



# WINNIPEG '96

GEOLOGICAL ASSOCIATION OF CANADA - MINERALOGICAL ASSOCIATION OF CANADA  
ASSOCIATION GÉOLOGIQUE DU CANADA - ASSOCIATION MINÉRALOGIQUE DU CANADA  
JOINT ANNUAL MEETING - RÉUNION ANNUELLE CONJOINTE  
27-29 MAY/MAI 1996 THE UNIVERSITY OF MANITOBA

## FIELD TRIP GUIDEBOOK

### PETROLOGY AND MINERALIZATION OF THE TANCO RARE-ELEMENT PEGMATITE, SOUTHEASTERN MANITOBA (FIELD TRIP A3)

by

Petr Cerny<sup>1</sup>, T.S. Ercit<sup>2</sup> and P.T. Vanstone<sup>3</sup>

- 1 - Department of Geological Sciences, University of Manitoba, Winnipeg, Manitoba, R3T 2N2
- 2 - Mineral Sciences Section, Canadian Museum of Nature, Ottawa, Ontario, K1P 6K1P
- 3 - Tantalum Mining Corporation of Canada Ltd., Box 2000, Lac du Bonnet, Manitoba, R0E 1A0

Recommended citation: Cerny, Petr, Ercit, T.S. and Vanstone, P.T., 1996. Petrology and Mineralization of the Tanco Rare-Element Pegmatite, Southeastern Manitoba - Field Trip Guidebook A4; Geological Association of Canada/Mineralogical Association of Canada Annual Meeting, Winnipeg, Manitoba, May 27-29, 1996.

© Copyright Geological Association of Canada, Winnipeg Section.



**Electronic Capture, 2008**

The PDF file from which this document was printed was generated by scanning an original copy of the publication. Because the capture method used was 'Searchable Image (Exact)', it was not possible to proofread the resulting file to remove errors resulting from the capture process. Users should therefore verify critical information in an original copy of the publication.

© 1996:

*This book, or portions of it, may not be reproduced in any form without written permission of the Geological Association of Canada, Winnipeg Section. Additional copies can be purchased from the Geological Association of Canada, Winnipeg Section. Details are given on the back cover.*

# THE TANCO RARE-ELEMENT PEGMATITE DEPOSIT, SOUTHEASTERN MANITOBA

## Table of Contents

Introduction .....	1
Location and regional geology .....	1
Location .....	1
General geology .....	1
Bird River Greenstone Belt .....	1
Granitoid intrusions .....	5
Pegmatite populations .....	5
Regional evolution .....	6
The Tanco pegmatite .....	6
Structural setting and morphology .....	6
Internal structure .....	9
Mineralogy .....	13
Potassium feldspar .....	13
Plagioclase .....	17
Quartz .....	17
Holmquistite .....	17
The mica group .....	17
Biotit	
Muscovite	
Lithian muscovite	
Lepidolite	
Cookeite .....	18
Illite-montmorillonite .....	18
Lithium aluminosilicates .....	20
Petalite	
Spodumene	
Eucryptite	
The tourmaline group .....	21
Dravite	
Uvite	
Schorl	
Elbaite	
Beryl .....	21
Pollucite .....	24
Cesian analcime .....	24
The zircon group .....	25
Zircon	
Thorite	
Coffinite (?)	
Ta,Nb,Sn,Ti,U-oxide minerals .....	27
The wodginite group	
The columbite-tantalite group	

Ferrotapiolite	
Cassiterite	
Rutile	
The microlite group	
Cesstibtantite	
Simpsonite	
Rankamaite-sosedkoite	
Uraninite	
Ilmenite	
Manganite . . . . .	28
Apatite group . . . . .	28
Fluorapatite	
Carbonate-hydroxylapatite	
Lithiophilite . . . . .	32
Amblygonite-montebrazite . . . . .	32
Lithiophosphate . . . . .	33
Minor secondary phosphates . . . . .	34
Whitlockite	
Fairfieldite	
Crandallite	
Overite	
Tancoite	
Dorfmanite	
Alluaudite	
Diomignite . . . . .	34
Native elements, alloys, sulfides and sulfosalts . . . . .	34
Lead	
Bismuth	
Arsenic	
Antimony	
Copper (?)	
Stibarsen	
Galena	
Sphalerite	
Hawleyite	
Pyrrhotite	
Pyrite	
Chalcopyrite	
Marcasite	
Arsenopyrite	
Molybdenite	
Cosalite	
Gladite	
Pekoite	
Gustavite	
Tetrahedrite	

Freibergite	
Bournonite	
Dyscrasite	
Pyrargyrite	
Miargyrite	
Cubanite	
Stannite	
Kesterite	
Černýite	
Carbonate minerals . . . . .	35
Calcite	
Rhodochrosite	
Dolomite	
Zabuyelite	
Barite . . . . .	36
Geochemistry . . . . .	36
Bulk composition . . . . .	36
Internal geochemical evolution . . . . .	38
Petrology . . . . .	40
Intrusive and solidification style . . . . .	41
P-T paths of consolidation . . . . .	42
Melt vs fluid evolution . . . . .	42
Exo- and endomorphism . . . . .	43
Internal subsolidus processes . . . . .	44
Petrogenesis . . . . .	44
Economic aspects . . . . .	46
History of the mine development . . . . .	46
Resources and reserves . . . . .	47
Products, specifications and uses . . . . .	47
Tantalum minerals	
Spodumene	
Montebrasite	
Pollucite	
Lepidolite	
Zonal distribution of commodities . . . . .	51
Mining . . . . .	52
Processing . . . . .	52
Tantalum mineral concentration	
Spodumene concentration	
Acknowledgements . . . . .	55
References . . . . .	55



## INTRODUCTION

The Tanco pegmatite has played a globally significant role in the production of tantalum ore concentrates, pyroceramic spodumene, pollucite and other materials since the late nineteen sixties. It has also been subject to numerous studies because of a very restricted extent of low-temperature alteration, and virtually complete preservation under the erosion surface which minimizes weathering effects. These features facilitate the study of bulk composition and of the primary petrologic phenomena which are commonly extensively disturbed by subsolidus and supergene events at other localities.

The extent of the present understanding of the Tanco pegmatite will become evident throughout the pages of this guidebook, with all relevant literature quoted in the list of references. Considerable amount of information still awaits publication, and many studies are in different stages of progress at the time of writing. Representative samples of data from the current research are included here to update the information as much as possible.

It is not possible to compile information relevant to the actual pre-meeting field trip half a year in advance, as the course of the excursion will depend on the state of the underground operations and accessibility of outcrops in late May 1966. Thus, this guidebook provides general background on all aspects of the Tanco deposit, and specific information concerning the field trip will be distributed to the participants shortly before the date of the excursion.

## LOCATION AND REGIONAL GEOLOGY

### Location

The Tanco pegmatite deposit is located about 180 km east-northeast of Winnipeg, close to the Manitoba-Ontario boundary (Figure 1) on the northwestern shore of Bernic Lake. The mine can be reached by float plane, or by road eastward from Lac du Bonnet. In turn, Lac du Bonnet is linked to the provincial road system in several directions, and has rail connection to Winnipeg.

### General Geology

The Tanco pegmatite is situated in the southern limb of the Bird River Greenstone Belt which flanks the exposed part of the Bird River Subprovince of the Superior Province, in the southwestern part of the Canadian Shield (Figure 1). This subprovince adjoins the batholithic belt of the Winnipeg River Subprovince in the south, and the Manigotogan gneiss belt of the English River Subprovince in the north (Figure 2; cf. Card & Ciesielski 1986, Černý 1990). Several remnants of lithologies dated at ~ 3 Ga are exposed in the broader vicinity of the map area shown in Figure 2 but most of the bedrock formations display ages in the range of 2780 - 2640 Ma (Table 1).

### Bird River Greenstone Belt

The following review of the Bird River Greenstone Belt is condensed from Trueman (1980) and from his chapters in Černý et al. (1981).

The Bird River Greenstone Belt is comprised of metavolcanic, related, and derived metasedimentary rocks (Figure 2) with synvolcanic to late tectonic intrusive rocks. The metavolcanics and metasediments compose six Formations, from the oldest Eaglenest Lake through Lamprey Falls, Peterson Creek, Bernic Lake and Flanders Lake to the

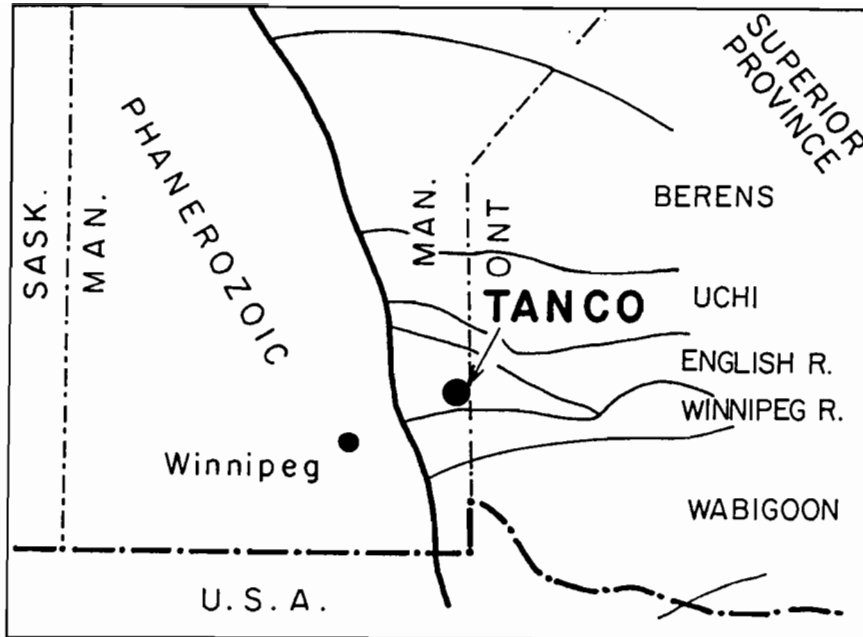


Figure 1. General location of the Tanco pegmatite.

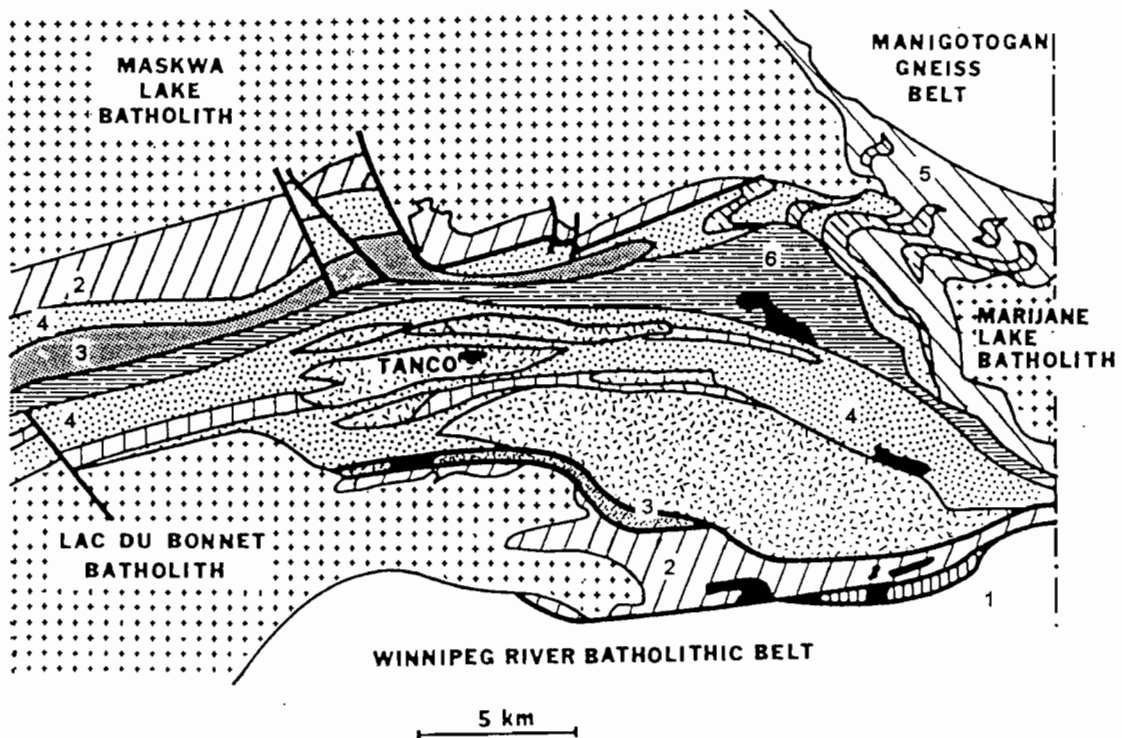


Figure 2. Geology of the Bird River Greenstone Belt, modified from Crouse et al. (1979, 1984) and Morgan & London (1987). 1 - Eaglenest Lake Formation, 2 - Lamprey Falls Formation, 3 - Peterson Creek Formation, 4 - Bernic Lake Formation, 5 - Flanders Lake Formation, 6 - Booster Lake Formation; see text for lithologies and subdivision into structural-cum-metamorphic subareas.

Table 1. Regional geochronology

Rock or event	Age, Ma	Method	Source
Winnipeg River tonalitic gneiss	~3010(?)	by analogy with zircon U-Pb by Krogh et al. (1976a) in adjacent n.w. Ontario	
Maskwa L. tonalite basement	2779±32	zircon U-Pb	Timmins et al. 1985
Bird R. greenstone belt, volcanism	2750 (min.) to 2715 (max.)	zircon U-Pb	Timmins et al. 1985
Main prograde metamorphism	~2710-2680(?); -2670	by analogy with n.w. Ontario (Krogh et al. 1976a, Gower & Clifford 1981), Corfu 1988), and n. Bird R. subprovince (Turek et al. 1989)	
Lac du Bonnet biotite granite	2665±20	zircon U-Pb	Krogh et al. 1976b
Shatford L. pegmatites	2652±5 2643±14	euxenite U-Pb monazite U-Pb	Baadsgaard & Černý 1993 Baadsgaard & Černý 1993
Shatford L. pegmatites	2579±8	uraninite U-Pb	Baadsgaard & Černý 1993
Tanco and Silverleaf pegmatites	2576±17 2583±4	muscovite Rb-Sr lepidolite Rb-Sr	Baadsgaard & Černý 1993 Baadsgaard & Černý 1993
Regional resetting of greenstone-belt lithologies	2587±32	average of 14 Rb-Sr isochron ages	A. Turek, pers. comm. 1990
Regional resetting of the Lac du Bonnet granite	2603±97	whole-rock Rb-Sr isochron	G.S. Clark, pers. comm. 1982
Regional resetting of the Lac du Bonnet leucogranite	2550±190	whole-rock Rb-Sr isochron	Černý et al. 1987

youngest Booster Lake Formation. Figure 2 also shows the principal structural elements of the belt, inclusive the major east-trending faults. Within the belt, these faults form internal lithologic, structural and metamorphic boundaries, and allow a subdivision of the belt into five subareas.

*Subarea A* consists of immature volcanoclastic sediments and mafic lavas of the Eaglenest Formation, which have suffered polydeformation and attendant metamorphism to greenschist facies.

*Subarea B* is comprised essentially of pillowed, amygdaloidal and hyaloclastic metabasalt, and is marked locally by glomeroporphyritic metabasalt (hi-alumina tholeiite), intercalated tuffs, and Algoman-type iron formation. These rocks which constitute the Lamprey Falls Formation have been intruded by hypabyssal metagabbro, the ultramafic-gabbroic chromite-bearing Bird River Sill (Trueman and Macek 1971), metagabbro stocks, quartz and quartz-feldspar porphyry dykes, and in the southern and eastern map area (Figure 2) by pegmatitic granite and pegmatite stocks and dykes.

The structural geology of subarea B is simple; these rocks form the basal part of a major east-trending synclinorium, unmodified by minor folding (Figure 2). All of the rocks of subarea B, excepting pegmatites, exhibit stable greenschist facies assemblages, and carry a weak to moderately well developed penetrative tectonic foliation.

*Subarea C* is comprised of three fundamental groups of rocks. These include: flow and clastic rocks of felsic composition (Peterson Creek formation), polymict metaconglomerate interlayered with mafic to felsic metavolcanic rocks (northern segment of the Bernic Lake Formation), and interbedded polymictic metaconglomerate and lithic arenite (Flanders Lake Formation). This latter group rests unconformably on the former two groups; of the three groups, the former two have been intruded by sills of quartz and quartz-feldspar porphyry, the latter by pegmatite dykes.

The structural geology of subarea C is complex, and involved two major periods of folding which yielded Ramsay's Type III interference fold patterns (Figure 2). Metamorphic assemblages evident in subarea C attained upper amphibolite facies and suffered, in part, subsequent retrogression.

*Subarea D* is equivalent in age to the interlayered polymictic metaconglomerate, metavolcanic rocks and iron formation of subarea C. It comprises the major fault-bounded segment of the Bernic Lake Formation. A fundamental difference between subarea C and D, however, is the synvolcanic emplacement in subarea D of large stocks of composite nature of gabbro, diorite, quartz-feldspar porphyry and granodiorite.

Structurally, subarea D occupies the core of the synclinorium formed by subareas A, B, and C, itself forming tightly close, near horizontally plunging Type III interference folds. Metamorphic assemblages in subarea D are of greenschist to lower amphibolite facies and all rocks (excepting pegmatite) display a strongly developed penetrative tectonic foliation.

*Subarea E* consists of a succession of greywacke-mudstone turbidites which, with interbedded iron formation, form the youngest stratified rocks of the Bird River Greenstone Belt (the Booster Lake Formation). These rocks rest unconformably above subareas A, B, C, and D, and have been intruded by sills and stocks of pegmatitic composition.

The structural geology of subarea E is simple; these rocks form a steep south-dipping, south-facing, monoclinial sequence marked by open flexures of bedding and schistosity. Pegmatites are essentially undeformed. Metamorphic assemblages in subarea E attained lower amphibolite facies, and were subsequently retrogressed.

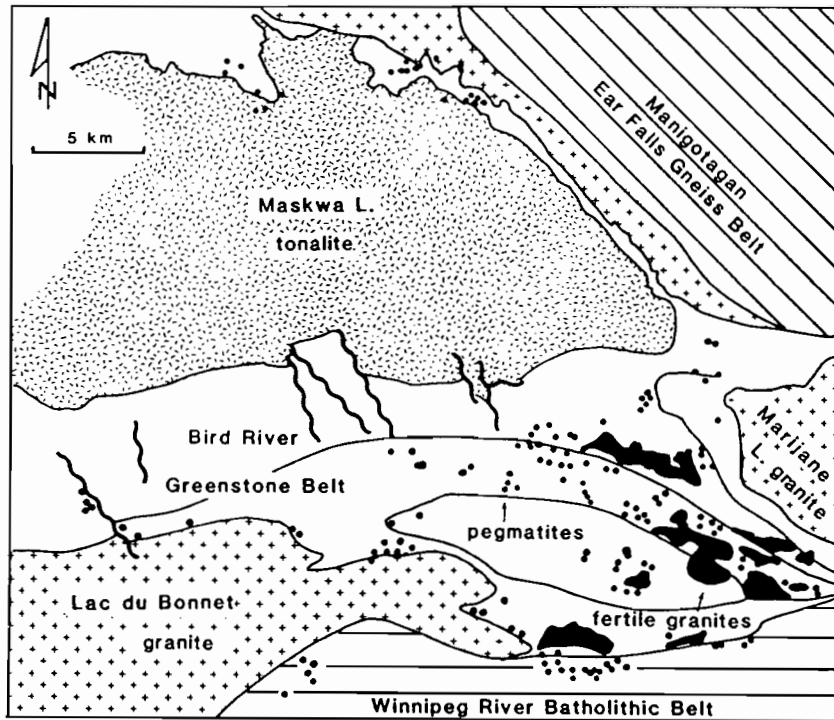


Figure 3. Distribution of batholithic granitoids, fertile granites (black) and pegmatites in the Cat Lake - Winnipeg River pegmatite field (after Černý 1991b); the pegmatites (dots) are in most cases only a schematic representation of densely populated pegmatite groups.

#### Granitoid Intrusions

The areas north, east and southwest of the Bird River Greenstone Belt are occupied respectively by the Maskwa Lake, Marijane Lake, and Lac du Bonnet batholiths (McRitchie 1971; Černý et al. 1982, 1987) which are shown in Figure 2. These intrusions consist of diapiric, tonalitic to granodioritic cores which appear to have been emplaced synchronously with development of tectonic foliation of layered rocks of the greenstone belt, and with the peak of regional metamorphism. Late tectonic biotite granites mantle and dissect the tonalitic diapirs, and in the Lac du Bonnet batholith they significantly predominate over other rock types.

#### Pegmatite Populations

Five intrusions of two-mica to garnet-muscovite leucogranites, in part tourmaline-bearing, were emplaced mainly along the east-trending faults segmenting the greenstone belt (Figure 3). Although locally sheared, they are late- to post-tectonic and represent the last intrusive event in the region. Most of the diverse pegmatite groups populating the Bird River Greenstone Belt were derived from residual melts generated by consolidation of these leucogranites (Greer Lake, Eaglenest Lake, Axial, Rush Lake, and Tin Lake groups). The Shatford Lake group is associated with the eastern termination of the Lac du Bonnet batholith, whereas the Bernic Lake group, a member of which is the Tanco pegmatite, has no fertile granite outcropping in reasonably close vicinity which could be its potential parent

(e.g., Černý et al. 1981, Černý 1991c).

### Regional Evolution

The oldest rock formations of the region are the tonalitic gneisses of the Winnipeg River belt in the south, and the tonalites of the Maskwa and Marijane Lake batholiths (Table 1). In the Bird River Greenstone Belt, the oldest formations are the metavolcanic and related rocks of subareas A and B. These rocks, largely basaltic and subaqueously deposited, were succeeded in age by felsic metavolcanic rocks of subarea C the deposition of which was both subaqueous and subaerial. Erosion of the emergent volcanic edifice yielded the clastic detritus interlayered with metavolcanic rocks of subareas C and D, and both clastic and nonclastic rocks of subarea D were intruded at this time by large gabbro-granodiorite composite stocks.

Detritus from the gabbro-granodiorite stocks is abundant in polymict metaconglomerate and lithic arenites of subarea C, as are reworked materials from subareas B and D. The deposition of these rocks presents a maximum age for the folding event in the greenstone belt.

The greywacke-mudstone turbidite of subarea E does not display evidence of the first period of folding, but is marked by the existence of the  $S_2$  foliation which generated the interference patterns of subarea C. This foliation, evident in all rocks of the greenstone belt except biotite granites and pegmatitic rocks, closely follows the boundaries of the Maskwa and Marijane batholiths and is thus interpreted as having originated during the diapiric emplacement of their tonalitic cores, which was roughly coeval with the peak of regional metamorphism (Table 1).

Some of the late biotite granites have also been affected by the above process but others, notably the Lac du Bonnet biotite granite, were emplaced during regional east-west faulting of the greenstone belt which yielded the final assembly of the lithologic-structural-metamorphic subareas shown in Figure 2. These faults also appear to have acted as channelways for the leucogranites and their pegmatite aureoles. Locally these intrusions show minor faulting and brecciation related to limited episodic movement along the faults.

Statistically, the ages of the batholithic biotite granites, leucogranites and pegmatites are largely identical but field relationships indicate a sequence from the strongly sheared A-type leucogranite in the eastern termination of the Lac du Bonnet batholith to the batholithic biotite granite (and its analogs in the broader vicinity, in part also dated) to the peraluminous leucogranites and their pegmatites.

A regional event of unknown nature and origin reset the whole-rock Rb-Sr ages of all lithologies about 60 to 90 Ma after the plutonic plus pegmatite consolidation (e.g., Penner & Clark 1971; Table 1). The Rb-Sr ages of micas in the pegmatites also were reset at that time, and other pegmatite minerals at least partly disturbed (Baadsgaard & Černý 1993).

## THE TANCO PEGMATITE

### Structural Setting and Morphology

The Tanco pegmatite is located in a subhorizontal position within a subvertically foliated metagabbro, close to its boundary with a synvolcanic granodiorite stock to the west (Figure 4). The emplacement of the pegmatite was controlled by gently E- and W-dipping joints and fractures, in a manner similar to the subhorizontal fractures hosting pegmatites

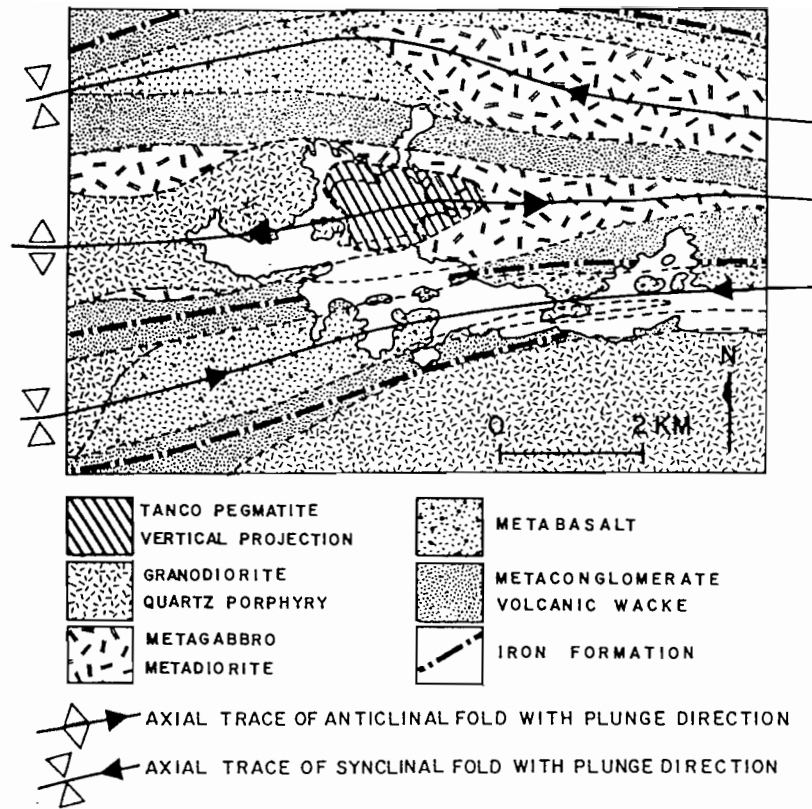


Figure 4. Geology of the lithologies and structural elements in the mine area, with the vertical projection of the Tanco pegmatite, from Crouse et al. (1984).

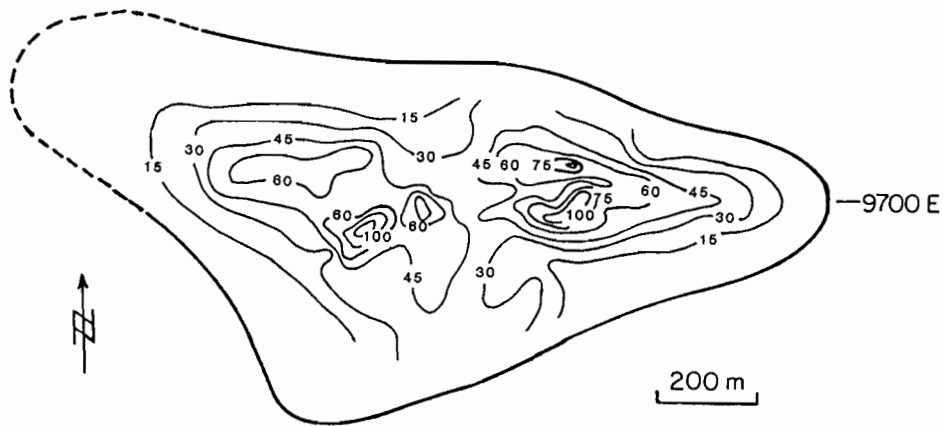


Figure 5. Isopachous map of the pegmatite, modified from Crouse et al. (1984).

Table 2. Zoning of the Tanco pegmatite.

Zone	Main constituents	Characteristic subordinate (accessory), and ((rare)) minerals	Textural and structural characteristics	Geochemically important major & (minor) elements
Exomorphic unit	biotite, tourmaline, holmquistite	(arsenopyrite)	fine-grained reaction rims and diffuse veins	K, Li, B (P,F)
(1) border zone	albite, quartz	tourmaline, apatite, (biotite) ((beryl, triphylite))	fine-grained layers	Na, (B,P,Be,LI)
(2) wall zone	albite, quartz, muscovite, Li-muscovite, microcline-perthite	<u>beryl</u> * (tourmaline)	medium-grained, with giant K-feldspar crystals	K, Na(LI,Be,F)
(3) aplitic albite zone	albite, quartz (muscovite)	muscovite, <u>Ta-oxide minerals</u> , <u>beryl</u> , (apatite, tourmaline, cassiterite) ((ilmenite, zircon, sulfides))	fine-grained undulating layers, fracture fillings, rounded blebs, diffuse veins	Na (Be,Ta,Sn,Zr,Hf,Tl)
(4) lower intermediate zone	microcline-perthite, albite, quartz, spodumene, amblygonite	Li-muscovite, lithiophilite ((lepidolite, petalite, Ta-oxide minerals))	medium- to coarse-grained inhomogeneous	K, Na, Li, P, F ((Ta))
(5) upper intermediate zone	<u>spodumene</u> , <u>quartz</u> , <u>amblygonite</u>	microcline-perthite, pollucite, lithiophilite (albite, Li-Muscovite), ((petalite, eucryptite, Ta-oxide minerals))	giant crystal size of major and most of the subordinate minerals	Li, P, F (K,Na,Cs,Ta)
(6) central intermediate zone	<u>microcline-perthite</u> quartz, albite, muscovite	<u>beryl</u> ( <u>Ta-oxide minerals</u> ), (zircon, ilmenite, spodumene, sulfides lithiophilite, apatite, cassiterite))	medium- to coarse-grained	K(Na,Be,Ta,Sn,Zr,Hf,Tl)
(7) quartz zone	quartz	((spodumene, amblygonite))	monomineralic	Si (LI)
(8) pollucite zone	pollucite	quartz, spodumene ((petalite, muscovite, lepidolite, albite, microcline, apatite))	almost monomineralic	Cs (LI)
(9) lepidolite zone	Li-muscovite, lepidolite, microcline-perthite	albite, quartz, <u>beryl</u> , ( <u>ta-oxide minerals</u> , cassiterite), (zircon)	fine-grained	Li,K,Rb,F (Na,Be,Ta,Sn, Zr,Hf,Ga)

\*Underlined minerals occur in economic quantities in the zones indicated.

at the eastern end of Bernic Lake, and at the nearby Rush Lake (Brisbin & Trueman 1982).

The boundaries of the Tanco pegmatite shown in Figure 5 are almost completely bracketed by diamond drilling. In form, the Tanco pegmatite is best described as a bilobate, shallowly north-dipping and doubly (E and W) plunging body, as partly shown in Figure 6. The pegmatite is fingering out in swarms of parallel dykes along most of its margins. The maximum thickness of the pegmatite is slightly in excess of 100 m, and along strike it can be traced for 1600 m; in the north-south direction the pegmatite is up to 820 m wide.

A series of small to sizeable pegmatites of related mineralogy accompanies the Tanco pegmatite immediately below, and below as well as above to the east, north and northwest. Most of these neighbouring pegmatites occupy the same system of shallow-dipping fractures that hosts the Tanco body; these pegmatites also display geochemical and paragenetic signatures similar to those of Tanco (Ferreira 1984).

#### Internal Structure

Nine zones of different mineral composition, texture and location can be distinguished within the pegmatite, and a halo of contact exomorphism in the mafic wall rock. Their compositional and textural characteristics as well as their economic significance are summarized in Table 2, and Figure 6 shows their relations in space.

Zones (1) and (2) compose shell-like concentric envelopes, commonly much thicker along the footwall contact. Units (4) and (5), whose mutual boundaries are gradational, can also be considered shell-shaped when taken as a single unit. In contrast, units (3), (6), (7), (8) and (9) occur as more or less discontinuous layers. Most of these flat lenticular bodies are confined to the upper central parts of the pegmatite and to the central parts of the eastern and western lobes.

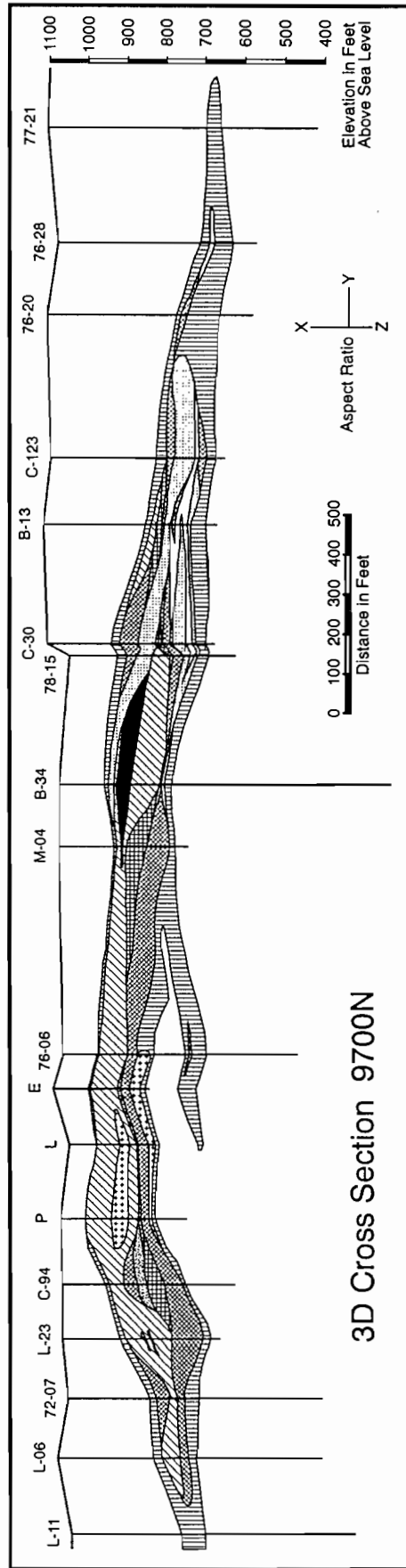
In a longitudinal E-W section, the pegmatite displays a distinct symmetry (Figure 6). At the crest of the pegmatite near its centre, most of its thickness is occupied by the Li-rich zones (4) and (5). These two are separated in both lobes by the intervening zone (6), overlain by quartz and pollucite bodies (7) and (8). Most of the segments of the lepidolite zone (9) occur within and just above the two segments of zone (6), in part transitional into this zone. Zone (3) follows the contacts of quartz core (7) with adjacent zones, and it penetrates particularly the zones (2) and (6). However, late stringers of albite which crosscut and replace most of the primary zones on small local scale are not necessarily connected with the albitic aplite (3).

Textural and paragenetic features strongly suggest that the bulk of all nine zones was produced by primary crystallization from a liquid/fluid phase. However, zones (1), (3) and in part also (9) show metasomatic relationships with adjacent zones, and small-scale plus very low-volume replacements can be seen within each of the zones (4) to (9).

*The border zone (1)* is dominantly a saccharoidal assemblage of albite and quartz along the pegmatite/wallrock contacts and replacing zone (2). Due to its negligible thickness which varies from a few to about 30 cm, zone (1) is not shown in Figure 5.

*The wall zone (2)* attains a thickness of 35 m along the footwall contact. Giant columnar microcline-perthite (up to 3 m) in a matrix of quartz, medium-grained albite and tabular greenish muscovite (up to 10 cm) are its main primary constituents. Other textural varieties of albite, columnar curvilamellar lithian muscovite and some of the accessory minerals display locally metasomatic features.

*The albitic aplite zone (3)* forms sheet-like layers up to 16 m thick as well as smaller,



3D Cross Section 9700N

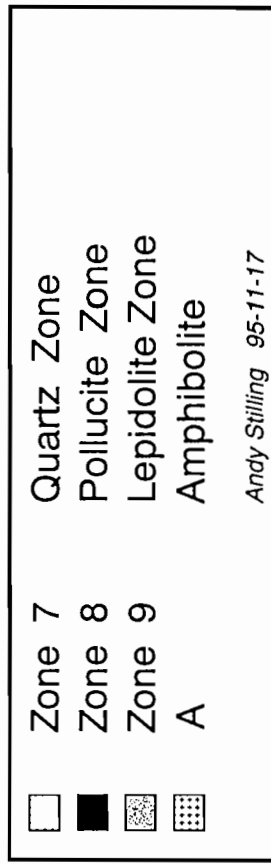
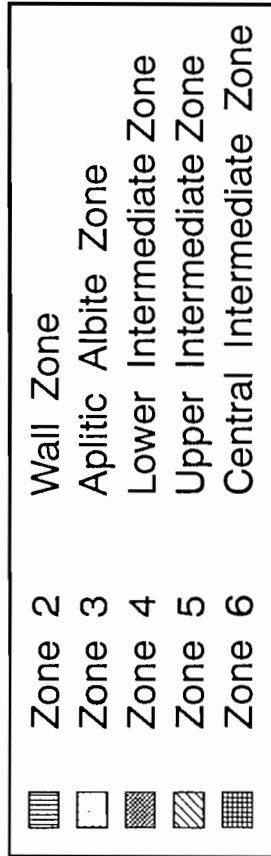


Figure 6. An E-W fence diagram through the Tanco pegmatite (unpublished data of A. Stilling); see Figure 5 for location of the section in plan.

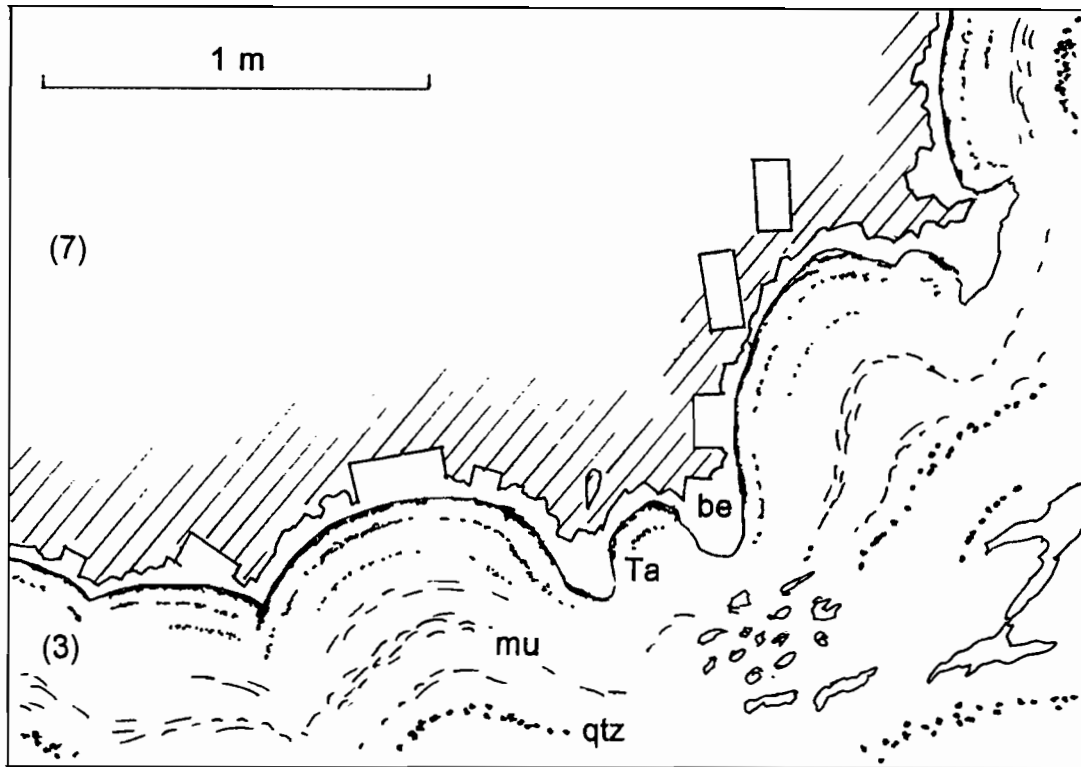


Figure 7. A typical conformation of albitic aplite zone (3) along contact with quartz zone (7) in the eastern wing of the pegmatite; the layering of the aplite is accentuated by accumulation of quartz (dots) and micas (dashes), and by increased concentration of Ta-oxide minerals close to the contact with quartz which is smoky (ruled) along the contact; the beryl fringe (white; crystals routinely up to 20 cm) is intermittent.

discontinuous and ragged lens-like bodies in the eastern lobe of the pegmatite, where they reside along the contacts of the wall zone (2) with the overlying zones (6) and (7) (Figure 7), or grade into the zone (6). In the western part of the pegmatite, zone (3) is dispersed as a network within the zone (6) and its contacts with zone (2) and (4); continuous and texturally well-defined layered sequences typical of the eastern part of the pegmatite are much less in evidence. The albite is mostly saccharoidal and only rarely medium-grained in texture, whereas cleavelandite is uncommon and only exceptionally in contact with the saccharoidal aggregates. This zone carries significant Ta,Nb mineralization along Be, Sn, Zr and Hf.

*Lower intermediate zone (4)* is located mainly in the lower central parts of the pegmatite, attaining a maximum thickness of about 25 m. A lack of textural and compositional uniformity appears to be characteristic: large crystals of microcline-perthite and spodumene + quartz pseudomorphs after petalite (up to 2 m) embedded in medium-grained quartz, albite and micas form one characteristic assemblage; the other one consists of quartz pods (0.5 - 2 m) with amblygonite-montebrazite and spodumene + quartz aggregates. Radial rims of cleavelandite and micas around the feldspar-rich assemblages usually separate them from the quartz accumulations (Figure 8).

*Upper intermediate zone (5)* evolves gradually from zone (4) mainly upwards, by

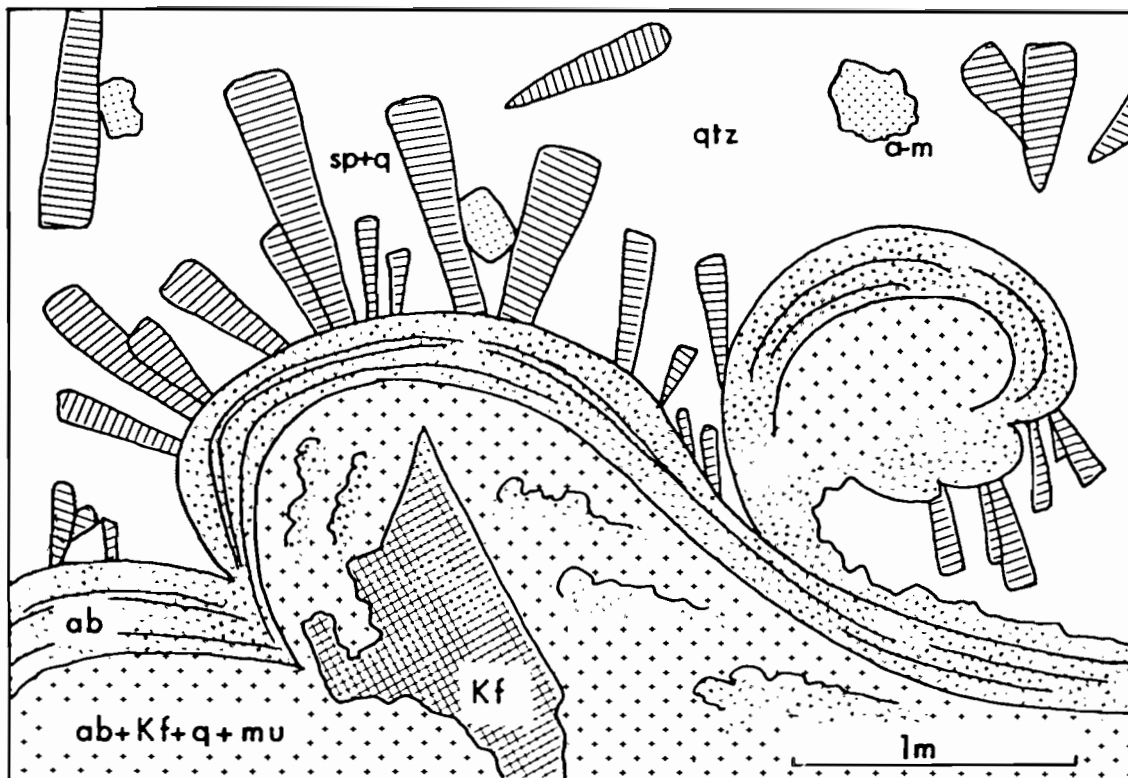


Figure 8. A typical texture from contacts of the wall zone (2) at the bottom ( $ab+Kf+q+mu$ ) with albitic aplite layers ( $ab$ ) approximating zone (3), in contact with a feldspar-poor segment of the lower intermediate zone (4) containing squi pseudomorphs after petalite, quartz and amblygonite-montebbrasite (lower central parts of the pegmatite; from Černý & Ferguson 1972).

almost total disappearance of albite and micas. Its thickness reaches locally 24 m. It is characterized by gigantic crystal size of most of its components (amblygonite to 2 m, microcline-perthite to 7 m, petalite to 13 m in length). This zone is the main source of petalite, spodumene + quartz pseudomorphs after petalite, amblygonite and quartz. Mirolitic cavities are rare, but leaching vugs with low-temperature mineral assemblages are locally abundant.

*Central intermediate zone (6)* is divided into two segments which reside in the central parts of the eastern and western flank of the pegmatite, inside the shell of the combined zones (4) and (5). It attains a maximum thickness of 45 m, and its overall shape approximates the contours of the whole pegmatite. Its contacts with the neighbouring units are usually sharp, but with locally gradual transitions into zones (3) and (9). Microcline-perthite and quartz (5-40 cm in size) and fine-grained greenish muscovite are the main constituents of this zone, which contains high concentrations of Ta,Nb oxide minerals, beryl and hafnian zircon, and rare mirolitic cavities.

*Quartz zone (7)* forms a true quartz core in some segments of the eastern part of the pegmatite but it is segmented and placed asymmetrically, predominantly upwards, in the other parts.

*Pollucite zone (8)* consists of several lenticular bodies located mainly along the

upper contacts of zone (5) with the hanging-wall parts of the wall zone (2). The largest of them is the only one in the eastern part of the pegmatite, 180 x 75 x 12 m in dimension. Petrologically, it belongs to zone (5) which contains numerous small blebs of pollucite but it is descriptively treated as a separate zone because of the huge dimensions of some of the pollucite bodies, and because of their distinctive location. This zone represents a rather unique economic concentration of pollucite, about 75% pure in the bulk of the zone composition. Coarse veining of pollucite by lepidolite, quartz and feldspars is widespread.

*Lepidolite zone (9)* forms two flat-lying, E-W elongated sheets up to 18 m thick, and several smaller bodies within the central intermediate zone (6) or along its contacts with the spodumene- (petalite-) rich zones (4) and (5). Fine-grained (0.1-2 mm) lithian muscovite predominates over true lepidolite, both commonly intergrown with the microcline-perthite and quartz along the contacts with zone (6). Lepidolite and Ta,Nb oxide minerals are of economic interest here.

### Mineralogy

The mineral paragenesis of the Tanco pegmatite is quite diversified, considering the restricted extent of low-temperature alteration which commonly generates the bulk of mineral species (Table 3). The pegmatite has yielded holotypes of four new minerals, černýite (Kissin et al. 1978), tancoite (Ramik et al. 1980), diomignite (London et al. 1987), and titanowodginite (Ercit et al. 1992), and it contributed to the original definition of wodginite (Nickel et al. 1963). Several other minerals are on the list of worldwide rarities, some of them being relatively abundant here (cesstibtantite, simpsonite, lithiophosphate, cesian analcime) but most of them scarce (ferrowodginite, lithiowodginite, rankamaite-sosedkoite, dorfmanite).

Figure 9 shows the distribution and abundances of the significant rock-forming and accessory minerals in the zonal structure of the pegmatite.

The following notes briefly summarize some of the important features of the Tanco minerals, and list the sources of detailed information.

#### Potassium feldspar

K-feldspar is present in zones (2), (4), (5), (6) and (9) as a substantial component, and in minor quantities in zones (1) and (8). It is mostly pale grey to beige in colour, with patchy rust coloration developed in close vicinity of the amphibolite wallrock or its xenoliths. *Microcline perthite* is the standard type of alkali feldspar at Tanco, with generally high degree of tetrahedral order ( $\Delta \geq 0.80$ ; Figure 10). Giant crystals in zone (5) that commonly display a striped grey and white pattern in their interior and pink-rusty outer zone show increasing degree of tetrahedral order and segregation of the perthite phases from grey to white to rusty (Černý & Macek 1972).

Veins of rusty- to flesh coloured, non-perthitic K-feldspar penetrate the pollucite of zone (8). This feldspar is non-perthitic but highly triclinic (Černý & Simpson 1978).

A late hydrothermal variety of K-feldspar, white to colourless in color and with typical *adularia* morphology is found in leaching cavities and as an alteration product of pollucite. In the cavities, the *adularia* is extremely close to a structural end-member high sanidine (Figure 10; Černý 1972b, Černý & Chapman 1984, Ferguson et al. 1991).

The bulk composition of K-feldspar shows an erratic decrease in Na but a steady increase in P, Rb, Cs and Tl from the outer to the inner pegmatite zones (Černý 1982b, London et al. 1990; Table 4, Figure 11), whereas the triclinic feldspar veining pollucite has



Mineral	EX	(1)	(2)	(3)	(4)	(5)	(6)	(7)	(8)	(9)
Holmquistite	#									
Epidote	+									
Biotite	#	+								
Chlorite	+									
Quartz	+	28	35	27	34	32	15	94	5	10
Albite	+	64	40	67	25	4	20	+	5	8
K-feldspar			15		23	10	50	2	2	10
Muscovite		1	3	3	1	+	12		2	
Lithian muscovite			3		2	+				40
Lepidolite				+	0.5	+	+		7	30
Petalite					10	35		11	1	
Spodumene						5	+	2	1	
Eucryptite						2				
Apatite	+	2	+	0.5	#	+	#		0.5	+
Lithiophilite	+	+	+	#	0.5	1	0.5			#
Amblygonite			0.5	+	3	10		0.5	0.5	0.5
Beryl		#	0.5	1	+	+	1			0.5
Pollucite					?				75	
Tourmaline	#	2	1	0.5	+	+	+			
Garnet		?								
Cassiterite			#	+	+	+				+
Rutile				+		+	+			
Ferrotapiolite				+			+			
Columbite group			#	+	#	#	+			#
Wodginite group				#		+	#		#	+
Microlite group				+	+	+	+		+	+
Simpsonite							+			
Ilmenite		?		?			?			
Uraninite						+	+			+
Zircon						+	+			+
Thorite						+	+			+
Sulfides	+			+	+	+	+			
Carbonates	#			+	+	+	+		+	

Figure 9. Zonal distribution and abundances of minerals, modified from Crouse et al. (1972) and Morgan & London (1987). A number of petrologically and economically less significant minerals were grouped or omitted; see Tables 3, 10, 13 and the text for further information; # - relatively abundant accessory phase, + - rare minerals.

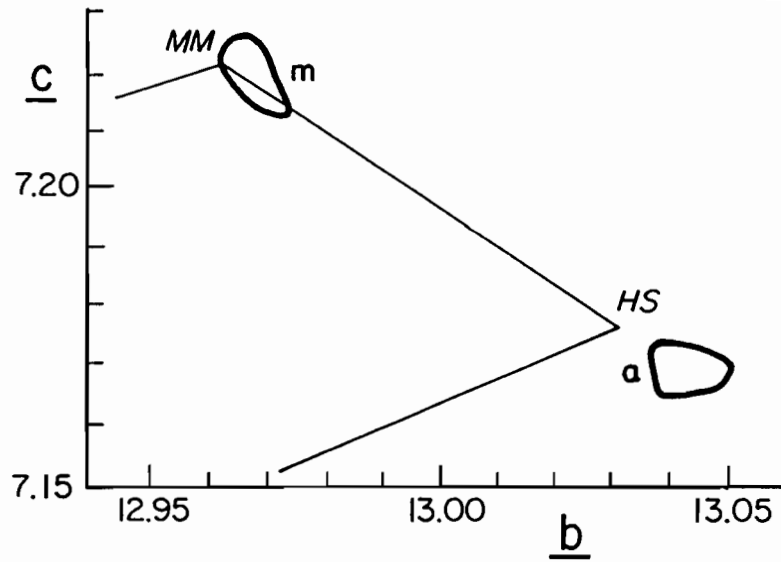


Figure 10. Structural state of the K-feldspar in the *b* vs *c* diagram of Stewart & Wright (1974); note the drift of Rb-enriched rock-forming microcline (*m*) outward from the maximum microcline apex, and the external location of the adularia plots (*a*) (after Černý & Chapman 1984).

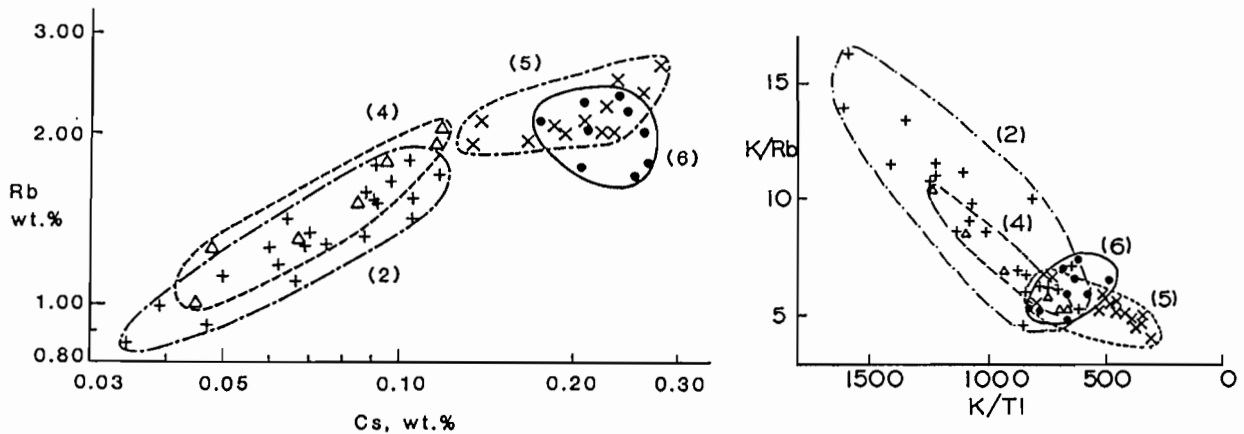


Figure 11. Graphs of Rb vs Cs and K/Rb vs K/Tl for the Tanco K-feldspar; numbers indicate pegmatite zones (unpublished data of P. Černý).

$\text{Na}_2\text{O} < 1$  wt.%. In contrast, the adularia from leaching cavities is virtually pure end-member potassium feldspar (Table 4). In the alteration assemblage after pollucite, adularia shows variable and locally dominant substitution of Rb for K (Table 4; unpublished data of D.K. Teertstra).

**Table 4. Compositional characteristics of K-feldspar.**

	K <sub>2</sub> O	Na <sub>2</sub> O	CaO	Li <sub>2</sub> O	Rb <sub>2</sub> O	Cs <sub>2</sub> O	P <sub>2</sub> O <sub>5</sub>	Ga*	Ti*
zone (2)	11.60 -13.70	0.79 -2.65	0.07 -0.34	0.016 -0.069	0.77 -0.069	0.02 -0.24	0.29 -0.39	50 -100	60 -167
zone (4)	11.20 -14.25	1.34 -3.66	0.011 -0.025		0.64 -2.19	0.02 -0.13		37 -89	85 -150
zone (5)	11.80 -14.55	0.56 -2.28	bdl -0.15	0.033 -0.132	1.67 -2.93	0.10 -0.30	0.36 -0.48	31 -110	150 -322
zone (6)	13.16 -14.64	0.55 -1.76	bdl -0.19	0.028 -0.099	1.80 -2.57	0.20 -0.28	0.45 -0.61	84 -116	145 -300
adularia I	-14.09 -16.91	0.00 0.12	bdl	-	bdl	bdl	bdl	-	-
adularia II	8.83 -16.81	0.0 -0.06	bdl	-	0.0 ~15.4	0.0 ~0.7	bdl	-	-

bdl - below detection limit; - not analyzed

\* - in p.p.m.

adularia I - in leaching cavities

adularia II - replacing pollucite

Unpublished data of P. Černý and D. K. Teertstra, except P<sub>2</sub>O<sub>5</sub> from London *et al.* (1990).

### Plagioclase

In the immediate vicinity of contacts with the mafic wallrock, plagioclase is as calcic as andesine An<sub>30</sub>. However, in most of the zone (1) and in all other zones, its composition corresponds to an almost pure albite, with An<sub>1-3</sub> at the maximum, and the structural state is invariably extremely close to fully ordered. Saccharoidal to finely lath-shaped albite is most common, grading to medium-grained in zone (2) and locally also (4) and (9). Cleavelandite is the only other variety, forming plates up to 10 cm across, typically in zones (4) and (5). It routinely occurs separately from saccharoidal albite, and the two varieties are rarely seen in direct contact.

### Quartz

Quartz is widespread, at its most abundant in zone (7) and relatively least common in zone (9) and (6). Crystals are sporadically found in miarolitic cavities of zones (5) and (6). The colour is whitish, rarely smoky in cavities or along contacts of zones (3) and (7) (Figure 3). In some parts of zones (4) and (5), quartz has a very slight but perceptible rose colour.

### Holmquistite

This violet to purplish orthoamphibole is found as subparallel fibrous aggregates on fractures of amphibolite in the exocontacts, at distances of up to 20 m outside the pegmatite. Locally it also forms three-dimensional networks penetrating the mafic wallrock, associated with biotite (cf. Morgan & London 1987).

### The Mica Group

The micas are represented by (magnesian) *biotite* in the exocontacts and in zone (1), platy silvery to greenish *muscovite* in zone (2), fine-flaked yellow-greenish muscovite

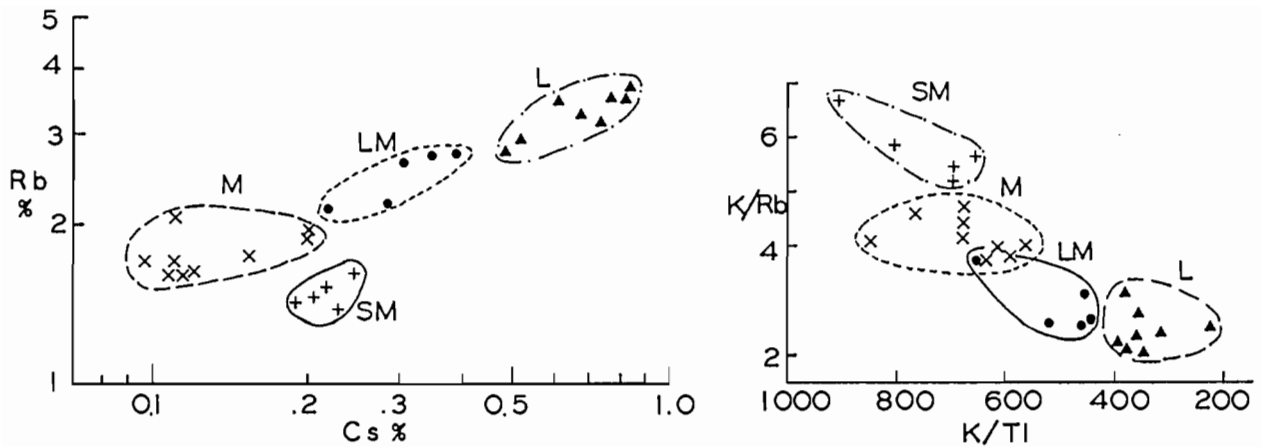


Figure 12. Graphs of Rb vs Cs and K/Rb vs K/Tl for the main types of Tanco micas; numbers indicate pegmatite zones (unpublished data of P. Černý). M - muscovite of zones (2) and (4); LM - lithian muscovite of zones (2), (4) and (5); L - lithian muscovite and lepidolite of zones (4), (5) and (9); SM - fine-grained muscovite of zone (6).

in zones (3), (6) and (8), rare extremely fine-flaked *rose muscovite* in zone (3), columnar curvilamellar *lithian muscovite* to *lepidolite* of silvery to purplish colour in zones (3), (4) and (5), and fine-flaked lithian *lepidolite* to *lepidolite* in zone (9). Brownish micas are rarely found associated with *lithiophilite* of zones (4) and (5).

The designation of lithian *lepidolite* is used for lithium-poor micas ( $\text{Li}_2\text{O} \leq 3.5$  wt.%) which display the normal muscovite polytype of  $2\text{M}_1$ ; true *lepidolite* is richer in Li and, at Tanco, it shows the  $1\text{M}$  polytype stacking (Rinaldi et al. 1972, unpublished data of P. Černý). The columnar curvilamellar micas of zones (3), (4) and (5) routinely show interlayering of lithian muscovite (silvery) and *lepidolite* (purple); the same feature characterizes the fine-flaked micas of the *lepidolite* zone (9) but at microscopic scale.

The chemistry of the Tanco micas shows considerable contents of rare alkalis in the exocontact biotite (Table 5, after Morgan & London 1987; including also Li - unpublished data of P. Černý). A conspicuous increase in the rare alkalis is observed from muscovite to *lepidolite* (Table 5, Figure 12). The brownish micas belong in part to muscovite, in other cases to *lepidolite*; they are typically enriched in Fe and Mn (Table 5). Gallium is very enriched in all types of Tanco micas, at levels of 250 to 900 ppm (Černý & Hawthorne 1989).

#### Cookeite

This Li,Al-based chlorite is quite widespread as an alteration product of *spodumene*, commonly intergrown with muscovite. Otherwise, cookeite also lines leaching cavities in zones (4) and (5), and it coats earlier phases in miarolitic vugs of zones (5) and (6) (Černý 1972b).

#### Illite-montmorillonite

Pale apple-green clay is commonly found as a late filling of leaching cavities in zones (4) and (5), or as a replacement of *spodumene* (Černý 1972b). On exposure to sunlight, it turns brown and disintegrates by dehydration. X-ray diffraction identified the two mineral components in random interstratification.

Table 5. Representative compositions of micas

	Biotite		Muscovite		Lithian Muscovite and Lepidolite			
	178	30	R.8	ZNTA-2A	R.7	REN.5	R.9	REN.1
SiO <sub>2</sub>	39.35	36.19	43.20	45.20	47.80	48.00	47.50	51.65
TiO <sub>2</sub>	0.73	1.36	----	0.27	----	----	----	----
Al <sub>2</sub> O <sub>3</sub>	17.53	17.30	34.36	35.75	28.64	28.31	28.64	26.65
Fe <sub>2</sub> O <sub>3</sub>	----	----	----	0.76	----	----	----	----
FeO	16.72	19.30	0.32	----	0.06	0.26	0.03	0.06
MnO	0.26	0.19	0.07	0.23	0.20	0.50	0.22	0.44
MgO	8.03	10.21	<0.01	0.01	<0.01	2.08	<0.01	0.90
CaO	0.07	0.07	----	0.05	----	----	----	----
Li <sub>2</sub> O	----	----	0.37	0.43	3.12	3.42	3.50	4.28
Na <sub>2</sub> O	0.16	0.10	0.22	0.70	0.19	0.17	0.19	0.40
K <sub>2</sub> O	7.73	8.35	10.12	8.57	9.98	8.61	9.45	8.68
Rb <sub>2</sub> O	1.96	0.58	1.69	2.00	2.91	5.10	3.59	4.47
Cs <sub>2</sub> O	1.46	0.37	0.21	0.12	0.50	----	0.71	----
F	2.41	0.84	0.64	----	2.73	1.44	4.08	1.51
H <sub>2</sub> O <sup>+</sup>	----	----	6.00	4.44	5.60	2.74	4.38	2.13
H <sub>2</sub> O <sup>-</sup>	----	----	0.80	----	0.48	----	0.21	----
O=F	-1.01	-0.35	-0.27	----	-1.15	-0.61	-1.72	-0.64
	<u>95.40</u>	<u>94.51</u>	<u>97.74</u>	<u>98.53</u>	<u>101.07</u>	<u>100.02</u>	<u>100.79</u>	<u>100.53</u>
<i>Atoms per 24(O,OH,F)</i>								
Si	----	----	6.112	6.108	6.559	6.440	6.514	6.758
Al	----	----	<u>1.888</u>	<u>1.892</u>	<u>1.441</u>	<u>1.560</u>	<u>1.486</u>	<u>1.242</u>
			8.000	8.000	8.000	8.000	8.000	8.000
Al	----	----	3.842	3.802	3.191	2.917	3.143	2.868
Ti	----	----	----	0.027	----	----	----	----
Fe <sup>3+</sup>	----	----	----	0.077	----	----	----	----
Fe <sup>2+</sup>	----	----	0.038	----	0.007	0.029	0.003	0.007
Mn	----	----	0.008	0.026	0.023	0.057	0.026	0.049
Mg	----	----	<0.002	0.002	<0.002	0.416	<0.002	0.176
Ca	----	----	----	0.007	----	----	----	----
Li	----	----	<u>0.211</u>	<u>0.234</u>	<u>1.722</u>	<u>1.845</u>	<u>1.930</u>	<u>2.252</u>
			4.101	4.175	4.945	5.264	5.104	5.352
Na	----	----	0.060	0.183	0.051	0.044	0.051	0.101
K	----	----	1.827	1.477	1.747	1.474	1.653	1.449
Rb	----	----	0.154	0.174	0.257	0.440	0.317	0.376
Cs	----	----	<u>0.013</u>	<u>0.007</u>	<u>0.029</u>	----	<u>0.042</u>	----
			2.054	1.841	2.084	1.958	2.063	1.926
F	--	--	0.286	----	1.185	0.611	1.770	0.625
OH	--	--	3.714	4.000	2.815	3.389	2.230	3.375
O	--	--	<u>20.000</u>	<u>20.000</u>	<u>20.000</u>	<u>20.000</u>	<u>20.000</u>	<u>20.000</u>
			24	24	24	24	24	24

178: Exocontact black-brown, <0.5 m from contact.

30: Exocontact black-brown, 1-2 m from contact.

R.8: Fine-grained green 2M<sub>1</sub>, zone (6).

ZNTA-2A: Tabular brownish 2M<sub>1</sub>, zone (4).

R.7: Massive violet 2M<sub>1</sub>, zone (9).

REN.5: Massive violet 2M<sub>1</sub>, zone (9).

R.9: Massive violet 2M<sub>1</sub> > 1M, zone (9).

REN.1: Columnar curvilamellar, violet 1M > 1M<sub>1</sub>, zone (9).

All H<sub>2</sub>O is measured, except for analysis (4), calculated. All formula OH is calculated for stoichiometry.

\*----\*: not measured. 178 and 30 from Morgan & London (1987), ZNTA-2A unpubl. data of P. Černý; others from Rinaldi *et al.* 1972.

Lithium aluminosilicates

*Petalite* was abundant at the time of pegmatite solidification in zone (4) and particularly plentiful in giant crystals in zone (5). However, most of it broke down at lower temperatures to a spodumene + quartz intergrowth (squi) which forms perfect pseudomorphs after the parent phase (Černý & Ferguson 1972). Primary *spodumene* forms columnar crystals up to 2 m long in zone (5) and mainly along margins of some segments of the quartz zone (7). It is white, in contrast to minor columnar spodumene of zone (6) which is pale greenish. *Eucryptite* forms irregular blebs in the squi pseudomorphs which are almost indistinguishable from massive quartz when greyish or white, but a large proportion of eucryptite is baby-pink or slightly rusty-red. Carmine-red fluorescence in UV light is shown only by mechanically undisturbed specimens; it is eliminated by impacts of hammer blows and by drilling (Černý 1972a). Crystals of eucryptite were found recently in open fissures (R.Gunther, pers. comm. 1995).

The chemical composition of petalite and spodumene is close to theoretical formulas, with only minor deviations from ideal stoichiometry and negligible substitution by other elements (Table 6). The deviations are within the limits of analytical error and minor

Table 6. Representative compositions of petalite, squi, spodumene and eucryptite

	Petalite		Squi		Spodumene		Eucryptite	
	13	25	33	34	SPD-1	33s	2	3a
SiO <sub>2</sub>	77.80	77.85	77.10	77.05	63.45	63.68	45.93	44.43
P <sub>2</sub> O <sub>5</sub>	----	----	0.05	0.05	0.02	0.08	----	----
Al <sub>2</sub> O <sub>3</sub>	16.55	16.60	16.30	16.83	27.40	27.40	42.74	44.84
Fe <sub>2</sub> O <sub>3</sub>	0.002	0.012	0.11	0.14	0.053	0.18	----	----
MgO	----	0.028	0.009	0.021	0.012	0.015	----	----
CaO	----	0.008	0.01	0.16	0.16	0.02	----	----
Li <sub>2</sub> O	4.55	4.54	4.49	4.46	7.87	7.55	11.33	10.73
Na <sub>2</sub> O	----	0.054	0.225	0.280	0.114	0.378	----	----
K <sub>2</sub> O	----	0.050	0.063	0.032	0.038	0.106	----	----
Rb <sub>2</sub> O	----	----	0.016	0.007	0.002	0.026	----	----
Cs <sub>2</sub> O	----	----	0.005	0.010	0.001	0.008	----	----
H <sub>2</sub> O <sup>+</sup>	0.29	0.32	0.25	0.30	0.30	0.42	----	----
H <sub>2</sub> O <sup>-</sup>	0.06	0.14	0.08	0.10	0.11	0.13	----	----
	99.25	99.60	98.71	99.44	99.53	99.99	100.00	100.00
<i>Atoms per formula unit</i>								
Si	8.020	8.012	8.008	7.960	7.948	7.967	5.796	5.621
P	----	----	0.004	0.004	0.002	0.008	----	----
Al	2.011	2.014	1.995	2.049	4.045	4.040	6.356	6.686
Fe <sup>3+</sup>	0.000	0.001	0.009	0.011	0.005	0.017	----	----
Mg	----	0.004	0.001	0.003	0.002	0.003	----	----
Ca	----	0.001	0.001	0.018	0.021	0.003	----	----
Li	1.886	1.879	1.875	1.853	3.965	3.798	5.749	5.459
Na	----	0.011	0.045	0.056	0.028	0.092	----	----
K	----	0.007	0.008	0.004	0.006	0.017	----	----
Rb	----	----	0.001	0.000	0.000	0.002	----	----
Cs	----	----	0.000	0.000	0.000	0.000	----	----
	11.917	11.929	11.949	11.960	16.023	15.947	17.901	17.766
O	20	20	20	20	24	24	24	24

13: Grey, zone (5).

25: White, zone (5).

33, 34: White, zone (5).

SPD-1: Log-shaped white crystals, zone (5/7).

33s: Recalculated from squi #33.

2, 3a: Pale pink massive, adjusted for impurities, zone (5).

\*----\*: not measured. From Černý & Ferguson (1972), except petalite from Černý and London (1983) and eucryptite from Černý (1972).

alteration (Černý & Ferguson 1972, Černý & London 1983). Compositions of eucryptite, adjusted for impurities, correspond to the intermediate members of its variation range, close to the ideal formula (Table 6; Černý 1972a).

#### The tourmaline group

Tourmaline is present as blackish-brown columnar to fibrous crystals in the exocontact, associated with biotite and arsenopyrite; black fine grains in zone (1), black columnar crystals with greenish-black outer zones and up to 25 cm long in zone (2), fine-grained black crystals in zones (3) and (6), and green or pink grains in zones (4) and (5). The abundance of tourmaline is moderate in zone (2), usually confined to the vicinity of contacts with amphibolite, but it is much greater here than in any other pegmatite zone. The light-coloured tourmaline of zones (4) and (5) is particularly scarce. A minor but distinct variety of blue tourmaline forms reaction rims around lithiophilite.

Representative compositions show that the exocontact tourmaline belongs to intermediate *dravite-uvite* with variable proportions of schorl component. This composition also characterizes a proportion of tourmaline in zone (1). However, most of the tourmaline of zone (1) is classified, along with tourmaline from zones (2), (3), (6) and from rims around lithiophilite as *schorl* with variable percentage of the elbaite component. Compositions close to the *elbaite* end member are typical of the light-coloured tourmaline of zones (4) and (5) (Table 7, unpublished data of J. Selway).

Compositional diagrams of Figure 13 show progressive changes in compositional parameters of the tourmaline minerals from the exocontact inwards. A general decrease in Ti, Mg and Fe is evident, along with an increase in Al, Mn, F (and implicitly Li). Na and F show an almost perfect 1:1 (at.) correlation, and both drop sharply in the most fractionated transition-metal-depleted elbaite. Calcium shows a sharp initial drop from relatively high values but a perceptible increase in late elbaite. A noteworthy feature is the presence of substantial vacancies in the alkali site, shown by tourmalines of most of the compositional types from most of the pegmatite zones (Figure 13; unpublished data of J. Selway).

#### Beryl

Beryl is found locally in the endocontact parts of zone (1) and scattered throughout zone (2). It forms prominent fringes along the outer margins of zone (3) against quartz (Figure 6; crystals up to 30x40 cm), but is rarely encountered in the intermediate zones (4) and (5). In zone (6), it is associated predominantly with the albite-rich assemblages but such a link is not in evidence in zone (9). Early beryl from the outermost zones is columnar in shape, and locally pale greenish in colour. However, most of the beryl in other zones is equidimensional to stumpy or tabular, flattened parallel to the basal pinacoid. The colour is mainly white to colourless but in the zones (4), (5) and (9) a slight salmon-pink colour is widespread.

The composition of beryl is highly variable, with increasing contents of Na, Li and Cs from the outermost pegmatite zones inwards; the Na/Li ratio decreases in the same direction but levels off when the increase in Cs becomes dominant (Figure 14; Černý & Simpson 1977). Representative compositions shown in Table 8 indicate unusually high contents of Cs in the primary beryl, normally associated with late cavity-grown beryl from miarolitic cavities. Beryl of this kind, lining miarolitic cavities or apparently associated with hydrothermal minerals in leaching vugs, is very rare at Tanco but some of its samples

Table 7. Representative compositions of tourmaline.

	Tt2	Tt21	Tt25	TtC18	TtC31	TtC22	TtC13	TtC11	TtC11	TtC19	TtC12	TtC40a	TtC40b	TtC2
SiO <sub>2</sub>	34.90	37.00	37.30	35.30	36.20	35.40	36.20	37.50	36.50	36.60	37.30	38.00	35.20	35.00
TiO <sub>2</sub>	0.87	0.09	0.15	0.70	0.19	1.14	0.37	0.08	0.02	0.53	0.11	0.03	0.10	0.53
Al <sub>2</sub> O <sub>3</sub>	27.10	32.80	38.10	32.50	36.00	27.00	34.50	37.80	36.70	35.90	39.00	41.10	36.30	34.20
MgO	5.60	5.06	1.32	1.11	0.12	7.30	0.04	0.12	0.10	0.41	0.00	0.00	0.01	0.05
CaO	2.29	0.47	0.20	0.17	0.07	3.12	0.02	0.14	0.08	0.05	0.30	0.13	0.04	0.08
MnO	0.01	0.04	0.04	0.19	0.21	0.00	0.21	1.28	0.37	0.21	2.08	2.52	0.64	0.35
FeO	12.90	6.70	5.07	13.60	8.33	10.50	10.10	4.66	7.83	8.10	2.69	0.11	9.08	12.20
ZnO	0.02	0.02	0.01	0.30	0.22	0.05	0.13	0.02	0.11	0.14	0.23	0.03	0.43	0.34
Na <sub>2</sub> O	1.41	2.39	2.50	1.88	2.40	1.14	2.31	2.31	2.59	2.48	2.24	2.06	2.11	1.94
F	0.34	1.38	1.36	0.28	1.08	0.59	0.74	1.07	1.22	1.05	1.16	1.06	0.88	0.44
O=F	-0.14	-0.58	-0.57	-0.12	-0.45	-0.25	-0.31	-0.45	-0.51	-0.44	-0.49	-0.45	-0.37	-0.19
total	85.30	85.37	85.45	85.91	84.37	85.99	84.31	84.53	85.01	85.03	84.62	84.59	84.42	84.94

Atoms per formula unit based on Si = 6

Si	6.000	6.000	6.000	6.000	6.000	6.000	6.000	6.000	6.000	6.000	6.000	6.000	6.000	6.000
Ti	0.112	0.111	0.018	0.089	0.024	0.145	0.046	0.010	0.002	0.065	0.013	0.004	0.013	0.068
Al	5.491	6.269	7.223	6.511	7.032	5.393	6.739	7.128	7.110	6.936	7.394	7.648	7.292	6.910
Mg	1.435	1.223	0.317	0.281	0.030	1.845	0.010	0.029	0.025	0.100	0.000	0.000	0.003	0.013
Ca	0.422	0.082	0.034	0.031	0.012	0.567	0.004	0.024	0.014	0.009	0.052	0.022	0.007	0.015
Mn <sup>2+</sup>	0.001	0.005	0.005	0.027	0.029	0.000	0.029	0.173	0.052	0.029	0.283	0.337	0.092	0.051
Fe <sup>2+</sup>	1.855	0.909	0.682	1.933	1.155	1.488	1.400	0.624	1.076	1.110	0.362	0.015	1.294	1.749
Zn	0.003	0.002	0.001	0.038	0.027	0.006	0.016	0.002	0.013	0.017	0.027	0.003	0.054	0.043
Na	0.470	0.751	0.780	0.620	0.771	0.375	0.742	0.717	0.825	0.788	0.699	0.631	0.697	0.645
F	0.185	0.708	0.692	0.151	0.566	0.316	0.388	0.541	0.634	0.544	0.590	0.529	0.474	0.239

exoccontact - Tt2, Tt21, Tt25

zone (3) - TTC19

zone (1) - TTC18, TTC31, TTC22

zone (4) and (5) - TTC12, TTC40

Zone (2) - black or brown - TTC13

TTC40a - pink rim, TTC40b - green core of same grain

zone (2) - green - TTC11

zone (6) - TTC2

B203, H<sub>2</sub>O<sup>+</sup>, and Li<sub>2</sub>O constitute the remainder to 100 wt%.

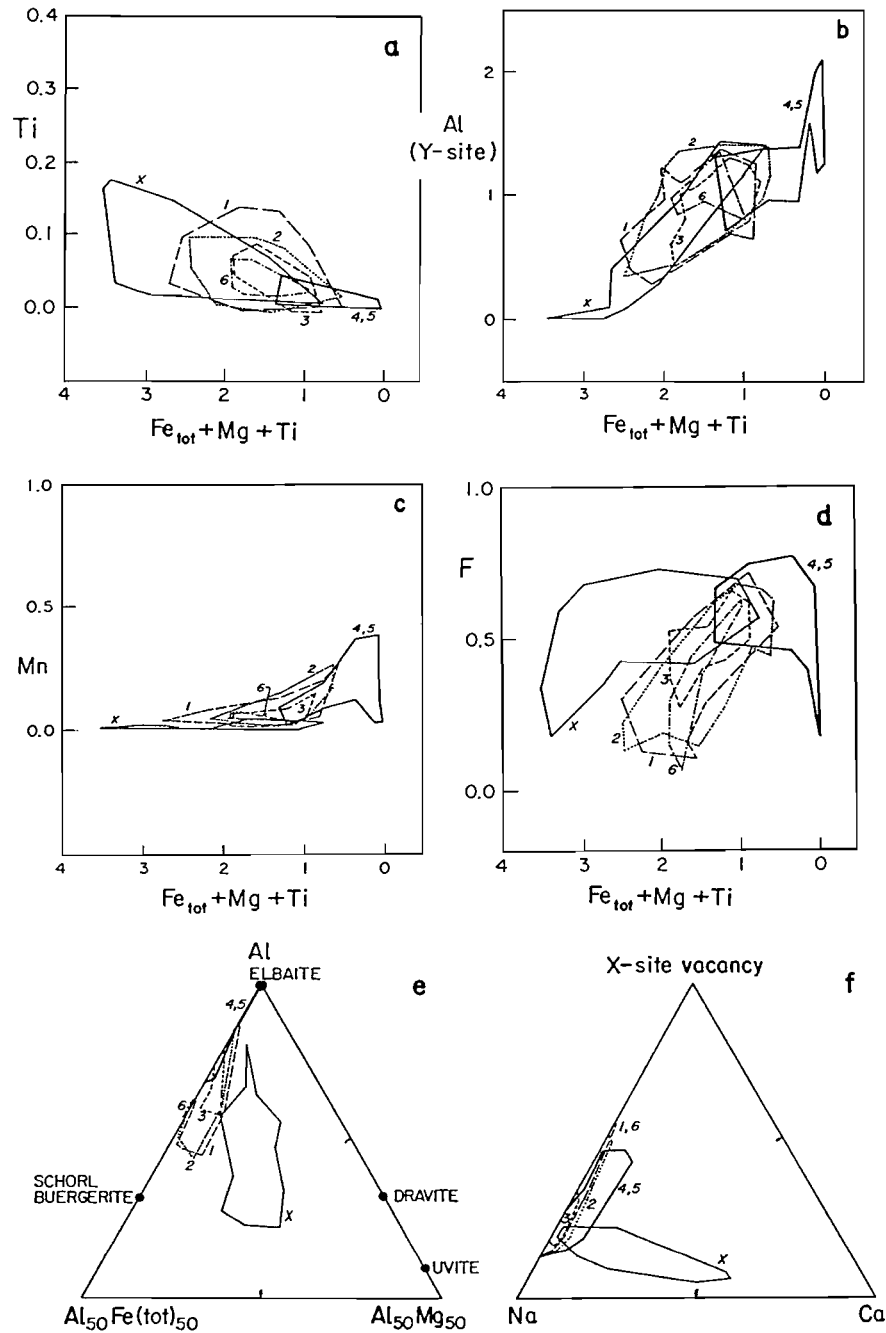


Figure 13. Compositional features of tourmaline (unpublished data of J. Selway and M. Novák); a - Ti, b - Al(Y site), c - Mn and d - F vs the sum of Fe<sub>tot</sub>+Mg+Ti which generally decreases during pegmatite fractionation; e - the Al - Al<sub>50</sub>Fe<sub>(tot)</sub><sub>50</sub> - Al<sub>50</sub>Mg<sub>50</sub> diagram of Henry & Guidotti (1985); f - the X-site diagram for Na - Ca - □. Bracketed numerals denote pegmatite zones (x - exocontact).

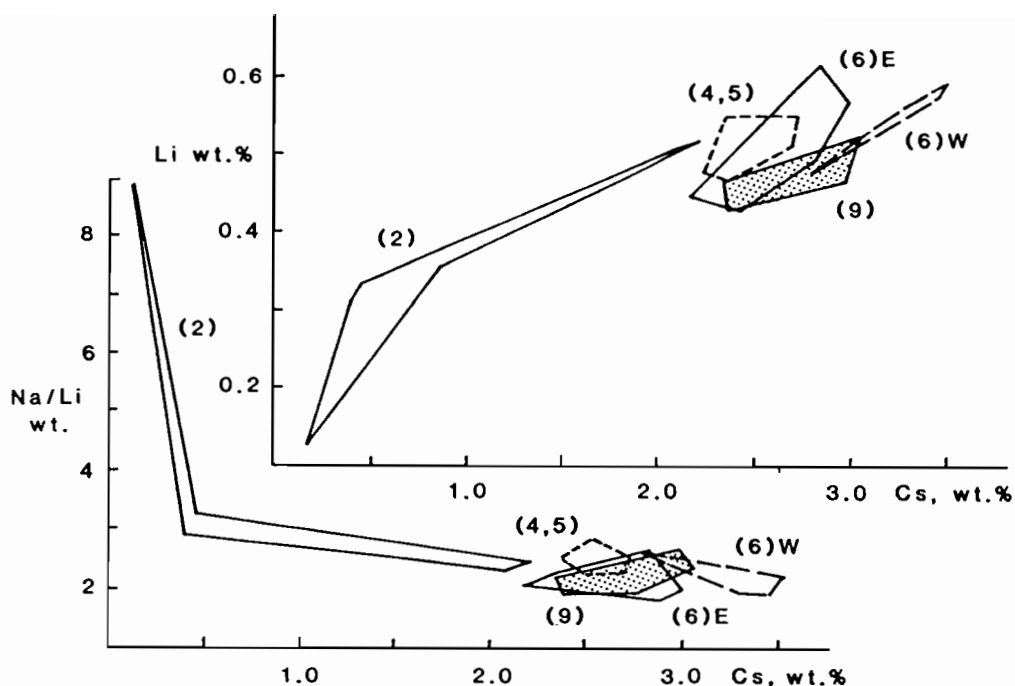


Figure 14. Alkali contents and ratio of beryl across the pegmatite zones, indicated by their numbers; from Černý & Simpson (1977).

attain  $\text{Cs}_2\text{O}$  contents of at least 7.16 wt.%, and probably much more in others which show extremely high refractive indices.

#### Pollucite

Large bodies and smaller pods of pollucite typically reside in the upper intermediate zone (5), attaining huge dimensions which earned them a descriptive designation of a separate zone (8). Pollucite is white to colourless waterclear, rarely with a violet tint caused by dispersed microflakes of lepidolite. It is commonly penetrated by subparallel to braided networks of white veinlets < 1 mm wide, consisting of muscovite and spodumene, locally accompanied by adularia.

Bulk composition of the pollucite (Table 8) corresponds to the data obtained at most of its localities elsewhere (Černý & Simpson 1978). Electron microprobe (unpublished data of D.K. Teertstra) reveals a great degree of heterogeneity in terms of both the Si/Al ratio and the CRK index (atomic ratio) which equals  $100(\text{Cs}+\text{Rb}+\text{K})/\Sigma\text{cations}$  (where the  $\Sigma\text{cations} = \text{Li}+\text{Na}+\text{K}+\text{Rb}+\text{Cs}+\text{Ca}+\text{Mg}$ ) and expresses the mole percentage of end-member pollucite. Primary pollucite is not far removed from one of the bulk composition but it shows bimodal distribution of data, clustered around CRK 80.7 and 85.6 (Figure 15). It is penetrated by several generations of progressively Cs- and Al-enriched veinlets, in part rimming inclusions, which attain CRK as high as 98.4. Superposed on these phenomena is a late process of analcimization, usually associated with clay minerals, which reduces the CRK index to values as low as 6.0 (Table 8).

#### Cesian analcime

In hydrothermal leaching vugs of zone (5), close to as well as remote from pollucite

Table 8. Representative compositions of beryl, pollucite and cesian analcime.

	1	2	3	4	5	6	7	8	9	10	11	12
SiO <sub>2</sub>	62.35	62.00	47.80	47.42	47.07	43.35	39.06	50.96	54.42	52.10	54.85	49.30
Al <sub>2</sub> O <sub>3</sub>	17.50	17.71	15.70	16.02	15.95	16.05	16.26	18.57	21.73	17.60	20.36	17.35
Fe <sub>2</sub> O <sub>3</sub>	0.03	0.02	0.01	0.01	0	0.01	0.01	0.01	0	–	–	0
P <sub>2</sub> O <sub>5</sub>	–	–	–	–	0.33	0.03	0.01	0	0.02	–	–	0
BeO	11.76	11.32	–	–	–	–	–	–	–	–	–	–
Li <sub>2</sub> O	0.98	1.13	0.28	0.29	–	–	–	–	–	–	–	–
Na <sub>2</sub> O	1.38	1.68	1.98	1.30	1.59	0.83	0.15	7.27	12.12	6.46	10.30	6.22
K <sub>2</sub> O	0.05	0.27	0.17	0.10	0	0.01	0	0.03	0.01	0.19	0.40	0.01
Rb <sub>2</sub> O	0.07	0.11	0.77	0.68	0.83	0.26	0.37	0	0	0.06	0.01	0
Cs <sub>2</sub> O	2.47	3.27	30.60	32.57	32.19	38.23	41.31	15.94	3.55	18.00	6.00	17.32
CaO	0.01	0.03	0.04	0.06	0	0.01	0	0.01	0	0.13	0.05	0.01
H <sub>2</sub> O	1.96	2.06	2.11	1.37	–	–	–	–	–	4.45	7.51	–
sum	98.54	99.68	99.54	99.87	97.96	98.78	97.18	92.80	91.87	99.13	99.89	90.20
Atomic contents based on 18 (beryl) and 6 (pollucite-analcime) atoms of oxygen per anhydrous formula unit.												
Si	11.976	11.911	2.998	2.150	2.144	2.094	2.021	2.101	2.042	2.146	2.093	2.128
Al	3.959	4.010	0.836	0.856	0.856	0.914	0.992	0.905	0.962	0.854	0.916	0.883
Fe	0.004	0.003	0.003	0.003	0	0	0	0	0	–	–	0
P	–	–	–	–	0.013	0.001	0	0	0.001	–	–	0
Be	5.376	5.225	–	–	–	–	–	–	–	–	–	–
Li	0.624	0.775	0.051	0.053	–	–	–	–	–	–	–	–
Na	0.513	0.626	0.174	0.114	0.140	0.078	0.015	0.583	0.882	0.516	0.761	0.521
K	0.011	0.065	0.010	0.006	0	0.001	0	0.002	0.001	0.010	0.019	0.001
Rb	0.009	0.013	0.022	0.020	0.024	0.008	0.012	0	0	0.002	0.001	0
Cs	0.202	0.268	0.590	0.630	0.625	0.788	0.912	0.281	0.057	0.316	0.098	0.319
Ca	0.001	0.006	0.002	0.003	0	0	0	0	0	0.006	0.002	0
Si/Al	–	–	2.58	2.51	2.50	2.29	2.04	2.33	2.12	2.51	2.28	2.41
CRK	–	–	73.3	79.3	82.2	91.1	98.4	32.7	6.1	38.6	13.3	38.1

“–”: not analysed; “0”: below limit of detection;

CRK = 100 (Cs+Rb+K)/(Li+Na+K+Rb+Cs+Ca).

1,2. Bulk composition of beryl from Tanco: Černý & Simpson (1977).

3. U39, bulk composition by wet chemical analysis: Černý & Simpson (1978).

4. B1207, bulk composition by wet chemical analysis: Černý & Simpson (1978).

5. Average of 31 EMP compositions of primary pollucite.

6. Quartz-containing Cs,Al-rich veinlet of pollucite.

7. Cs,Al-rich pollucite adjacent to spodumene inclusion.

8,9. Cesian analcime resulting from analcimization of primary pollucite.

10,11. Secondary cesian analcime, bulk composition by wet chemical analysis of Tanco crystals #1 and #2: Černý (1972b).

12. EMP composition of core of zoned crystal; rim has Si/Al = 2.18 CRK = 10.2.

bodies, crystals of analcime are found displaying the dominant form {211}, occasionally slightly modified by {100}. Individual crystals are as large as 2 cm in diameter, associated with adularia, cookeite, calcite and illite-montmorillonite (Černý 1972b).

Chemical composition is highly variable among the different crystals as well as internally. The content of Cs is commonly very low but some crystals show CRK of 38.6 in their bulk composition (Table 8). Strong concentric zoning in Na and Cs is locally observed, with sector-bound variations in Si/Al (unpublished data of D.K. Teertstra and P. Černý).

The zircon group

*Hafnian zircon* is found in anhedral, in part skeletal grains to euhedral crystals a few mm in maximum size in zone (3), in the albite-rich parts of zone (6), and in zone (9). It

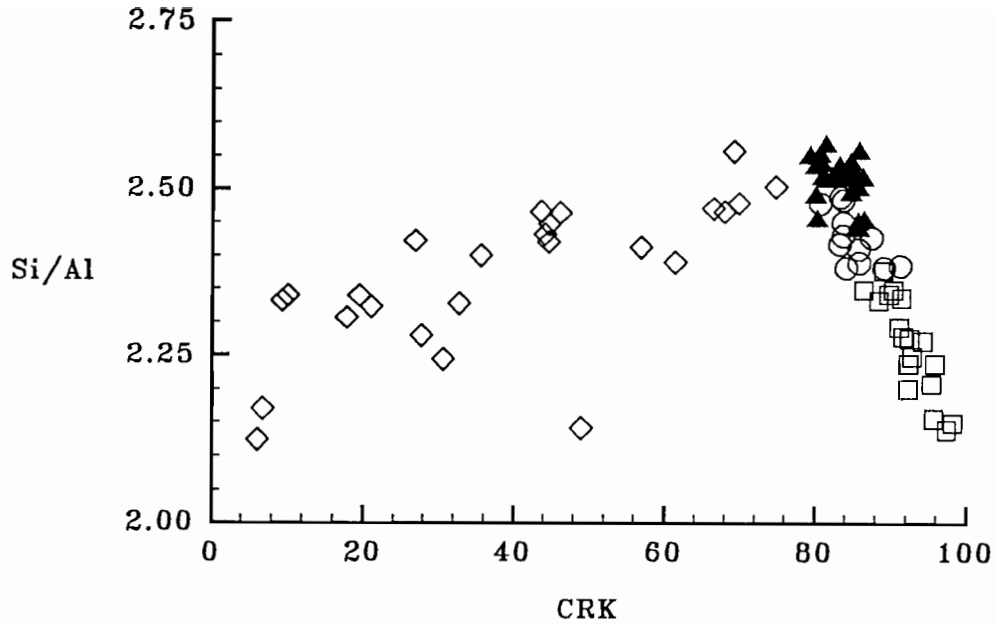


Figure 15. Composition of the primary homogeneous pollucite (solid triangles), Cs,Al-enriched blebs (circles), Cs,Al-rich veinlets (squares) and cation-exchanged analcimized regions (diamonds). Note the divergence of the analcimization trend from the Cs,Al-concentrating reequilibration (unpublished data of D.K. Teertstra).

Table 9. Composition of zircon.

	ZH-1		ZH-3/11		ZH-4/17		ZH-5/10	
	S	C	S	C	S	C	S	C
SiO <sub>2</sub>	32.2	31.4	29.4	28.4	28.5	28.5	30.6	32.3
ZrO <sub>2</sub>	50.4	38.4	52.8	49.3	53.0	49.4	52.6	47.4
HfO <sub>2</sub>	17.4	17.5	17.9	13.3	17.6	14.8	17.3	15.3
Al <sub>2</sub> O <sub>3</sub>	.0	.0	.0	.0	.8	.8	.7	.7
FeO	.04	.9	.1	.8	.03	.5	.01	.0
MnO	.2	1.0	.6	.9	.02	.3	.1	.3
CaO	.02	2.3	.3	3.6	.0	.4	.0	.4
	100.26	91.5	101.1	96.3	99.95	94.7	101.3	96.4
	Atoms per formula unit							
Si	1.041		.969		.951		.989	
Zr	.794		.848		.862		.829	
Hf	.161		.168		.167		.160	
Al	-		-		.031		.027	
Fe	.001		.003		.001		-	
Mn	.005		.017		.001		.003	
Ca	.001		.011		-		-	
	2.003		2.016		2.013		2.008	

S - homogeneous birefringent subsurface zones.  
 C - inhomogeneous near-isotropic central parts.  
 Atomic contents based on 4 oxygens per formula.  
 From Černý & Štívolová (1980)

tends to be associated with the oxide minerals of Nb and Ta, and cassiterite. Crystals up to 15 mm in size are sporadically present in zone (5), associated with the squi pseudomorphs after petalite. In all cases, zircon displays a pale pink-brownish colour and {101} dominant over occasional narrow facets of {100} and {110}.

Internally, the zircon crystals are heterogeneous, with turbid metamict cores and much fresher but transversally cracked outer zones. Primary zoning is not related to the Hf content, which is rather constant between 15 and 18 wt.% oxide (Table 9). Zoning is related primarily to variable U and Th. The U, Th-enriched core and zones in the oscillatorily heterogeneous outer parts were preferentially attacked by late fluids, hydrated and enriched in Ca, Fe, Mn and traces of S; simultaneous loss of Hf and Zr was accompanied by segregation and in part sulfidation of radiogenic Pb (Table 9; cf. Černý & Siivola 1980).

*Thorite* was identified only as microscopic inclusions in the oxide minerals of Ta and Nb, and probably also in zircon.

*Coffinite* was tentatively identified only as microscopic inclusions in zircon.

#### Garnet

Garnet was reported from endocontacts of the pegmatite by D.L. Trueman (pers. comm. 1976).

#### Ta, Nb, Sn, Ti, U oxide minerals

This is the economically most important mineral class in the Tanco pegmatite, and very diversified. Sixteen mineral species are represented by members of the wodginite, columbite and microlite groups, ferrotapiolite, cassiterite, rutile, cesstibtantite, simpsonite, and the rare rankamaite-sosedkoite, uraninite and ilmenite.

Identification of many of those minerals in the field is close to impossible in some cases, as some of them closely resemble each other, and some are indistinguishable from components of the silicate matrix in daylight.

*Wodginite-group minerals* are generally dark brown to black in colour, occasionally pale cinnamon-brown, as in the case of the wodginite-lithiowodginite solid solution. Single crystals (mm- to cm-scale) are columnar to fibrous, characteristically sector-twinned and diamond-shaped in cross-section. *Columbite-group minerals* are similar to wodginite-group minerals in colour and size, tending, however, toward stout, brick- or barrel-shaped crystals in zones (4) and (5) and more elongate crystals in zone (6). *Ferrotapiolite* forms mm-scale, lustrous, deep red-black equant crystals. *Cassiterite* forms mm-scale, lustrous bipyramidal crystals, similar to wodginite-group minerals in outline, but untwinned. *Rutile* forms nondescript, mm-scale, irregular black grains. *Microlite* forms mm-scale, equant crystals ranging from brown to black (uranoan) to white and green varieties. *Simpsonite* forms mm-scale to cm-scale quartz-like white to yellow-pink crystals which fluoresce blue-white in short-wave UV light. Rankamaite-sosedkoite, cesstibtantite and lithiowodginite are rare species found only in the most highly fractionated parts of zone (6) of the western limb of the pegmatite.

*Cesstibtantite*, a cesium-antimony-bearing microlite, forms orange-yellow crystals which fluoresce orange in UV light. *Rankamaite-sosedkoite* has been found in only one sample, and is opaque white and micro-fibrous. *Stibiotantalite* was tentatively identified by XRD in an ore concentrate. *Uraninite* and *ilmenite* are black and are extremely rare; ilmenite has only been located in ore concentrates to date. The distribution of oxide

Table 10. Summary of oxide mineral distribution.

Internal Unit	WD	MC	TN	CT	RU	TP	UR	SM	CS	RS
[2] Wall			■	■						
[3] Aplitic Albite	■	x	x	x	x	x				
[4] Lower Intermediate		x	■	x						
[5] Upper Intermediate	x	x	■	x	x		x			
[6] Central Intermediate	■	x	x	x		x		x	x	x
[8] Pollucite	■	x								
[9] Lepidolite	x	x	x	■						

WD wodginite group, MC microlite group, TN columbite group, CT cassiterite, RU rutile, TP ferrotapiolite, UR uraninite, SM simpsonite, CS cesstibtantite, RS rankamaite-sosedkoite

■ dominant, x subordinate to rare

minerals in the individual zones is given in Table 10.

Representative compositions of oxide minerals are given in Table 11 (Ercit 1986, Ercit et al. 1992, 1993, and unpublished data), and compositional ranges in terms of the most significant components are shown in Figure 16. Variations in mineral chemistry are smooth and continuous over the evolutionary history of the pegmatite (T.S. Ercit, unpublished data). Minerals of the columbite and wodginite groups (Figures 16 a, c) show sympathetic increases in Mn and Ta. Ferrotapiolite is symptomatic of the relatively Fe- and Ta-rich assemblage of zone (3), and is found again in zone (6) as a late product of increased activity of Ta. Titanium gradually fades out, up to complete substitution by Sn, with progressive fractionation of the wodginite minerals (Figure 16 d). In the microlite group, an increase in Na+Mn+Fe+Pb parallels increasing Ta, at the expense of Ca+Sn+Sb+U (Figure 16 b).

### Manganite

Manganite is found in the form of sooty coating or finely fibrous, black tufts with the clay minerals in the hydrothermal assemblage of cesian analcime, cookeite, calcite and related minerals (unpublished data of P. Černý).

### Apatite group

This most widespread phosphate is present in virtually all zones of the Tanco pegmatite except, possibly, the quartz zone (7). Several varieties were generated during the course of pegmatite consolidation: primary *manganoan fluorapatite*, columnar to massive granular, pale-blue to black-blue in zones (1), (2), (4), (5), (6) and (8), and pale-green in zone (3); secondary fibrous *carbonate-hydroxylapatite*, pink to purplish in squi of zone (5), mainly as a replacement of lithiophosphate; and secondary *carbonate-hydroxylapatite*, beige to chocolate-brown in radial fibrous botryoidal coatings or equidimensional complex crystals, lining leaching cavities in zones (4), (5) and (6). Main concentrations of the primary apatite are encountered in zones (5), along the margins of the pollucite bodies (8), and in local accumulations in zone (3).

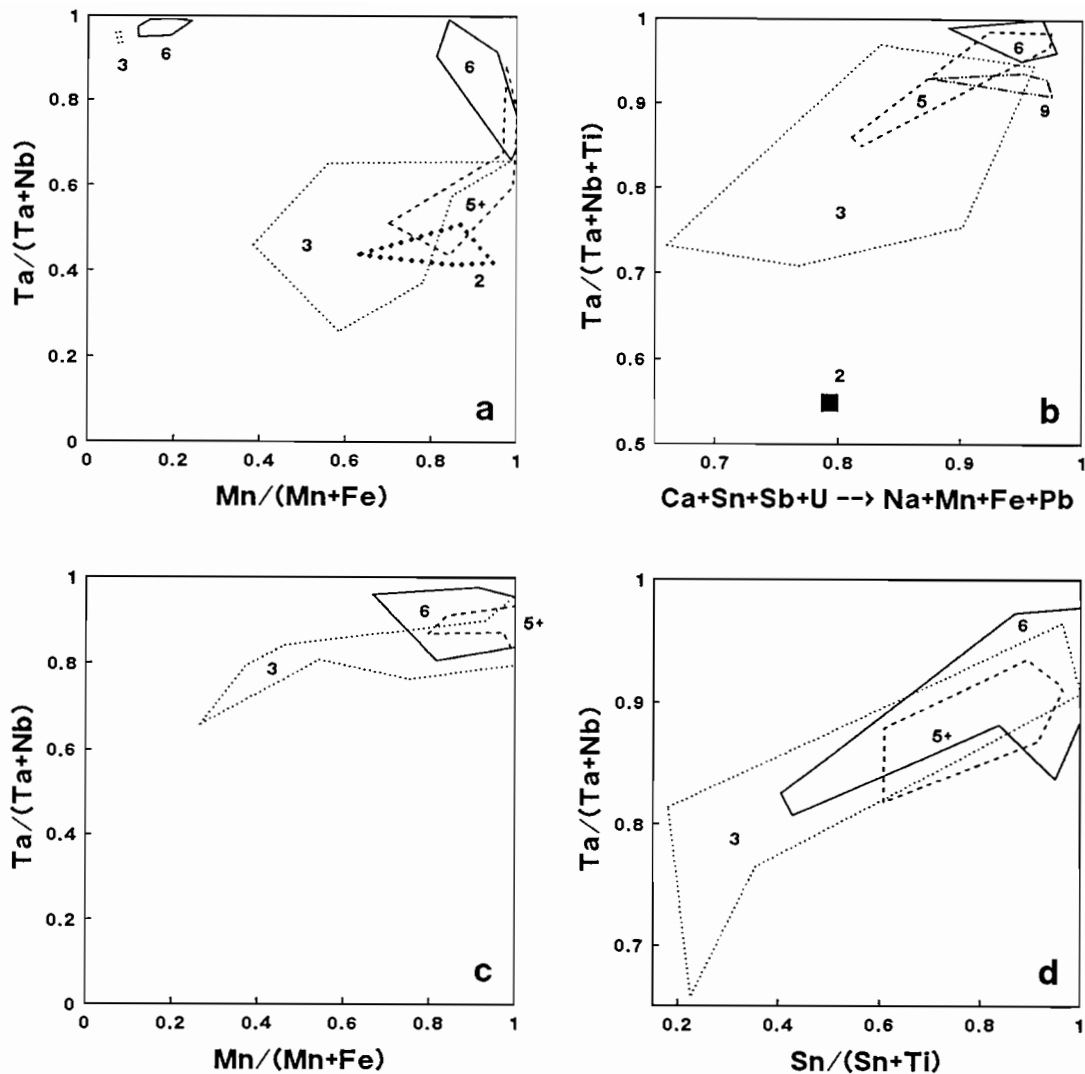


Figure 16. Variations in major element chemistry for various oxide minerals (unpublished data of T.S. Ercit): a - columbite-group minerals and ferrotapiolite (top left); b - microlite and uranmicrolite (the square for zone 2 represents a single sample); c and d - wodginite-group minerals. Numerals in the fields of the plots are zone numbers; "5+" denotes data covering zones (4), (5), (8) and (9).

Besides these three principal varieties, less conspicuous but equally widespread types of apatite are found as grey to black, fine-grained replacement products of amblygonite-montebbrasite, and as pale- to dark-blue reaction rims around lithiophilite. White massive apatite of chalky appearance locally forms after amblygonite-montebbrasite, and cinnamon-coloured massive apatite is occasionally found filling interstices among other minerals and their fragments in zone (4).

The dark-blue primary fluorapatite in zones (4), (5), (6) and (8) is locally altered. It shows a sequence of colour changes, from the relics of the primary phase outwards, to dull pale-blue, matt bluish-grey, brownish-beige and rusty brown in the outermost parts.

Representative compositions of the principal varieties of apatite are shown in Table

Table 11. Representative compositions of oxide minerals

	1	2	3	4	5	6	7	8	9	10	11	12	13	14	15
Li <sub>2</sub> O *	0.00	0.08	0.08	1.21	----	----	----	----	----	----	----	----	----	----	----
Na <sub>2</sub> O	----	----	----	----	----	----	----	----	4.13	1.30	2.18	----	1.88	----	----
K <sub>2</sub> O	----	----	----	----	----	----	----	----	----	----	0.03	----	2.84	----	----
Cs <sub>2</sub> O	----	----	----	----	----	----	----	----	0.01	0.00	5.27	----	----	----	----
CaO	0.08	----	0.00	0.00	0.00	----	----	----	8.96	6.79	0.58	----	0.00	----	1.60
MnO	10.64	4.43	9.00	4.91	13.33	2.06	0.33	0.04	0.24	0.48	----	----	----	2.65	----
FeO	0.00	6.91	2.98	0.00	2.45	12.04	0.49	5.14	0.34	1.58	----	----	0.00	45.14	----
SnO	----	----	----	----	----	----	----	----	0.77	0.32	0.05	----	----	----	----
PbO	----	----	----	----	----	----	----	----	0.50	2.79	6.67	----	----	----	15.40
Al <sub>2</sub> O <sub>3</sub>	----	----	----	----	----	----	----	----	----	----	----	22.95	1.45	----	----
Sc <sub>2</sub> O <sub>3</sub>	0.00	----	----	0.00	0.38	0.06	0.07	0.09	----	----	----	----	----	----	----
Fe <sub>2</sub> O <sub>3</sub> *	1.16	1.58	0.15	0.27	----	----	----	1.40	----	----	----	0.00	----	----	----
Sb <sub>2</sub> O <sub>3</sub>	----	----	----	----	----	----	----	----	1.16	0.65	9.07	----	----	----	----
Bi <sub>2</sub> O <sub>3</sub>	----	----	----	----	----	----	----	----	----	----	0.80	----	----	----	----
TiO <sub>2</sub>	0.24	4.57	9.21	0.00	1.46	0.17	0.26	59.40	1.16	0.99	----	0.00	----	52.10	----
ZrO <sub>2</sub>	0.00	----	----	0.00	0.12	----	----	----	----	----	----	----	----	----	----
SnO <sub>2</sub>	16.66	9.32	7.41	3.42	0.62	0.67	93.36	1.18	----	----	----	1.20	----	0.00	----
UO <sub>2</sub>	----	----	----	----	0.03	----	----	----	1.47	10.54	----	----	----	----	79.80
Nb <sub>2</sub> O <sub>5</sub>	2.49	8.61	11.11	4.81	21.87	1.50	0.25	4.29	3.64	1.54	0.97	0.85	1.57	0.00	0.00
Ta <sub>2</sub> O <sub>5</sub>	68.42	63.67	59.89	85.00	58.61	83.45	5.67	28.90	73.41	64.11	71.55	72.25	88.38	0.00	2.10
WO <sub>3</sub>	0.00	----	----	0.00	0.16	0.00	----	----	0.02	0.00	----	----	----	----	----
H <sub>2</sub> O *	----	----	----	----	----	----	----	----	----	----	----	1.02	----	----	----
F	----	----	----	----	----	----	----	----	2.55	1.08	----	0.00	0.00	----	----
O=F	----	----	----	----	----	----	----	----	-1.07	-0.45	----	----	----	----	----
	99.69	99.16	99.84	99.61	99.03	99.95	100.43	100.44	97.29	91.72	97.17	98.27	96.12	99.90	98.90
<i>Atoms per formula unit</i>															
Li	0.00	0.13	0.12	2.13	----	----	----	----	----	----	----	----	----	----	----
Na	----	----	----	----	----	----	----	----	0.712	0.267	0.425	----	0.551	----	----
K	----	----	----	----	----	----	----	----	----	----	0.004	----	0.548	----	----
Cs	----	----	----	----	----	----	----	----	0.000	0.000	0.226	----	----	----	----
Ca	0.04	----	0.00	0.00	0.00	----	----	----	0.854	0.771	0.062	----	0.000	----	0.080
Mn	3.93	1.52	2.92	1.83	3.33	0.59	0.014	0.001	0.018	0.043	----	----	----	0.057	----
Fe <sup>2+</sup>	0.00	2.35	0.95	0.00	0.61	3.40	0.021	0.142	0.025	0.140	----	----	----	0.957	----
Sn <sup>2+</sup>	----	----	----	----	----	----	----	----	0.031	0.015	0.002	----	----	----	----
Pb	----	----	----	----	----	----	----	----	0.012	0.080	0.180	----	----	----	0.194
Al	----	----	----	----	----	----	----	----	----	----	----	3.986	0.258	----	----
Sc	0.00	----	----	0.00	0.10	0.02	0.003	0.003	----	----	----	----	----	----	----
Fe <sup>3+</sup>	0.38	0.48	0.04	0.09	----	----	----	0.035	----	----	----	0.000	----	----	----
Sb	----	----	----	----	----	----	----	----	0.043	0.028	0.376	----	----	----	----
Bi	----	----	----	----	----	----	----	----	----	----	0.021	----	----	----	----
Ti	0.08	1.40	2.65	0.00	0.32	0.04	0.010	1.479	0.078	0.079	----	0.000	----	0.993	----
Zr	0.00	----	----	0.00	0.02	----	----	----	----	----	----	----	----	----	----
Sn <sup>4+</sup>	2.90	1.51	1.13	0.60	0.07	0.09	1.867	0.016	----	----	----	0.071	----	0.000	----
U	----	----	----	----	0.00	----	----	----	0.029	0.249	----	----	----	----	0.830
Nb	0.49	1.58	1.93	0.96	2.92	0.23	0.006	0.064	0.146	0.074	0.044	0.057	0.107	0.000	0.000
Ta	8.11	7.03	6.24	10.16	4.70	7.66	0.077	0.260	1.776	1.847	1.956	2.895	3.634	0.000	0.027
W	0.00	----	----	0.00	0.01	0.00	----	----	0.000	0.000	----	----	----	----	----
	15.93	16.00	16.00	15.76	12.08	12.03	1.997	2.000	3.724	3.593	3.296	7.008	5.099	2.007	1.131
OH	--	--	--	--	--	--	-	-	----	----	----	1	----	-	-
F	--	--	--	--	--	--	-	-	0.717	0.362	----	0	----	-	-
O	<u>32</u>	<u>32</u>	<u>32</u>	<u>32</u>	<u>24</u>	<u>24</u>	<u>4</u>	<u>4</u>	<u>6.021</u>	<u>6.501</u>	<u>6.167</u>	<u>13</u>	<u>10.29</u>	<u>3</u>	<u>2</u>
	32	32	32	32	24	24	4	4	6.738	6.863	6.167	14	10.29	3	2

1. Wodginite (sample TSE-90).  
 2. Ferrowodginite (TSE-117).  
 3. Titanowodginite (A-25).  
 4. Lithiowodginite (TSE-76).  
 5. Columbite-Tantalite (average).

6. Ferrotapiolite (average).  
 7. Cassiterite (average).  
 8. Rutile (average).  
 9. Microlite (average).  
 10. Uranmicrolite (average).

11. Cesstibantite (average).  
 12. Simpsonite (average).  
 13. Rankamaite-Sosedkoite.  
 14. Ilmenite (average).  
 15. Uraninite (TRT-42).

\* Calc. stoichiometrically, except Li<sub>2</sub>O for analysis (4), measured. "0.00": not detected; "----": not measured.

Table 12. Representative compositions of apatite, lithiophilite and amblygonite-montebbrasite

	Apatite				Lithiophilite			Amblygonite-Montebbrasite			
	1	2	3	4	5	6	7	8	9	10	11
Li <sub>2</sub> O	----	----	0.16	0.05	9.02	9.30	9.08	9.90	10.29	9.90	9.52
Na <sub>2</sub> O	0.12	0.12	0.72	0.59	0.13	0.01	0.00	0.047	0.044	0.015	0.139
K <sub>2</sub> O	0.030	0.058	0.011	0.011	0.02	0.01	0.00	0.004	----	0.004	0.005
CaO	54.61	52.33	52.78	54.94	1.51	0.68	0.81	0.132	0.074	0.030	0.085
SrO	0.094	0.075	0.059	0.42	----	----	----	----	----	----	----
MgO	0.008	0.008	0.022	0.006	1.52	0.01	0.00	0.002	0.002	0.002	0.003
MnO	0.32	2.72	1.00	0.33	22.73	36.89	43.55	----	----	----	----
FeO	0.051	0.078	0.03	0.021	18.56	7.31	0.63	----	----	----	----
Al <sub>2</sub> O <sub>3</sub>	0.045	0.074	0.08	0.03	----	----	----	32.86	34.86	34.46	35.10
Fe <sub>2</sub> O <sub>3</sub>	----	----	----	----	----	----	----	----	0.028	----	----
RE <sub>2</sub> O <sub>3</sub>	0.091	0.006	0.005	0.007	----	----	----	----	----	----	----
P <sub>2</sub> O <sub>5</sub>	42.25	41.63	39.41	40.89	44.93	44.66	45.25	49.26	49.26	49.26	49.11
CO <sub>2</sub>	0.05	0.10	3.33	1.11	----	----	----	----	----	----	----
F	3.31	3.22	0.09	0.27	----	----	----	6.30	4.51	3.44	1.40
H <sub>2</sub> O <sup>+</sup>	----	----	0.94	1.08	----	----	----	3.21	3.30	4.43	5.25
H <sub>2</sub> O <sup>-</sup>	0.06	0.21	----	----	----	----	----	0.06	0.08	0.05	0.07
Insol.	0.53	0.46	0.17	0.11	1.49	0.61	----	----	----	----	----
O=F	-1.39	-1.36	-0.04	-0.11	----	----	----	-2.65	-1.90	-1.45	-0.59
	<u>100.18</u>	<u>99.74</u>	<u>98.77</u>	<u>99.75</u>	<u>99.91</u>	<u>99.48</u>	<u>99.32</u>	<u>99.12</u>	<u>100.55</u>	<u>100.14</u>	<u>100.09</u>
<i>Atoms per formula unit</i>											
Li	----	----	0.108	0.034	3.818	3.954	3.836	1.960	2.019	1.939	1.867
Na	0.039	0.040	0.235	0.193	0.027	0.002	0.000	0.004	0.004	0.001	0.013
K	0.006	0.013	0.002	0.002	0.003	0.001	0.000	0.000	----	0.000	0.000
Ca	9.882	9.575	9.520	9.954	0.170	0.077	0.091	0.007	0.001	0.002	0.004
Sr	0.009	0.007	0.006	0.041	----	----	----	----	----	----	----
Mg	0.002	0.002	0.006	0.002	0.238	0.002	0.000	0.000	0.005	0.000	0.000
Mn	0.046	0.393	0.143	0.047	2.026	3.303	3.875	----	----	----	----
Fe <sup>2+</sup>	0.007	0.011	0.004	0.003	1.634	0.646	0.055	----	----	----	----
Al	0.009	0.015	0.016	0.006	----	----	----	1.907	2.005	1.978	2.017
Fe <sup>3+</sup>	----	----	----	----	----	----	----	----	0.001	----	----
RE	0.006	0.000	0.000	0.000	----	----	----	----	----	----	----
P	6.041	6.018	5.617	5.854	4.003	3.997	4.024	2.053	2.035	2.031	2.027
C	<u>0.012</u>	<u>0.023</u>	<u>0.765</u>	<u>0.256</u>	----	----	----	----	----	----	----
	<u>16.059</u>	<u>16.098</u>	<u>16.422</u>	<u>16.393</u>	<u>11.919</u>	<u>11.983</u>	<u>11.882</u>	<u>5.932</u>	<u>6.071</u>	<u>5.951</u>	<u>5.929</u>
F	1.768	1.739	0.048	0.144	--	--	--	0.981	0.696	0.530	0.216
OH	----	----	1.056	1.218	--	--	--	1.054	1.074	1.439	1.708
O	<u>24.232</u>	<u>24.261</u>	<u>24.896</u>	<u>24.638</u>	<u>16</u>	<u>16</u>	<u>16</u>	<u>7.965</u>	<u>8.230</u>	<u>8.031</u>	<u>8.076</u>
	26	26	26	26	16	16	16	10	10	10	10

1. BLM-508: pale greenish, zone (3).

2. AP-11: dark blue, zone (8).

3. AP-16: dark brown in leaching cavities, zone (5).

4. AP-31: beige crusts, zone (4).

5. TRT-2: grey at wallrock contact, zone (1).

6. TRT-14: pale brown, zone (5).

7. TRT-61: orange-pink, zone (5).

8. A-29: white, zone (5).

9. A-5: pink, zone (5).

10. A-98: yellow, zone (4).

11. A-22: secondary brownish, zone (4).

\*----\*: not measured. Formula contents calculated assuming all RE as Ce. Unpublished data of P. Povondra (apatite) and A.-M. Fransolet (lithiophilite); amblygonite-montebbrasite by P. Povondra, from Černá *et al.* (1972).

12. The green and dark-blue primary fluorapatite contains up to 5.6 wt.% MnO, and corresponds to a virtually pure fluorapatite. The secondary varieties are less manganiferous but tend to be enriched in Sr, and some of them contain low concentrations of Cl, but they correspond to carbonate-hydroxylapatite in their bulk composition. The contents of radiogenic Sr and Pb also are high in the secondary apatite (unpublished data of P. Černý and B.J. Fryer). The colour changes featured by the altered primary

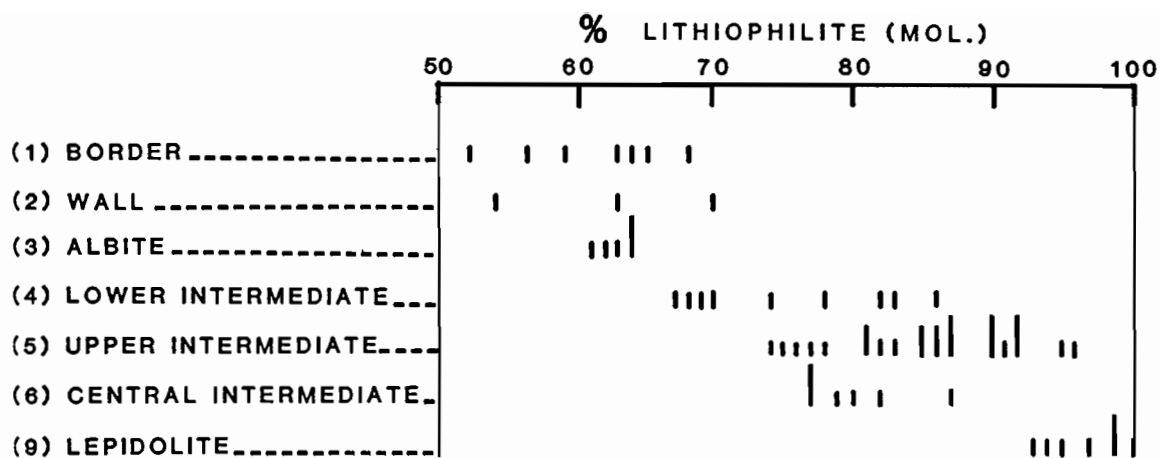


Figure 17. Compositional trend of lithiophilite in the zonal sequence (unpublished data of A.-M. Fransolet, P. Černý and F.C. Hawthorne).

fluorapatite are accompanied by modest increases in Sr, Cl, H<sub>2</sub>O and CO<sub>3</sub>, and loss of F (unpublished data of P. Povondra and P. Černý).

#### Lithiophilite

Mn-dominant members of the triphylite-lithiophilite series are found throughout the zones (1) to (6), and in the lepidolite zone (9). Subhedral crystals are very rare, coarse-grained aggregates and single-crystal blocks attaining up to 40 cm in size are standard. Dark-grey lithiophilite rims biotitized xenoliths of amphibolite in zone (1). In zones (2) to (5), the colour progresses from medium brown to pale orange, but pale brown to greenish beige is typically encountered in zone (6). Pale orange is again characteristic of lithiophilite in zone (9). The main concentration of this phosphate is found in zone (5).

The grey to brown varieties of the two outermost zones are relatively Fe-rich, and also show the highest contents of Mg (Table 12, Figure 17). The average Mn content then increases in the inward zonal sequence, at the expense of Fe and Mg; the latter is virtually absent in Mn-rich lithiophilite, which also shows Fe below the detection limit of electron microprobe in zone (9) (unpublished data of A.-M. Fransolet, F.C. Hawthorne and P. Černý).

#### Amblygonite-montebbrasite

Members of this series occur with increasing abundance in the zonal sequence (2), (3), (4) and (5), and are scarce in zone (9). Primary amblygonite-montebbrasite is predominantly coarse-grained to blocky; individual crystals (which commonly show polysynthetic lamellar twinning) attain a maximum size of 1.5 m in zone (5). However, amblygonite-montebbrasite of zones (3) and (9) is thin tabular (1-3 cm) in skeletal or dendritic-like aggregates imbedded in the respective albitic and lepidolite matrices.

The blocky crystals of zone (4) and (5) display a set of different colours, correlatable with the crystallization sequence and decreasing F content. From the earliest to the latest phase, the colour changes from pink to white to yellow, and the average F content

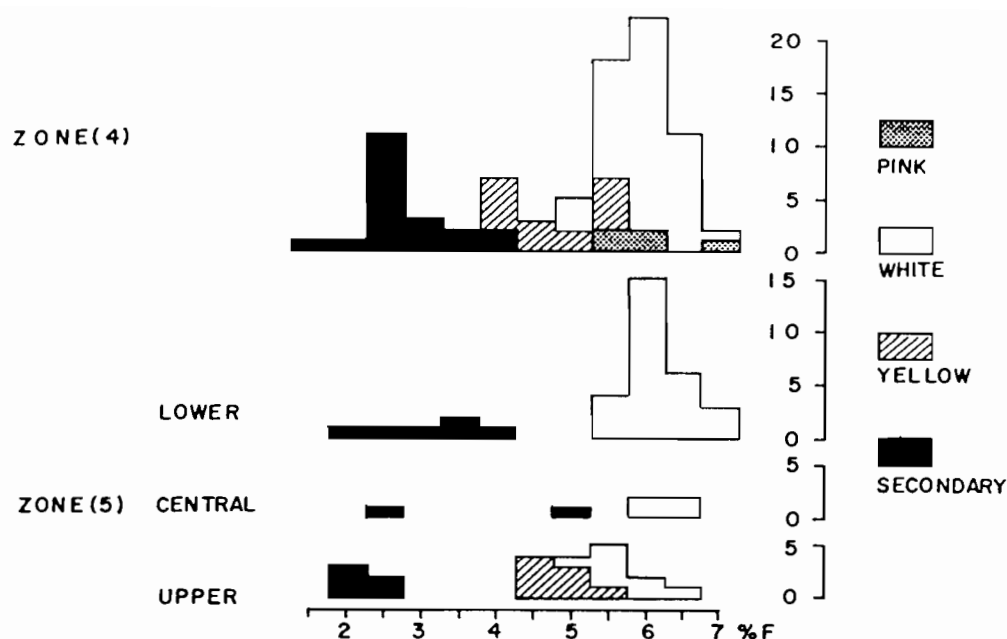


Figure 18. The F content and colour of primary amblygonite-montebrasite and secondary montebrasite in the zones with maximal accumulation of these minerals (from Černá et al. 1972).

decreases from ~6.5 to 5.75 to 4.5 wt.%, respectively (Figure 18 and Table 12; Černá et al. 1972; see also Groat et al. 1990). The skeletal aggregates of platy amblygonite from zones (3) and (9) are F- rich, with 6 - 8.5 wt.% F. Other miscellaneous varieties are rarely found associated with cleavelandite, very F-poor but enriched in Na, K and Ca.

All of the above types of primary amblygonite-montebrasite were subject to late alteration into secondary montebrasite, which averages at 3 to 4 wt.% F less than the parent primary phase (Table 12 and Figure 18; Černá et al. 1972). The secondary montebrasite forms along the margins of the primary grains, and along fractures and twinning boundaries as grey, beige, greenish or brownish diffuse streaks, apparently by anion exchange without recrystallization of the primary textures.

Amblygonite-montebrasite of all generations also is subject to alteration along its contacts with silicates; mixtures of apatite and muscovite are the most common product, rarely pure apatite.

#### Lithiophosphate

This mineral is found in parts of zones (4) and (5) that were subject to widespread low-temperature alteration and consequently also carry leaching cavities with cesian analcime and associated phases. Lithiophosphate was considered a member of this association, based on the first few specimens found before 1971 (Černý 1972b). However, numerous finds in the eighties indicated that lithiophosphate is an alteration product after rounded blebs of amblygonite-montebrasite enclosed in squi. Its grains attain maximum size of 15 cm. Their good cleavages and milky white colour make them difficult to distinguish from spodumene; however, widespread alteration into pink-purplish fibrous apatite and conspicuous surficial leaching after exposure to atmospheric moisture on dumps greatly aid in its identification in hand specimen.

### Minor secondary phosphates

Ramik et al. (1980) described *tancoite* as a new mineral species from white coatings of microscopic crystals (up to 1 mm) on altered lithiophosphate and pink secondary apatite. It was accompanied by a hydrated sodium phosphate, defined more or less concurrently as a new species *dorfmanite* by Kapustin et al. (1980) from Kola Peninsula. R.A.Ramik (pers.comm. 1983) also identified *whitlockite*, *crandallite*, *overite* and *fairfieldite* from altered amblygonite-montebrazite (cf. also Groat et al. 1990 for *crandallite*). *Alluaudite* was found as an extremely rare alteration product of lithiophilite (unpublished data of A.-M. Fransolet).

### Diomignite

This natural form of lithium tetraborate was described as a new mineral from Tanco, the first species ever characterized from fluid inclusions (London et al. 1987). It occurs in euhedral crystals  $\leq 30 \mu\text{m}$  in size, associated with albite, cookeite, quartz, analcime-pollucite, microlite and carbonate in fluid inclusions in spodumene of the squi intergrowths, and possibly also in their petalite precursor. London et al. considered this phase quite widespread but Anderson (1993) questioned this claim, suspecting misidentification of abundant zabuyelite.

Table 13. Sulfide mineral assemblages.

Mode of occurrence	Assemblage # in zones (4) and (5)		Assemblage # in zones (3) and (6)		
Contacts with amphibolite xenoliths	-	-	(6,3A)	arsenopyrite pyrrhotite chalcopyrite	
Dispersed isolated grains	(4,5A) (4,5B)	sphalerite molybdenite	(6,3B)	sphalerite	
Cavity- and fissure- filling aggregates	(4,5C)	bismuthian antimony antimonian bismuth bismuthian stibarsen arsenic galena sphalerite chalcopyrite tetrahedrite dyscrasite	(6,3C)	bismuth bismuthian antimony pyrrhotite sphalerite hawleyite pyrite arsenopyrite cubanite chalcopyrite galena	stannite kesterite černýite cosalite gustavite gladite-pekoite tetrahedrite freibergite bournonite pyrargyrite miargyrite
Miarolitic cavities	-	-	(6,3D)	pyrite marcasite	

### Native elements, alloys, sulfides and sulfosalts

Minerals which belong to the above systematic categories are extremely numerous in the Tanco pegmatite in terms of the number of species (collectively surpassing the silicates) but their abundances are largely negligible. Nevertheless, their paragenetic and

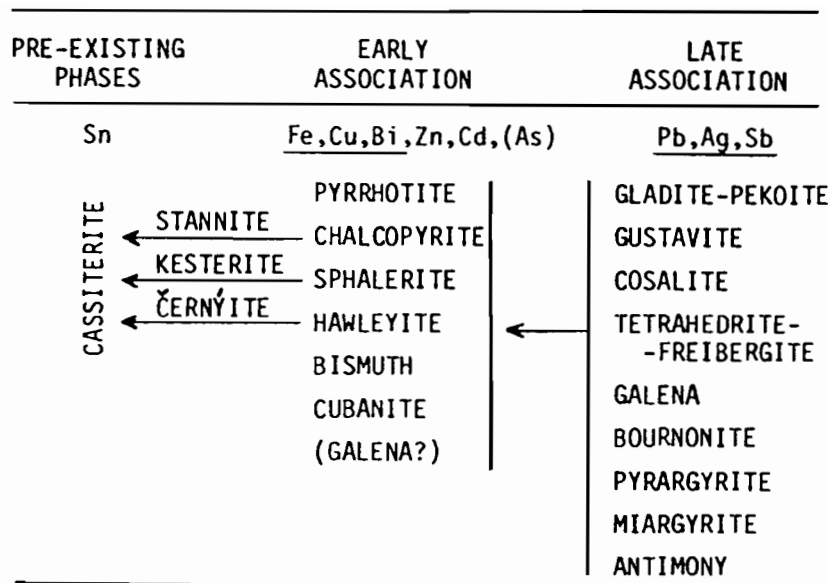


Figure 19. Probable evolution of sulfides and sulfosalts of the assemblage (6,3C) (from Černý & Harris 1978).

compositional features are quite remarkable.

The distribution of the mineral species in different assemblages of diverse pegmatite zones is summarized in Table 13, modified from Černý & Harris (1978). Arsenopyrite from the exocontacts is the most commonly found sulphide, followed in relative frequency of encounters by the dispersed grains of sphalerite and clusters of molybdenite. All the other assemblages are rather rare. Genetically, the most interesting assemblage is (6,3D), with two associations of distinctly different bulk chemistry and mineralogy: the first originated in part at the expense of cassiterite, the second by reaction of newly introduced metals with the first (Figure 19).

Noteworthy among these minerals are the composition of Cd-rich sphalerite and the presence of hawleyite *per se*, the Fe-, Zn- and Cd-dominant members of the stannite group, freibergite with up to 32 wt.% Ag, the exsolution intergrowths of gladite and pekoite, and the high TI content of the late sprinkling of pyrite and marcasite on crystals lining miarolitic cavities ( $\leq 900$  ppm; unpublished data of P. černý). The paper by Černý & Harris (1978) provides additional information on all the minerals listed in Table 13, including chemical composition of most of them.

#### Carbonate minerals

*Rhodochrosite* is frequently encountered in zone (5), as late filling of interstices between spodumene blades or in a quasi-graphic intergrowth with lithiophilite. Its reddish-pink colour is commonly tarnished by brownish oxidation products. It is locally replaced, on microscopic scale, by slightly manganoan calcite.

*Calcite* forms crystals of diverse morphologies in miarolitic cavities of zone (6), occasionally coated by pyrite and/or marcasite.

*Dolomite* was found so far only twice, as whitish microcrystalline masses with albite of zone (6). It may be, however, more widespread because it is very difficult to spot in this

Table 14. Representative compositions of carbonates.

	Calcite			Rhodochrosite			Dolomite	
	A-19B2	H-2	H-3B	A-19B1	H-3A	H-5	H-6	A-19A
CaO	51.31	55.13	49.93	0.32	0.21	0.14	1.09	30.55
MnO	4.43	1.13	7.71	57.06	55.98	55.56	59.08	7.88
FeO	0.00	0.00	0.00	4.30	5.53	6.04	1.27	5.25
MgO	0.88	0.00	0.00	0.00	0.00	0.00	0.00	10.89
CO <sub>2</sub>	43.93	43.97	43.94	38.25	38.25	38.25	38.25	43.93
	100.55	100.23	101.58	99.93	99.97	99.99	99.69	98.50
Atoms per two formula units								
Ca	1.833	1.968	1.783	0.013	0.009	0.006	0.045	1.091
Mn <sup>2+</sup>	0.125	0.032	0.218	1.851	1.816	1.802	1.916	0.223
Fe <sup>2+</sup>	0.00	0.00	0.00	0.138	0.177	0.193	0.041	0.146
Mg	0.044	0.00	0.00	0.00	0.00	0.00	0.00	0.541
C	1.999	2.000	1.999	1.999	1.999	1.999	1.999	1.999
	4.001	4.000	4.001	4.001	4.001	4.001	4.001	4.001

CO<sub>2</sub> contents calculated

Unpublished electron microprobe data of M. A. Wise

association.

The chemistry of the carbonates mentioned above is summarized in Table 14 (unpublished data of M.A. Wise). The composition of calcite is close to ideal, whereas rhodochrosite contains 5 - 20 mole % of the siderite component and dolomite shows substantial proportions of ankerite and particularly kutnahorite end-members.

Anderson (1994) described recently the lithium carbonate *zabuyelite* as a common solid constituent of fluid inclusions in spodumene.

Barite

Barite was identified as only a single mm-size crystal associated with secondary phosphates formed at the expense of lithiophosphate (Ramik et al. 1980; R.A. Ramik, pers. comm. 1980).

## Geochemistry

Bulk composition

Mineralogy of the Tanco pegmatite indicates that it belongs to the petalite subtype of the complex type, in the rare-element pegmatite class. However, the proportions of lepidolite and amblygonite (and to a degree of primary spodumene), which define subtypes of their own if dominant, are relatively high. This is a feature characteristic of most of the highly mineralized large pegmatite deposits in general (such as those at Varuträsk,

Table 15. Bulk composition of rare-element pegmatites.

	2	3	4	5	6
	Siberia USSR	Harding NM	Tanco MB	Pidlite NM	INCO MB
SiO <sub>2</sub>	70.62	75.24	69.74	74.5	73.70
TiO <sub>2</sub>	0.04	0.05	0.01	-	0.01
Al <sub>2</sub> O <sub>3</sub>	17.69	14.42	16.50	14.8	16.53
Fe <sub>2</sub> O <sub>3</sub>	0.60				0.18
FeO	0.20	0.65*	0.18*	-	0.08
MnO	0.03	0.18	0.21	-	0.16
MgO	0.28	0.01	-	-	0.05
CaO	0.65	0.20	0.89	0.2	0.13
Li <sub>2</sub> O	1.05	0.65	1.18	0.7	1.41
Na <sub>2</sub> O	4.84	4.23	2.69	3.3	3.78
K <sub>2</sub> O	1.95	2.74	4.42	5.4	1.73
Rb <sub>2</sub> O	0.21	0.19	1.10	-	0.36
Cs <sub>2</sub> O	1.31	0.05	0.42	-	0.03
P <sub>2</sub> O <sub>5</sub>	0.90	0.13	1.18	-	<0.01
B <sub>2</sub> O <sub>3</sub>	-	-	0.24	-	-
F	0.65	0.64	0.20	0.9	-
H <sub>2</sub> O*	0.75	-	-	0.6	0.10
total	101.77	99.38	98.96	100.4	98.33
-F+O <sub>2</sub>	-0.28	-0.27	-0.08	-0.4	-
Σ	101.49	99.11	98.88	100.00	98.33

\*total Fe as FeO, - not determined

2: Spodumene-subtype of complex pegmatite with pollucite

3: Spodumene-subtype of complex pegmatite

5: Lepidolite-subtype of complex pegmatite

6: Albite-spodumene type of pegmatite

From Černý (1991, Table 5)

Sweden; Bikita, Zimbabwe; Greenbushes, Australia and elsewhere; cf. Solodov 1971). It indicates a substantial role of volatile components which affect the liquidus and solidus temperatures, influence the course of melt consolidation, and may play a significant role in transport and deposition of rare metals. Nevertheless, the contents of rare elements indicated by the conspicuous volumes of their minerals commonly are rather low in these bodies, which tend to be granitic in their overall make-up (Černý 1991a).

Morgan & London (1987) made the first attempt to calculate the bulk composition of the Tanco pegmatite. The results are shown in Table 15, in comparison with some other pegmatite bodies of similar compositional complexity from the literature. Generally, the

Tanco composition conforms to the expectation of a peraluminous granitic chemistry but with elevated contents of rare alkalis, boron and phosphorus. This calculation is based on a broad east-west section which does not encompass most of the outer zones in the southern and northern parts of the pegmatite. This, and the somewhat irregular distribution of quartz bodies of zone (7), may explain the low silica plus high alumina and potash contents relative to the other pegmatites shown in Table 15. The bulk composition of Tanco is currently being reexamined by A. Stilling (M.Sc. thesis project).

The limited set of geochemical indicators available from the bulk composition quoted in Table 15 shows a very high degree of fractionation attained by the Tanco pegmatite as a whole:  $K/Rb = 3.6$ ,  $K/Cs = 2.9$ ,  $Rb/Cs = 2.5$ , and  $Fe/Mn = 0.82$ . As the value for  $Rb_2O$  seems to be somewhat high, compared to the mineral compositions shown in Tables 4 and 5, the  $K/Rb$  and  $Rb/Cs$  ratios may be slightly low and high, respectively. Nevertheless, the general range of these ratios should be reasonable.

It must be kept in mind that the bulk composition of the pegmatite, as it is estimated today and as it will be refined in the future, does not represent the composition of its parent melt. During the consolidation of the Tanco pegmatite, extensive loss of volatile components and some highly mobile elements took place, particularly of K, Na, Li, Rb, Cs,  $H_2O$ ,  $CO_2$ , F and B; quantitative considerations are given in Morgan & London (1987).

#### Internal geochemical evolution

The great abundance of rare elements and the high degree of fractionation attained by the bulk of the pegmatite are combined with steep gradients in abundances of these elements across the pegmatite, and in correspondingly steep gradients in their fractionation ratios. Tables 4, 5, 7, 8, 11 and 12, and Figures 11, 12, 13, 14, 16 and 17 were introduced earlier to document the chemistry of individual minerals but they also illustrate the evolution of mineral chemistry during the pegmatite evolution. Table 16 summarizes the ranges of contents and ratios of elements resulting from fractionation processes covering the whole history of pegmatite solidification (limited, of course, for some minerals by restrictions of their zonal distribution).

Potassium feldspar shows rapid evolution in zone (2) and (4) but with an extensive overlap in zones (5) and (6) in terms of  $K/Rb$  and  $K/Cs$  but a rather smooth and steady fractionation of  $Rb/Tl$  throughout the whole range (Tables 4 and 16, Figure 11).

The relationship is very similar in the mica group, except a sharp deviation in the Li-poor zone (6), where the muscovite approximates the fractionation values of the associated K-feldspar (Tables 5 and 16, Figure 11 and 12).

Tourmaline starts crystallizing as dravite-uvite in exocontacts and dravite-schorl in endocontacts, but the limited quantities of this mineral precipitated in the internal zones grade from schorl to a near-end-member elbaite composition (Table 7, Figure 13).

Beryl seems to be slightly affected by contamination from wallrocks in the Fe-bearing greenish crystals of zones (1) and (2), but rapidly evolves afterwards with increasing alkali contents, particularly Cs. Its compositions largely overlap in this respect in zones (4), (5), (6) and (9) (Table 8, Figure 14).

Extensive geochemical evolution is exhibited by the oxide minerals of Nb and Ta. In terms of their typical fractionation indicators, zones (2) and (3) are less fractionated than zones (4), (5), (8) and (9), which are in turn less fractionated than zone (6) (Figure 16, Table 16). However, columbite-group minerals (including ferrotapiolite), and possibly also those of the wodjonite group, display a late-stage reversal of the normal fractionation trend

Table 16. Geochemically significant trace elements and fractionation ratios in minerals.

	Rb	Cs	Tl	Ga	K/Rb	K/Cs	Rb/Cs	Rb/Tl	Al/Ga	Fe/Mn	Nb/Ta	Zr/Hf	Zn/Cd
K-feldspar	0.59-3.30	0.02-0.29	60-322	31-116	16.3-4.0	508-42	37-6	188-54	3300-900				
adularia I	bdl	bdl											
adularia II	~0-14	~0.0-0.7			2.21-0.52	2.30-22	104-26						
albite				39-123					2570-828				
muscovite	1.3-2.1	0.09-0.23	80-125	528-800	6.7-3.7	80-34	18.6-5.9	210-141	370-270				
lithian muscovite	2.2-2.8	0.21-0.39	131-160	392-580	3.7-2.6	30-18	9.9-7.0	202-148	415-300				
"lepidolite"	2.7-3.8	0.48-0.83	200-300	380-383	2.7-1.9	15-10	5.8-4.2	176-92	465-240				
pollucite			47-169	51-64				82-63	1740-1387				
spodumene				69-107					2284-1384				
petalite				45-64					1880-1380				
amblygonite				42-84									
benyl			1-7	58-125				310-103	1400-870				
tourmaline				364-415					500-430	~1000-0.044			
lithiophilite				8-27						0.98-0.00X			
ilmenite										3.45			
columbite-tantalite				295-325						1.61-0	1.465-0.004		
ferrotapiolite										13.37-3.20	0.035-0.004		
wodginite group										2.98-0	0.352-0.011		
microlite group											0.352-0		
zircon												6-4.5	
sphalerite													41.0-2.5
hawleyite													0.7
černýite													0.7

bdl - below detection limit of electron microprobe.

adularia I - in leaching cavities

adularia II - after pollucite

Unpublished data of P. Černý, T. S. Ercit, A.M. Franolet, F. C. Hawthorne, J. Selway and D. K. Teertstra, except spodumene and petalite (Černý & London 1983) and sulfides (Černý & Harris 1978).

of increasing Mn at the expense of Fe (Figure 16a). The oxide minerals also show distinct trace- to minor-element trends not recorded in Figure 16: Ti and Sc consistently behave as compatible elements. Furthermore, columbite-tantalite and the wodginite minerals of the less fractionated outer zones of the pegmatite exhibit lesser degrees of cation ordering than those of the more fractionated inner zones.

Lithiophilite shows low Mg contents in the outermost zones. Otherwise, it is characterized by progressive fractionation of Mn from Fe throughout its crystallization history, comparable with the fractionation trends in most minerals and element pairs, notably the oxide minerals of Nb and Ta (Tables 12 and 16, Figure 17).

Gradual increase in the activity of Li is documented by its increasing involvement in the mica evolution, and in the onset of massive crystallization of petalite, spodumene and amblygonite in the inner zones. The conspicuous lack of Li-bearing minerals in the central intermediate zone (6) is analogous to that displayed by similar K-feldspar-rich central zones of complex spodumene- and petalite-subtype pegmatites such as Mongolian Altai # 3 (e.g., Beus 1960). The crystallization of primary petalite vs. primary spodumene is a function of pressure regime (London 1984). The crystallization of these anhydrous Li-aluminosilicates vs. amblygonite vs. lepidolite is controlled by the relative chemical potentials of  $\text{PFO}_2$ , HF, LiF and KF (Burt & London 1982, London 1982).

Precipitation of highly incompatible Cs is modest in K-feldspar and micas, and is triggered on massive scale only in the late bodies of pollucite of zone (8), genetically linked to the concluding stages of consolidation of the upper intermediate zone (5).

A high degree of fractionation is indicated even by the sulphides. The Zn/Cd ratio in sphalerite is very low, rarely encountered in other environments, and grades into the Cd-dominant hawleyite. A similar trend is shown by the members of the stannite group by the presence of Cd-dominant černýite (Table 16; Kissin et al. 1978).

In contrast to all of the above features of the Tanco pegmatite which document extensive geochemical evolution of the consolidating magma, three pairs of elements show highly independent behaviour.

The Rb/Tl ratio shows some but very limited fractionation in K-feldspar and the micas, but as a whole it does not exceed the limits established for crustal rocks in general (Figure 20). The only exception are some samples of pollucite which are invariably the most Tl-enriched of all Rb,Tl-bearing pegmatite minerals (e.g., Černý 1988).

The Al/Ga ratio is highly variable among different minerals but relatively stable within a single mineral phase (Figure 20). This is best illustrated by the micas which show the ranges of Al/Si for different mica types largely overlapping, despite the otherwise enormous differences in their rare-alkali contents and overall chemistries. The controlling factor here is not so much a possible evolution of the parent medium but crystal-chemical characteristics of the individual minerals (Černý & Hawthorne 1989).

The Zr/Hf ratio is virtually constant in hafnian zircon from different zones, as far as it can be established in partially metamict and disturbed crystals (Table 9). This is in marked contrast with strongly zoned compositions of zircon crystals from some other pegmatites, and with much more advanced Zr-Hf fractionation established in pegmatites of much lower overall degree of geochemical evolution (Černý et al. 1985).

### Petrology

The Tanco pegmatite became a testing ground for interpretation of the internal evolution of complex pegmatites since the early nineteen eighties, because of its good

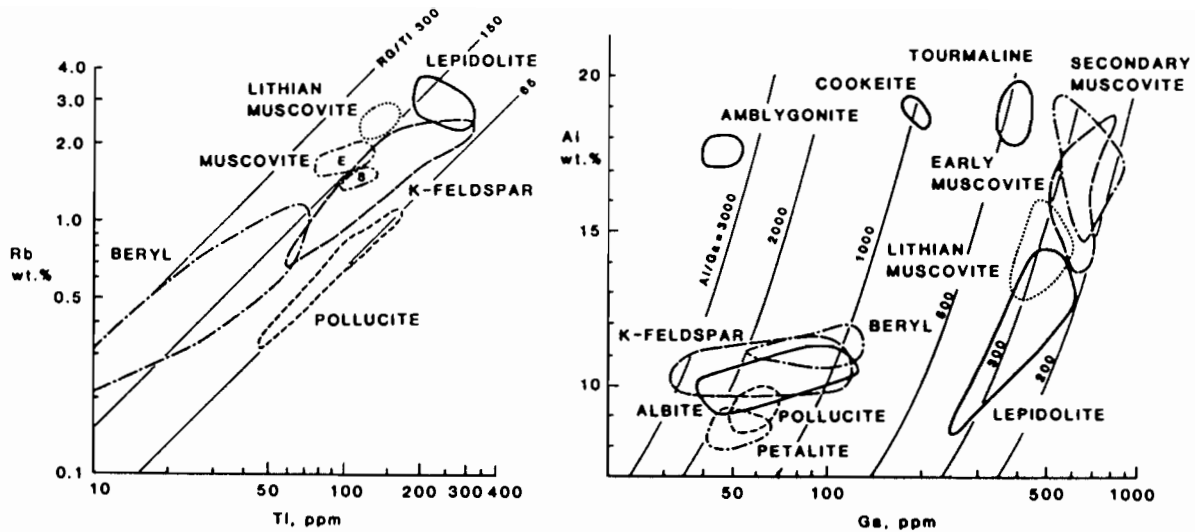


Figure 20. The Rb - Tl and Al - Ga contents and ratios in the main minerals carrying these elements, from Černý (1982; based on unpublished data); The Rb and Tl contents of beryl are multiplied 10x to fit into the diagram.

underground exposure, detailed 3d documentation, mineralogical studies and very low intensity of low-temperature hydrothermal as well as supergene alteration. Two schools of thought have developed over the past 15 years which partly coincide in their interpretations but also differ in several fundamental respects. Thomas and associates (Thomas & Spooner 1988 a,b, Thomas et al. 1988, 1990) favour the classic model of Jahns & Burnham (1969), which claims crystallization from coexisting melt and fluid throughout the evolution of the pegmatite. In contrast, London (1986 a,b; 1992) developed a new model of his own, followed by his consocii; it claims crystallization from a highly hydrous but homogeneous melt during most of the pegmatite consolidation, with exsolution of a coexisting fluid only in late stages.

#### Intrusive and solidification style

Brisbin & Trueman (1982) and Brisbin (1986) documented the forcible manner of intrusion of the melt, which consolidated as the Tanco pegmatite, into an environment of rigid host rocks.

The course of internal solidification was initially interpreted as a concentric, inward-oriented process for several primary zones, overprinted by metasomatism generating albitic, muscovite-rich and lepidolitic assemblages (e.g., Černý 1982). Thomas & Spooner (1984, 1987) first pointed out the lack of replacement features along the margins of the albitic aplite zone (3), and the upward sequence of crystallization in the lower parts of the pegmatite, and other local features.

Textural evidence indicates that the consolidation proceeded in some parts of the pegmatite from the footwall contact through zones (1), (2) and (3) to the quartz bodies (7), in others the zones (1) and (2) were followed by the lower and upper intermediate zones (4) and (5) well into the upper parts of the body. However, a downward trend is indicated in the uppermost parts of zone (5); although transitional into each other in terms of mineral

Table 17. Crystallization history of the Tanco pegmatite.

	Thomas <i>et al.</i> (1988, 90)		London (1986), Morgan & London (1987)			
(1) Border zone	680° C	2.9-2.7 kbar	700-600° C	~ 3 kbar		
(2) Wall zone	600-500	↓	↓	↓		
(4) Lower Intermediate zone	475				600-500	3-2.8
(5) Upper intermediate zone	475				600-500	
(8) Pollucite zone	475				~ 500	~2.5
Pet → Spd + Qz inversion					475	~2.8
(6) Central intermediate zone	~320					
(3) Aplitic zone	316-291				470-420	
(7) Quartz zone	475-265					
(9) Lepidolite zone					~ 450	~2
Spd → Ecr + Qz inversion					~ 275	~1.5

assemblages, zones (4) and (5) apparently crystallized inwards in their footwall and hangingwall segments, forming collectively a shell-like concentric zone. The central intermediate zone (6), lepidolite-zone segments (9) and most of the quartz bodies (7) crystallized within this innermost concentric shell, the upper parts of which contain the pollucite concentrations (8) as their late but integral part.

#### P-T paths of consolidation

Table 17 summarizes the interpretation of pressure and temperature regime of Tanco solidification, based on experimental petrology of Li-aluminosilicates (London 1984, 1986a) and on studies of fluid inclusions (London 1986a, Morgan & London 1987, Thomas & Spooner 1988a,b, Thomas *et al.* 1988, 1990).

Thomas and associates favour a near-isobaric process, whereas London observes a ~ 0.5 kbar decline during the main course of consolidation from the initial pressure of 3 kbar.

Differences in interpretation of primary vs secondary inclusions and other considerations lead the two groups of authors to different interpretations of the thermal regime. Thomas *et al.* see a relatively rapid decrease in temperature already during the main stages of consolidation (680 - ~300°C), extended to quite low levels in the near-final stages (265°C). In contrast, London *et al.* advocate a shorter temperature span for the main stages, including some of the late zones (~700 - 450°C).

#### Melt vs fluid evolution

Thomas & Spooner (1988a) and Thomas *et al.* (1990) interpret the results of their studies as indicative of the presence of coexisting melt and supercritical fluid from the onset of pegmatite crystallization to the very last stages at low temperatures. They claim the persistence of a residual melt phase down to 265°C.

In contrast, London (1986a,b) and London *et al.* (1988, 1989) provide evidence for crystallization from a highly hydrous but generally volatile-undersaturated melt well into the late stages, up to exsolution of a hydrous fluid at the time of tourmaline and Li-

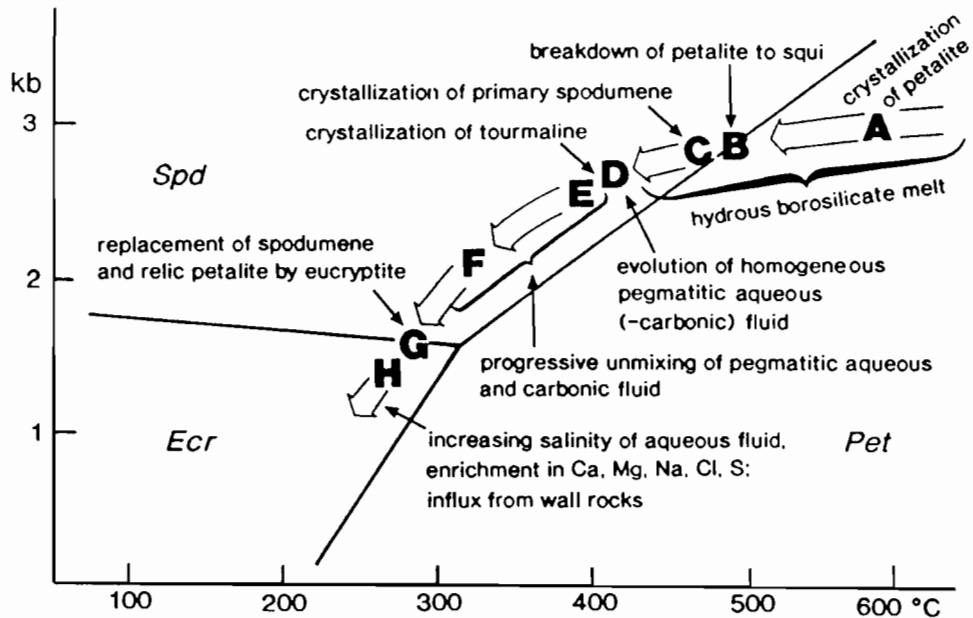


Figure 21. Evolution of the Tanco pegmatite melt, fluids and solid phases, based on stabilities of Li-aluminosilicates and studies of fluid inclusions (modified from London 1986a, 1990).

aluminosilicate consolidation ( $\sim 450^\circ\text{C}$ ). Rapid solidification of the residual melt by a chemical quench at this temperature level concludes magmatic crystallization; further processes are precipitation from supercritical-to-hydrothermal fluids and fluid-induced recrystallization or reequilibration. Figure 21 illustrates the crystallization pathway and changes in the character of the melt and fluid phases with decreasing pressure and temperature.

#### Exomorphism and endomorphism

Morgan & London (1987) distinguished three episodes of metasomatic alteration of the host amphibolitic wallrocks around the Tanco pegmatite. In an apparent sequence from early to late, the first event was B ( $\pm \text{Li}$ ) metasomatism in the form of tourmalinization, followed by (K-Rb-Cs-F ( $\pm \text{Li}$ )) metasomatism expressed by formation of biotite, and by propylitic alteration generating hornblende plus plagioclase, and superimposed epidote, chlorite, titanite, calcite and clay minerals with concomitant influx of Li and  $\text{CO}_2$ . Holmquistite is present in all three assemblages and served as the primary sink for Li, besides the rare-alkali biotite of the second episode. Wallrock metasomatism was preceded by a period of textural recrystallization at the conditions of lower amphibolite facies.

Recrystallization may have been caused by heat loss from the pegmatite, but is more probably an artifact of pre-emplacement metamorphism. The pegmatite-induced metasomatism took place at greenschist-facies conditions ( $\leq 500\text{-}550^\circ\text{C}$ , 3 kbar). Morgan

& London (1987) correlate the tourmalinization with the formation of the albitic aplite zone (3) within the pegmatite. Fluids responsible for the biotitization (at 460-450°C) are reported to have been generated by acidic, F-rich fluids during the late crystallization of zone (3) and consequent sericitization of primary microcline and pollucite. The propylitic alteration, which is the most pervasive type of alteration around Tanco, occurred during the entire duration of wallrock metasomatism but became dominant when the fluids cooled to  $\leq 420^\circ$  C. Morgan & London (1987) provide rough estimates of the losses of mobile components from the pegmatite, based on the composition and abundances of the exomorphic minerals. The loss of H<sub>2</sub>O, CO<sub>2</sub>, B, F and alkalis must have been very extensive.

Endomorphic phenomena inside the pegmatite/wallrock contacts are rather restricted. Mineralogical expression is found in the form of tourmaline in zone (1) and in part also (2), confined to the close vicinity of amphibolite in wallrock or xenoliths. Its composition is variable from dravite to schorl. Negligible amounts of biotite in zone (1) also indicate an influx of mafic components from outside. Otherwise, it is the modest content of Ti and Sc in the Nb,Ta oxide minerals, Ti in tourmaline, and Mg (plus possibly some Fe) in lithiophilite, which are at their highest in the outermost pegmatite zones and fade out rather quickly inwards, that probably reflect slight assimilation of the wallrock components.

#### Internal subsolidus processes

Restricted as they are in their general extent, and occasionally strongly localized in specific parts of the pegmatite, low-temperature processes triggered by reaction of supercritical to hydrothermal fluids are a significant part of the present constitution of the pegmatite.

Exsolution affects K-feldspar (Černý & Macek 1972), petalite breaks down to spodumene + quartz (Stewart 1963,1978, Černý & Ferguson 1972, London 1984, 1986a), and spodumene to eucryptite + quartz (Černý 1972a, London 1984, 1986a). Metastable pollucite (Lagache 1995) gradually exsolves and reequilibrates (unpublished data of D.K. Teertstra).

Secondary minerals form at the expense of primary phases such as K-feldspar (albite, muscovite, lepidolite), phosphates (apatite, tourmaline, alluaudite, lithiophosphate, crandallite, overite, fairfieldite, whitlockite, tancoite, dorfmanite; Černý 1972b, Ramik et al. 1980; unpublished data of R.A. Ramik, M. Novák and P. Černý), Li-aluminosilicates (muscovite, cookeite, adularia, calcite), beryl (calcite, apatite), pollucite (microcline, albite, lepidolite, muscovite, spodumene, adularia, calcite; Černý & Simpson 1978, unpublished data of D.K. Teertstra), and early oxide minerals of Nb and Ta (ferrotapiolite, rankamaite-sosedkoite; Ercit 1986 and unpublished data). "Alpine" assemblages coating fissures and leaching cavities are of hydrothermal origin (albite, adularia, quartz, calcite, cookeite, cesian analcime, montmorillonite-illite, apatite; Černý 1972b), as are the late minerals in miarolitic vugs (apatite, cookeite, marcasite, pyrite). All the native elements, alloys, sulfides and sulfosalts of the internal zones are late hydrothermal features (Černý & Harris 1978).

#### Petrogenesis

The question of derivation of the Tanco pegmatite is part and parcel of the general problem of the genesis of highly mineralized, peraluminous, LCT-family pegmatites of the rare-element class. It has been demonstrated by numerous investigators that this pegmatite category is generated by igneous differentiation of fertile granitic magmas of plutonic dimensions (e.g., Beus 1948, 1960, Ginsburg et al. 1979, Černý 1982a, Shearer

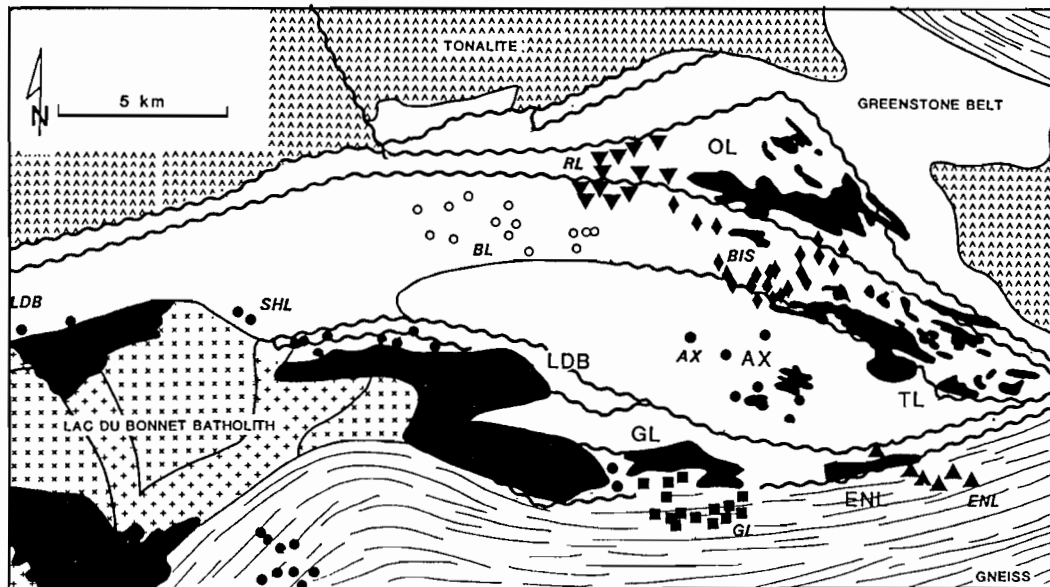


Figure 22. Distribution of cogenetic peraluminous, LCT-family fertile leucogranites and their pegmatite groups in the Winnipeg River district (modified from Černý 1990). Leucogranites: OL - Osis Lake, TL - Tin Lake, AX - Axial, GL - Greer Lake, ENL - Eaglenest Lake intrusions. Pegmatite groups (*italics*): RL - Rush Lake, BIS - Birse Lake, AX - Axial, GL - Greer Lake, ENL - Eaglenest Lake. The SHL (Shatford Lake) pegmatites of the NYF affiliation are related to the Lac du Bonnet batholith.

& Papike 1987, Trumbull 1990, 1991, Breaks & Moore 1992, Mulja et al. 1995, Morteani et al. 1995). Derivation by any other mechanisms meets with extensive petrologic problems, and was not convincingly demonstrated to date by experiment or field-based geochemical research (cf. Černý 1991b, 1992 for discussion).

The Tanco pegmatite is a member of the Bernic Lake pegmatite group in the Winnipeg River district of southeastern Manitoba (Figure 22). This group harbours the most fractionated and largest pegmatites of the whole Cat-Lake - Winnipeg River pegmatite field (Černý et al. 1981, Černý & Lenton 1995). The Bernic Lake group lacks any outcrops of potentially parent granites, as is commonly the case in similar situations elsewhere. Nevertheless, other pegmatite groups of the Winnipeg area, which locally contain pegmatites very similar to Tanco in mineralogy and geochemistry, are genetically connected with intrusions of peraluminous, two-mica to muscovite-garnet leucogranites, in part pegmatitic. Some of the leucogranites contain internal pods identical in texture, mineralogy and geochemistry to the pegmatites in their exterior aureoles (Černý et al. 1981, Goad & Černý 1981).

Thus it is conceivable that the Tanco deposit also belongs to a halo of pegmatites surrounding a fertile granite, and more specifically to the top part of the halo above the parent intrusion. Internal mineralogy and geochemistry of the Tanco pegmatite shows a slight progressive fractionation gradient to the west (Černý et al. 1981, Ercit 1986), whereas the pegmatites in the eastern part of the Bernic Lake group show a distinct eastward trend of intrusion and fractionation (Černý & Lenton 1995). The granite which

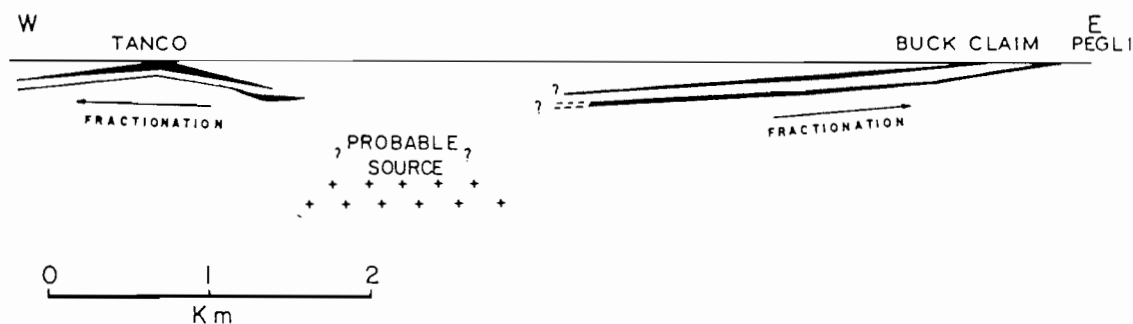


Figure 23. Schematic section through the Bernic Lake pegmatite group, showing the Tanco pegmatite at its western extremity and the Buck and Pegli pegmatites at the eastern termination (from Černý et al. 1981). Trace-element fractionation and paragenetic trends in the east, and the paragenesis and geochemistry of the internal zones of the Tanco deposit in the west suggest the presence of an igneous source between these pegmatites, and probably north of the section plane; the eastern pegmatites dip WNW, and the Tanco pegmatite dips gently northwards.

could have generated the Bernic Lake group could be hidden under its central parts (Figure 23).

#### Economic Aspects

The Tanco deposit, historically also known as Montgary or Chemalloy, is remarkable, and partly unique, in several respects. Among pegmatites of its petrological and geochemical type, the size of this pegmatite is surpassed, to the best of our knowledge, only by the Bikita deposit in Southern Rhodesia (Cooper 1964) and the metamorphosed Greenbushes pegmatite system in western Australia (Hatcher & Bolitho 1982, Bettenay et al. 1988). Another comparable pegmatite of the same type but smaller in size is the Varuträsk locality in Sweden (Quensel 1956).

The Tanco pegmatite contains the largest and highest-grade pollucite concentration known to date, and at present it is one of the largest primary producers of tantalum in the world, and the only significant producer in North America. Its substantial spodumene reserve consists mainly of refractory-grade high-purity material secondary after petalite, available in commercial quantities from only a handful of other localities.

Also, as in all complex pegmatite deposits, the Tanco pegmatite contains a wide variety of rare and trace elements, and industrial minerals as well. These can be utilized only by careful management and specifically tailored processing methods, occasionally with inevitable loss dictated by technical or economic necessities.

#### History of the mine development

In 1929 the property containing the present-day Tanco was acquired by Jack Nutt Tin Mines Ltd., to explore a cassiterite occurrence which outcropped on the north shore of Bernic Lake. The Tanco pegmatite, being completely hidden, was found accidentally during a diamond drilling program carried out by Consolidated Tin Mining Co., Ltd.

During the years 1954-1957, Montgary Exploration Ltd. (Later Chemalloy Minerals

Ltd.) completed 7900 m of diamond drilling and sank a three-compartment shaft to a depth of 93 m. In 1957 the property was optioned to American Metal Co. Ltd.) and an additional 2000 m of drilling was done. From 1959 to 1961 Chemalloy Minerals Ltd. deepened the shaft to 103 m, completed 8800 m of diamond drilling and 1800 m of drifting and raising in the spodumene, pollucite and lepidolite zones. It was during this period that the pollucite bodies were discovered and the abundance of tantalum minerals recognized. In 1962 the mine was allowed to flood and remained flooded until March 1967.

The dewatering, exploration, development, mining and the formation of the Tantalum Mining Corporation of Canada Ltd. was the result of a 1967 joint venture agreement between Chemalloy Minerals Ltd. and Northern Goldfields Investments Ltd., triggered by the demand for tantalum. Within a year, sufficient reserves of ore had been developed for the decision to be reached to construct a 500 ton per day mine/mill complex. Construction progressed rapidly, and operations commenced in 1969. Capacity increases followed and operations continued until the end of 1982, when low prices and poor markets resulted in a suspension of operations.

Attention was once again turned to the lithium reserves. Tanco's lithia reserves are in the form of very iron-poor squi, a contraction of 'spodumene-quartz intergrowths', and as such are suitable for ceramic and speciality glass production. The opportunity was taken to utilize parts of the tantalum plant to 'pilot' spodumene production, and in the spring of 1984 Tanco entered the spodumene business. Two years later, Tanco had constructed a 300 tonne per day dedicated spodumene plant, concomitant with the tantalum mill, which itself returned to full production in the fall of 1988.

The Tanco mine, owned today 100 % by the Cabot Corporation of Boston, Massachusetts, has also produced small-scale shipments of lepidolite (Rb ore), pollucite (Cs ore), amblygonite, quartz and feldspar.

### Resources and reserves

The Tanco deposits contain sizeable quantities of tantalum, lithium, cesium, rubidium, gallium, beryllium and of industrial minerals such as spodumene (plus minor petalite), amblygonite-montebrazite, rubidian K-feldspar, and quartz. Current market conditions dictate the use of spodumene for ceramic applications rather than as a Li ore mineral for lithium carbonate. The reserves of Be are insufficient for profitable recovery. Lepidolite was used as a Rb-ore mineral in the past; however, Rb will become a byproduct of Cs extraction from pollucite, and the lepidolite zone will be exploited for tantalum/mineral concentrates. Utilization of micas as sources of Ga was discontinued.

However, Tanco is engaged not only in exploration for new tantalum deposits in the vicinity of the mine, but is also investigating further diversification in the Industrial Minerals sector. Reject from the spodumene heavy medium plant could, with grinding and minimal upgrading be a first-class source of rubidium-rich feldspar, with applications in the electrical and dinnerware industry. The orebody also contains a high grade quartz 'pod' which was investigated as a source of silicon but found unsuitable.

Table 18 provides a list of preproduction reserves of the most significant commodities.

### Products, specifications and uses

The current product line at Tanco consists of the following:

Tantalum concentrates, 36% Ta<sub>2</sub>O<sub>5</sub>

**Table 18. Preproduction ore and mineral reserves.**

	Tons	Grade
Tantalum	2,071,358	0.216% Ta <sub>2</sub> O <sub>5</sub>
Lithium	7,301,735	2.76% Li <sub>2</sub> O
Cesium	350,000	23.3% Cs <sub>2</sub> O
Beryllium	920,000	0.20% BeO
Lepidolite	107,700	2.24% Li <sub>2</sub> O
Lepidolite	107,700	3% Rb <sub>2</sub> O
Quartz	780,800	-

Spodumene standard concentrate, 7.25% Li<sub>2</sub>O  
 Spodumene -200 mesh concentrate, 7.15% Li<sub>2</sub>O  
 Spodumene "6.8" grade concentrate, 6.8% Li<sub>2</sub>O  
 Spodulite concentrate, 5.0% Li<sub>2</sub>O  
 Montebrasite concentrate, 7% Li<sub>2</sub>O, 8% P<sub>2</sub>O<sub>5</sub>  
 Pollucite ore, 24% Cs<sub>2</sub>O

#### *Tantalum minerals*

Tanco has the capacity to produce 240,000 lbs of tantalum mineral concentrate annually which makes it one of the largest primary producers of tantalum in the world, and the only significant producer in North America. Global tantalum production was badly effected by the recession in the early 1980's, but has since returned to the historical production levels close to 3 million lbs. Tanco is one of the few primary producers of tantalum mineral concentrates without also producing tin concentrates - however, even Tanco's product does contain a subordinate amount of tin.

A typical tantalum concentrate contains the following:

Ta <sub>2</sub> O <sub>5</sub>	35 - 38%
SnO <sub>2</sub>	14 - 18%
Nb <sub>2</sub> O <sub>5</sub>	5 - 8%
TiO <sub>2</sub>	2 - 4%

Much of Tanco's tantalum production is sold under contracts to tantalum processors in West Germany and the United States. This, and other parcels which are available, are packed in 180-200 kg steel drums.

All tantalum minerals are converted to either the metal, or to tantalum compounds.

The major uses for tantalum are in the electronics industry and for cutting tools. High quality capacitors is the major single use for tantalum. In Japan, capacitors account for close to 70% of the total consumption of tantalum, in the form of powder or wire; in the U.S.A., it is closer to 50%, whereas in Europe it is little over 25%.

Europe is the major consumer of tantalum carbide, for the production of hardmetal alloys for cutting tools. Other tantalum alloys are important constituents of aero engines, armour-piercing shells and acid-resistant pipes and tanks used in the chemical industry.

One minor, but important, use of tantalum is in the medical industry, for "spare-part"

Table 19. Typical specifications for Tanco's spodumene-based concentrates.

	Concentrate Type (contents shown in wt. %)				
	Standard	"6.8"	Spodulite	-200 mesh	Montebrasite
Li <sub>2</sub> O	7.25 <sub>+0.1</sub>	6.8 min.	>5.0	7.10 min.	7.0 <sub>+0.25</sub>
Fe <sub>2</sub> O <sub>3</sub>	0.07 max.	0.07 max.	<0.08	0.12 max.	0.13 max.
Al <sub>2</sub> O <sub>3</sub>	26.0 typ.	25 min.	22 typ.	25.0 typ.	26.5 <sub>+ 0.9</sub>
Na <sub>2</sub> O	0.35 max.	0.35 max.	<0.75	0.35 typ.	0.3 max.
K <sub>2</sub> O	0.20 max.	0.25 max.	<0.50	0.35 typ.	0.6 <sub>+ 0.25</sub>
MnO <sub>2</sub>	0.06 max.		<0.05	0.06 typ.	0.2 typ.
P <sub>2</sub> O <sub>5</sub>	0.30 max.	0.25 max.	<0.10	0.35 typ.	8.5 <sub>+ 0.4</sub>
SiO <sub>2</sub>					50-55 typ.
F					1 <sub>+ 0.5</sub>

Concentrate Sizing				
+500 $\mu$	0.10% max.			nil
-100 $\mu$			<15%	
-75 $\mu$	50.0 <sub>+ 3%</sub>	40-45% typ.		94% min. 35% typ.

max. = maximum; typ. = typical; min. = minimum

surgery - tantalum pins are used for such areas as hip-joint replacements, as it is the only metal that is not rejected by body fluids.

### Spodumene

Tanco is one of three major suppliers of high-grade spodumene concentrates to the world market. Tanco's annual production has risen steadily since the first production in 1984, and the plant operates at close to its design capacity of 18,000 tonnes per annum. The other two major suppliers have combined sales (in terms of spodumene equivalents) of 25,000 - 30,000 tonnes.

Tanco's "6.8" grade production capability is of the order of 1,500 tonnes per year, compared to the current sales of approximately 40,000 tonnes by the leading producer of a glass-grade spodumene.

Production of -200# grade concentrate is to order only; however, approximately 1,500 tonnes are currently produced annually.

Different clients require different levels of impurity control, or different impurities controlled, depending on their specific use of the material. Typical specifications of Tanco standard grade, "6.8" grade, spodulite, and -200# concentrates are shown in Table 19.

Spodumene concentrate is supplied to all the major sectors of the market; the majority is shipped to plants in U.S.A., with other important markets in South Korea and Taiwan, and to various locations throughout Europe. Standard spodumene can be shipped in a variety of packaging. Larger North American customers, with the appropriate facilities can have the material delivered in 90 tonne railcars. Elsewhere the material is shipped to customers by 20 tonne container or by "piggyback", usually packed in 1 tonne non-

returnable 'big bags', although other packaging that can be used is container liners (one liner per container, holding all 20 tonnes), or even in 25 kg paper bags.

The spodumene "6.8" concentrate is packaged, when required, in 1 tonne 'big bags', or dispatched in bulk railcars.

The -200 mesh spodumene concentrate is made to order, for customers who require a finer product than Tanco's standard or "6.8" grade; clients to date are in the United States and South Korea. It can be packaged in 1 tonne 'big bags', 25 kg bags, or dispatched in bulk.

Spodumene can be used either as a feedstock for the production of lithium carbonate and metal, or be used directly, in its mineral form in the glass and ceramics industries.

Since the development of the "salars" in the U.S.A. and Chile, most lithium carbonate is recovered from these sources, and little spodumene is now used for chemical production.

High-grade spodumene concentrates are used in pyroceramics, speciality glasses, frits and glazes, continuous steel casting powders and traditional Japanese "cooking pots". Lithium reduces the melt temperature and reduces the viscosity of the melt; in pyroceramics, the very low coefficient of thermal expansion of lithium minimizes "thermal shock" and permits production of "from freezer to cooker" type cookware.

A comparatively new, and growing, use for lower-grade spodumene is in the container glass industry. Small additions (0.05 - 0.2% Li<sub>2</sub>O) in the batch will lower the melt temperature, improve viscosity and provide a good finish. Tanco's "6.8" spodumene is being investigated for such use.

### *Montebrasite*

Tanco's production capacity is 3,000 tonnes per year of montebrasite. It is a unique product, although small amounts of pure amblygonite are hand-cobbed at some small operations in Africa and South America. Typical specifications are shown in Table 20.

The concentrates are packaged in 1 tonne 'big bags' or 25 kg paper bags.

Montebrasite has relatively few applications at present; one application is in the manufacture of high phosphate frits, another in ceramic glazes. Tanco is developing markets for this material, which has an even higher lithium content than high-grade spodumene.

### *Pollucite*

So far, pollucite has been mined and crushed to order. Tanco's current annual production was over 1,000 tonnes, about three quarters of the pollucite ore produced worldwide. Characteristic specifications are

Cs <sub>2</sub> O	24.0% minimum
Rb <sub>2</sub> O	1.5% typical
Li <sub>2</sub> O	0.75% typical
size	-12 mm crushed

Tanco's pollucite ore was sold to cesium processors worldwide. The largest producer of cesium is in West Germany, which used to be the destination for over half of Tanco's production. Other buyers were in Denmark, the United States and Japan. It was normally sold in bulk, crushed to -12 mm in size, although small quantities could be sized to special order. However, all pollucite ore is expected to be processed on site in the

**Table 20.** Distribution of economically significant (or potential) minerals and elements.

Zone (4), (5):	K-feldspar* (Ga,Rb,Cs); amblygonite-montebbrasite* petalite*, spodumene*, spodumene + quartz*, eucryptite* (Li); quartz*
Zone (3), (6):	wodginite, microlite, tantalite and related oxide minerals (Ta,Sn); K- feldspar*, muscovite* (Ga,Rb,Cs); albite* (Ga); quartz*; beryl (Be); hafnian zircon (Zr,Hf)
Zone (7):	quartz*
Zone (8):	pollucite (Cs)
Zone (9):	lepidolite (Rb,Cs,Ga)

\*industrial mineral

future, once the new cesium extraction plant is ready to operate. Rb is a possible byproduct of the Cs production.

Essentially all pollucite is converted to cesium metal, or to cesium compounds such as cesium chloride. Major uses are in biomedical engineering, photoemissive devices, welding rods, scintillation counters, night-vision lenses, as a catalyst in the petrochemical and sulphuric acid industries, and in organic synthesis. The density and solubility of cesium chloride is ideal for the "dense medium" concentration of DNA and other macromolecules - an example of a mineral processing technique being applied to the high-tech biomedical field.

#### *Lepidolite*

Approximately 100 tonnes per year of lepidolite have been mined, hand-picked, crushed, and sold for its rubidium content in the past. Tanco was the world's only significant supplier of rubidium-rich lepidolite. The specifications were

Rb <sub>2</sub> O	3.0% typical
size	-12 mm crushed

The only processor of lepidolite for the production of rubidium is in the United States, and Tanco used to supply all its needs. The material was sold in bulk, crushed to -12 mm in size.

Rubidium has properties similar to those of cesium, for which it can be substituted. However, being rarer and more expensive, cesium is generally preferred, and the market for rubidium remains small.

The lepidolite bodies of zone (9) will be exploited as sources of tantalum mineral concentrates.

#### Zonal distribution of commodities

Table 20 summarizes the distribution of diverse ore and industrial minerals in the internal zonal structure of the pegmatite. A significant aspect of this distribution is a good separation of most of the economically important minerals in space. For example, the ore-bodies of tantalum minerals, spodumene + petalite and lepidolite are mutually totally divorced, which facilitates separate mining and simplifies ore processing. On the other hand, the best concentrations of K-feldspar and amblygonite-montebbrasite are commonly associated with spodumene + petalite, acting as mutual contaminants. Also, pollucite is

separated from the tantalum orebodies and lepidolite but its contacts with minerals of zone (5) tend to be gradational.

### Mining

The pegmatite is situated some 60 m below Bernic Lake, and is accessed by both a shaft and a 20° decline from surface. The only “outcropping” part of the pegmatite is a small patch of zone (5) in the southern part of the body, covered by 15 m of glacial drift on lake bottom.

Mining is carried out using a room and pillar method. Originally rooms were 16 m square; however, rock-mechanics studies have shown that the rooms can be increased to 22 m square, by shaving off of the pillars. However, the maximum width of the rooms at 22 m is the main limiting factor. The roof averages 20 m above the current working levels, and in places reaches 50 m; due to the nature of the ore and the mining method, rock-bolting is rarely required. However, the back is carefully monitored from custom designed Giraffes (areal lifting devices). Mining is carried out using a two-boom hydraulic jumbo for drifting and benching, and a single-boom Simba long-hole drill for pillar recovery. Broken ore is transported by 3.8 to 5.3 m<sup>3</sup> L.H.D. units to the various orepasses, from which it is transported to the shaft by train, and hoisted to the coarse-ore bins on the surface.

Ventilation is downcast through the old Jack Nutt shaft and a 1.2 m diameter raise, and upcast through the decline. Fresh air volume exceeds 3,400 m<sup>3</sup> per minute.

### Processing

Due to land constraints, the concentrator is constructed on a peninsula formed by two bays of Bernic Lake. The building is multi-floored, with equipment on a total of six levels. The major items of concentration equipment are on two levels, with feed preparation equipment, filters and driers on the upper levels, and with pumps on the lower levels.

The first stage of processing, common to all three types of ore is crushing, where the coarse ore from underground (-300 mm size) is broken down to -12 mm size. The tantalum and spodumene ores are crushed into different fine-ore storage bins; the pollucite is crushed to covered stockpiles for direct sale.

The two main ores are concentrated by different processes. Tantalum is processed by gravity concentration, a process which makes use of the fact that tantalum minerals are much heavier than the waste minerals. Spodumene, on the other hand, is primarily processed by flotation which makes use of the different physical and chemical characteristics of the surfaces of the different minerals.

#### *Tantalum mineral concentration*

There are three main elements in the gravity concentration of minerals: liberation of the valuables from the gangue; feed preparation of the ground product into different size fractions; and concentration of the different fractions. At Tanco, the plant is split effectively into four fractions - grinding/spiral circuit, coarse sand circuit, fine sand circuit and slime circuit (Figure 24).

Fine ore is first ground to pass 2 mm. The - 2 mm product passes to the spirals, which recover the coarse free tantalum minerals, which may otherwise have been ground too fine for their effective recovery. The spiral tailing is sized at 0.25 mm, with screen

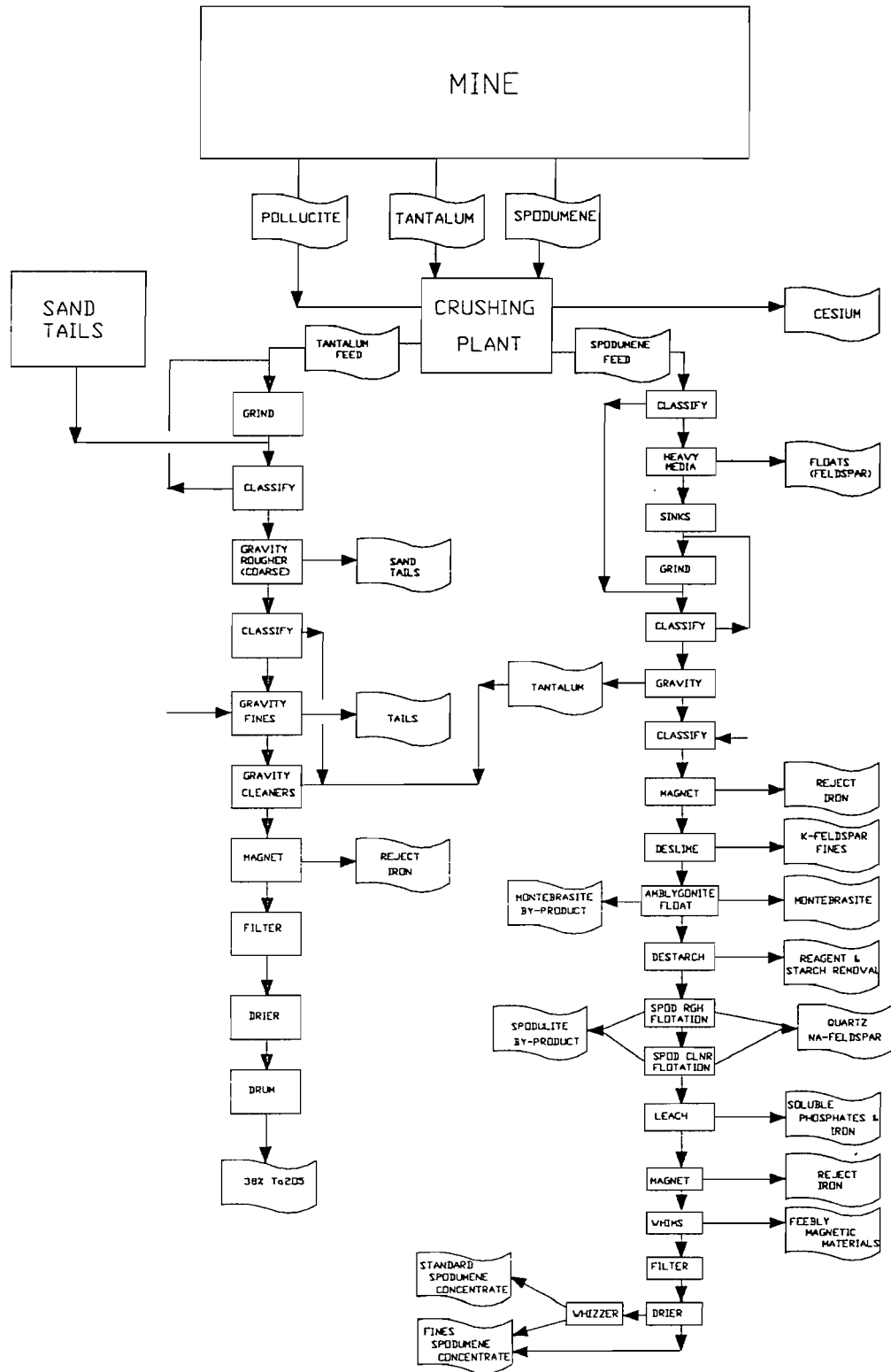


Figure 24. Schematic mill flowsheet of the Tanco processing plants.

**Table 21. Typical metallurgical balance.**

Product	Wt. tpd	Assay % Ta <sub>2</sub> O <sub>5</sub>	Distribution
Coarse concentrate	0.66	37	35
Sand concentrate	0.35	40	20
Fine concentrate	0.26	35	13
Slime concentrate	0.14	30	5
Tailing	718.6	0.026	27
<b>Feed</b>	<b>720</b>	<b>0.1</b>	<b>100</b>

oversize recirculating to the main grinding mill.

Effective feed preparation is essential for satisfactory separation on shaking tables, and this is carried out with cyclones, followed by Bartles-Stokes hydrosizers. The hydrosizers contain four spigots and an overflow. The spigot products, or coarse sands fractions, are distributed to a total of nine triple-deck Concenco tables. These tables each produce a low-grade concentrate, a recirculated middling, and a final tailing product.

Hydrosizer overflow is thickened in another bank of cyclones, and treated on a total of twelve Holman fine-sand tables. These tables produce a rougher concentrate, which passes to the cleaner circuit, a recirculating middling, and a final tailing.

Rougher concentrate from all of the above three sections is collected in a storage tank from which the cleaner section is fed at constant flowrate and density. Classification in cyclones and a hydrosizer sizes feed to five cleaner tables, which produce a final, 40% Ta<sub>2</sub>O<sub>5</sub> concentrate, a recirculated middling, and a tailing.

Overflows from the various cyclones constitute the feed to the slime circuit. The first stage consists of six Bartles-Mozley separators; the low-grade rougher concentrate passes to two Bartles-Crossbelt concentrators, which produce a 2% concentrate. The Crossbelt concentrate is dewatered in a bank of cyclones, and upgraded to a final concentrate, on a further Crossbelt concentrator.

Overall recovery of tantalum ranges from 72 - 74%, upgrading the ore from 0.1% to 38% Ta<sub>2</sub>O<sub>5</sub> as shown in Table 21.

During the summer months, accumulated tailings are processed along with the ore by the same flowsheet. Recovery from the tailing portion of the feed is of the order of 60%, upgrading the feed from 0.05% to 30% Ta<sub>2</sub>O<sub>5</sub>.

#### *Spodumene concentration*

Concentration of spodumene is also carried out in stages, not only to concentrate the spodumene mineral, but also to remove impurities. The first stage is heavy-medium separation, the purpose of which is to control the level of K-feldspar. A Triflo separator treats the -12 + 0.5 mm material in a mixture of ferrosilicon and magnetite, giving a density of separation medium which is higher than that of the feldspar but lower than that of the spodumene minerals. Heavy-medium lights are currently rejected, but could in the future be cleaned, ground and sold as K-feldspar for ceramic production.

Heavy-medium sinks and fines are ground to pass 0.25 mm. Spirals remove the

small amount of tantalum which occurs in the ore; the concentrate is recycled to the main tantalum plant, as a valuable addition to that plant. Iron is removed from the ground product by two-stage low-intensity magnetic separation.

One of the main contaminants in the Tanco spodumene ore is montebrasite-amblygonite; its removal not only controls the phosphate and fluorine levels in the final product but, unfortunately, also results in some loss of lithium. Controlled flotation with starvation quantities of reagent and starch depressant is used; montebrasite is produced without cleaning.

Montebrasite float 'tailing' is dewatered, and then floated, after conditioning and addition of reagents in rougher and cleaner cells, to remove the soda-feldspar and quartz and produce a concentrate grading 7.25%  $\text{Li}_2\text{O}$ . The level of impurities is controlled to the specifications required by customers. Cleaner tailing is combined with scavenger concentrate: this can be cleaned, in two stages, to produce a small amount of secondary concentrate grading 6.8%  $\text{Li}_2\text{O}$ .

After removal of iron minerals by low- and high-intensity magnetic separators, and of reagents from the flotation stage by an acid wash, the concentrate is dried and stored in 180 t storage bins for later bagging.

#### ACKNOWLEDGEMENTS

Research into the Tanco pegmatite was supported by numerous agencies quoted individually in the literature listed below. The authors would like to acknowledge specifically the financing provided by Research, Equipment and Major Installation Grants to P. Černý and F.C. Hawthorne by the National Science and Engineering Research Council of Canada, other research grants by the Canada Department of Energy, Mines and Resources, Manitoba Department of Energy and Mines, the University of Manitoba and the Canada Museum of Nature. The management of the Tanco mine at Bernic Lake and the parent companies provided generous financial and logistic support since 1967. The authors express their thanks to colleagues and students who provided unpublished data from their current research, namely A.-M. Fransolet, B.J. Fryer, M. Novák, R.A. Ramik, J. Selway, A. Stilling, and D.K. Teertstra, and to the past and present personnel of the Tanco mine, specifically the managers C.T. Williams and R.O. Burt, and the geologists R.A. Crouse and D.L. Trueman.

#### REFERENCES

- Anderson, A.J. 1994. Zabuyelite ( $\text{Li}_2\text{CO}_3$ ) in spodumene-bearing pegmatites. Geological Association of Canada–Mineralogical Association of Canada Annual Meeting Waterloo. Program with Abstracts, **19**, A3.
- Armstrong, C.W. 1969. The role of replacement in the formation of complex lithium pegmatites. Ph.D. thesis, University of Western Ontario, London, Ont.
- Ayres, L.D., and Černý, P. 1982. Metallogeny of granitoid rocks in the Canadian Shield. *Canadian Mineralogist*, **20**: 439-536.
- Baadsgaard, H., and Černý, P. 1993. Winnipeg River pegmatite populations, southeastern Manitoba. Geological Association of Canada–Mineralogical Association of Canada

- Annual Meeting Edmonton. Program with Abstracts, **18**, A5.
- Bannatyne, B.B. 1985. Industrial minerals in rare-element pegmatites of Manitoba. Manitoba Energy and Mines, Geological Services, Economic Geology Report, ER 84-1.
- Beakhouse, G.P. 1985. The relationship of supracrustal sequences to a basement complex in the western English River subprovince. *In* Evolution of Archean supracrustal sequences. *Edited by* L.D. Ayres, P.C. Thurston, K.D. Card, and W. Weber. Geological Association of Canada Special Paper, **28**: 169–178.
- Bettenay, L.F., Partington, G.A., Groves, D.I., and Paterson, C. 1988. Nature and emplacement of the giant rare-metal pegmatite at Greenbushes, Western Australia. Proceedings of the 7th IAGOD Symposium: 401-408.
- Beus, A.A. 1948. Vertical zoning of pegmatites on the example of the pegmatite field Aksu Pushtiru (Turkestan Range). Doklady Academy of Sciences U.S.S.R., **60**: 1235-1238.
- Beus, A.A. 1960. Geochemistry of beryllium and the genetic types of beryllium deposits. Academy of Sciences U.S.S.R., Moscow, in Russian. English translation Freeman & Co. 1966.
- Breaks, F.W., and Moore, J.M. 1992. The Ghost Lake batholith, Superior Province of northwestern Ontario: a fertile, S-type, peraluminous granite-rare-element pegmatite system. Canadian Mineralogist, **30**: 835-875.
- Brisbin, W.C. 1986. Mechanism of pegmatite intrusion. American Mineralogist, **71**: 644-651.
- Brisbin, W.C., and Trueman, D.L. 1982. Dilational mechanics of fractures during pegmatite emplacement, Winnipeg River area, Manitoba. Geological Association of Canada–Mineralogical Association of Canada Annual Meeting Winnipeg, Program with Abstracts, **7**: 40.
- Bristol, N.A. 1962. An x-ray powder examination of some pegmatite minerals from southeastern Manitoba. M.Sc. thesis, University of Manitoba, Winnipeg, Man.
- Burt, R.O., Flemming, J., and Trueman, D.L. 1982. Ore processing at Tantalum Mining Corporation. *In* MAC Short Course Handbook, **8**, Granitic Pegmatites in Science and Industry. *Edited by* P. Černý, 495-504.
- Burt, D.M., and London, D. 1982. Subsolvus equilibria. *In* Mineralogical Association of Canada Short Course Handbook, **8**, Granitic Pegmatites in Science and Industry. *Edited by* P. Černý: 329-346.
- Card, K.D. and Ciesielski, A. 1986. DNAG # 1. Subdivisions of the Superior Province of the Canadian Shield. Geoscience Canada, **13**: 5-13.
- Černá, I. 1970. Mineralogy and paragenesis of amblygonite-montebbrasite with special references to the Tanco (Chemalloy) pegmatite, Bernic Lake, Manitoba. M.Sc. thesis, University of Manitoba, Winnipeg, Man.
- Černá, I., Černý, P., and Ferguson, R.B. 1972. The Tanco pegmatite at Bernic Lake, Manitoba. III, Amblygonite-montebbrasite. Canadian Mineralogist, **11**: 643-659.
- Černá, I., Černý, P., and Ferguson, R.B. 1973. The fluorine content and some physical properties of the amblygonite-montebbrasite minerals. American Mineralogist, **58**: 291-301.
- Černý, P. 1972a. The Tanco pegmatite at Bernic Lake, Manitoba. VII, Eucryptite. Canadian Mineralogist, **11**: 708-713.
- Černý, P. 1972b. The Tanco pegmatite at Bernic Lake, Manitoba. VIII, Secondary minerals

- from the spodumene-rich zones. *Canadian Mineralogist*, **11**: 714-726.
- Černý, P. 1975. Granitic pegmatites and their minerals: selected examples of recent progress. *Fortschritte der Mineralogie*, **52**: 225-250.
- Černý, P. 1978. Alteration of pollucite in some pegmatites of southeastern Manitoba. *Canadian Mineralogist*, **16**: 89-95.
- Černý, P. 1982a. Petrogenesis of granitic pegmatites. *In* Mineralogical Association of Canada Short Course Handbook, **8**: Granitic Pegmatites in Science and Industry. *Edited by* P. Černý: 405-461.
- Černý, P. 1982b. The Tanco pegmatite at Bernic Lake, southeastern Manitoba. *In* Mineralogical Association of Canada Short Course Handbook, **8**: Granitic Pegmatites in Science and Industry. *Edited by* P. Černý: 527-543.
- Černý, P. 1988. The rubidium-thallium relationship in complex granitic pegmatites. Geological Association of Canada–Mineralogical Association of Canada Annual Meeting St. John's. Program with Abstracts, **13**: A 19.
- Černý, P. 1989a. Contrasting geochemistry of two pegmatite fields in Manitoba: products of juvenile Aphebian crust and polycyclic Archean evolution. *Precambrian Research*, **45**: 215-234.
- Černý, P. 1989b. Characteristics of pegmatite deposits of tantalum. *In* Lanthanides, Tantalum and Niobium. *Edited by* P. Möller, P. Černý, and F. Saupé. Springer-Verlag, SGA Special Publication, **7**: 192-236.
- Černý, P. 1990. Distribution, affiliation and derivation of rare-element granitic pegmatites in the Canadian Shield. *Geologische Rundschau*, **79**: 183-226.
- Černý, P. 1991a. Rare-element granitic pegmatites. Part I: Anatomy and internal evolution of pegmatite deposits. *Geoscience Canada*, **18**: 49-67.
- Černý, P. 1991b. Rare-element granitic pegmatites, Part II: Regional to global environments and petrogenesis. *Geoscience Canada*, **18**: 68-81.
- Černý, P. 1991c. Fertile granites of Precambrian rare-element pegmatite fields: is geochemistry controlled by tectonic setting or source lithologies? *Precambrian Research*, **51**: 429-468.
- Černý, P. 1992. Geochemical and petrogenetic features of mineralization in rare-element granitic pegmatites in the light of current research. *Applied Geochemistry*, **7**: 393-416.
- Černý, P., and Bristol, N.A. 1972. New mineral occurrences in pegmatites of southeastern Manitoba. *Canadian Mineralogist*, **11**: 560-563.
- Černý, P., and Chapman, R. 1984. Paragenesis, chemistry and structural state of adularia from granitic pegmatites. *Bulletin de Minéralogie*, **107**: 368-384.
- Černý, P., Ercit, T.S., and Wise, M.A. 1991. The tantalite-tapiolite gap: natural assemblages vs. experimental data. *Canadian Mineralogist*, **30**: 587-596.
- Černý, P., and Ferguson, R.B. 1972. The Tanco pegmatite at Bernic Lake, Manitoba. IV, Petalite and spodumene relations. *Canadian Mineralogist*, **11**: 660-678.
- Černý, P., Fryer, B.J., Longstaffe, F.J., and Tammemagi, H.Y. 1987. The Archean Lac du Bonnet batholith, Manitoba: igneous history, metamorphic effects, and fluid overprinting. *Geochimica Cosmochimica Acta*, **51**: 421-438.
- Černý, P., and Harris, D.C. 1978. The Tanco pegmatite at Bernic Lake, Manitoba. XI, Native elements, alloys, sulfides, and sulfosalts. *Canadian Mineralogist*, **16**: 625-640.
- Černý, P., and Hawthorne, F.C. 1989. Controls on gallium concentration in rare-element

- granitic pegmatites. Geological Association of Canada–Mineralogical Association of Canada Annual Meeting Montreal. Program with Abstracts, **14**: A 21.
- Černý, P., and London, D. 1983. Crystal chemistry and stability of petalite. *Tschermak's Mineralogische und Petrographische Mitteilungen*, **31**: 81-96.
- Černý, P., and Macek, J. 1972. The Tanco pegmatite at Bernic Lake, Manitoba. V, Coloured potassium feldspars. *Canadian Mineralogist*, **11**: 679-689.
- Černý, P., Meintzer, R.E., and Anderson, A.J. 1985. Extreme fractionation in rare-element granite pegmatites: selected examples of data and mechanisms. *Canadian Mineralogist*, **23**: 381-421.
- Černý, P., and Siivola, J. 1980. The Tanco pegmatite at Bernic Lake, Manitoba. XII, Hafnian zircon. *Canadian Mineralogist*, **18**: 313-321.
- Černý, P., and Simpson, F.M. 1977. The Tanco pegmatite at Bernic Lake, Manitoba. IX, Beryl. *Canadian Mineralogist*, **15**: 489-499.
- Černý, P., and Simpson, F.M. 1978. The Tanco pegmatite at Bernic Lake, Manitoba. X, Pollucite. *Canadian Mineralogist*, **16**: 325-333.
- Clark, G.S. 1982. Rubidium-strontium isotope systematics of complex granitic pegmatites. *In* *Granitic pegmatites in science and industry. Edited by P. Černý. Mineralogical Association of Canada Short Course Handbook*, **8**: 347-372.
- Clark, G.S., and Černý, P. 1987. Radiogenic  $^{87}\text{Sr}$ , its mobility, and the interpretation of Rb-Sr fractionation trends in rare-element granitic pegmatites. *Geochimica et Cosmochimica Acta*, **51**: 1011-1018.
- Cooper, D.G. 1964. The Geology of the Bikita pegmatites. *In* *The Geology of Some Ore Deposits in Southern Africa II*: 441-462.
- Crouse, R.A., and Černý, P. 1972. The Tanco pegmatite at Bernic Lake, Manitoba. I. Geology and paragenesis. *Canadian Mineralogist*, **11**: 591-608.
- Crouse, R.A., Černý, P., Trueman, D.L., and Burt, R.O. 1979. The Tanco pegmatite, southeastern Manitoba. *Canadian Institute of Mining and Metallurgy Bulletin*, 1979, No. 2: 1-10.
- Crouse, R.A., Černý, P., Trueman, D.L., and Burt, R.O. 1984. The Tanco pegmatite, southeastern Manitoba. *In* *CIM Special Volume 29. The Geology of Industrial Minerals in Canada*: 169-176.
- Davies, J.F. 1952. Geology of the Oiseau (Bird) River area, Lac du Bonnet mining division. *Manitoba Mines Branch*, **51-3**, 24 pp.
- Davies, J.G. 1956. Manitoba lithium deposits. *Canadian Mining Journal*, **77**, April No. 4: 78-79.
- Dawson, K.R. 1974. Niobium (columbium) and tantalum in Canada. *Geological Survey of Canada Economic Geology Report*, **29**, 157 pp.
- Ercit, T.S. 1986. The simpsonite paragenesis; the crystal chemistry and geochemistry of extreme Ta fractionation. Ph.D. thesis. University of Manitoba, Winnipeg, Man.
- Ercit, T.S., and Černý, P. 1982. The paragenesis of simpsonite. Geological Association of Canada–Mineralogical Association of Canada Annual Meeting Winnipeg, Program with Abstracts, **7**: 48.
- Ercit, T.S., and Černý, P. 1986. Oxide mineralogy of the Tanco pegmatite. Geological Association of Canada–Mineralogical Association of Canada Annual Meeting Ottawa, Program with Abstracts, **11**: 67.
- Ercit, T.S., Černý, P., Hawthorne, F.C., and McCammon, C.A. 1992. The wodginite group II. Crystal chemistry. *Canadian Mineralogist*, **30**: 613-631.

- Ercit, T.S., Černý, P., and Hawthorne, F.C. 1992b. The wodginite group III. Classification and new species. *Canadian Mineralogist*, **30**: 633-638.
- Ercit, T.S., Hawthorne, F.C., and Černý, P. 1992c. The wodginite group I. Structural crystallography. *Canadian Mineralogist*, **30**: 597-611.
- Ercit, T.S., Černý, P., and Hawthorne, F.C. 1993. Cesstibtantite—a geologic introduction to the inverse pyrochlores. *Mineralogy and Petrology*, **48**: 235-255.
- Feldman, L.G., and Ginsburg, A.I. 1973. Die Einzelartige Tantal-Cesium-Lagerstätte von Bernic Lake (Montgary) in Kanada. *Zeitschrift für Angewandte Geologie*, **19**: 410-413. *Translated from Razvedka i Ochrana Nedr, Moscow, 1971, 61-65.*
- Ferguson, R.B., Ball, N.A., and Černý, P. 1991. Structure refinement of an adularian end-member high sanidine from the Buck Claim pegmatite, Bernic Lake, Manitoba. *Canadian Mineralogist*, **29**: 543-552.
- Ferguson, R.B., Hawthorne, F.C., and Grice, J.D. 1976. The crystal structures of tantalite, ixiolite and wodginite from Bernic Lake, Manitoba. II, Wodginite. *Canadian Mineralogist*, **14**: 550-560.
- Ferreira, K.J. 1984. The mineralogy and geochemistry of the lower Tanco pegmatite, Bernic Lake, Manitoba, Canada. M.Sc. thesis, University of Manitoba, Winnipeg, Man.
- Gaupp, R., Möller, P., and Morteani, G. 1984. Tantal-Pegmatite: Geologische, Petrologische und Geochemische Untersuchungen. Monograph Series on Mineral Deposits, **23**. Borntraeger Berlin-Stuttgart. 124 pp.
- Ginsburg, A.I., Timofeyev, I.N., and Feldman, L.G. 1979. Principles of Geology of The Granitic Pegmatites. Nedra, Moscow, 296 pp, in Russian.
- Goad, B.E., and Černý, P. 1981. Peraluminous pegmatitic granites and their pegmatite aureoles in the Winnipeg River district, southeastern Manitoba. *Canadian Mineralogist*, **19**: 177-194.
- Grice, J.D. 1970. The nature and distribution of the tantalum minerals in the Tanco (Chemalloy) mine pegmatite at Bernic Lake, Manitoba. M.Sc. thesis, University of Manitoba, Winnipeg, Man.
- Grice, J.D. 1973. Crystal structure of the tantalum oxide minerals tantalite and wodginite, and of millerite NiS. Ph.D. thesis, University of Manitoba, Winnipeg, Man.
- Grice, J.D., Černý, P., and Ferguson, R.B. 1972. The Tanco pegmatite at Bernic Lake, Manitoba. II, Wodginite, tantalite, pseudo-ixiolite and related minerals. *Canadian Mineralogist*, **11**: 609-642.
- Groat, L.A., Raudsepp, M., Hawthorne, F.C., Ercit, T.S., Sherriff, B.L., and Hartman, J.S. 1990. The amblygonite-montebrasite series: characterization by single-crystal structure refinement, infrared spectroscopy, and multinuclear MAS-NMR spectroscopy. *American Mineralogist*, **75**: 992-1008.
- Halden, N.M., Meintzer, R.E., and Černý, P. 1989. Trace element characteristics and controls of element mobility in the metasomatic aureole to the Tanco pegmatite. Manitoba Energy and Mines, Minerals Division, Report of Field Activities, 152-155.
- Hatcher, M.I., and Bolitho, B.C. 1982. The Greenbushes pegmatite, south-west western Australia. *In Granitic Pegmatites in Science and Industry. Edited by P. Černý. Mineralogical Association of Canada Short Course Handbook*, **8**: 513-525.
- Hawthorne, F.C., and Černý, P. 1977. The alkali-metal positions in Cs-Li beryl. *Canadian Mineralogist*, **15**: 414-421.
- Heinrich, E.W. 1965. Holmquistite and pegmatitic lithium exomorphism. *Indian*

- Mineralogist, **6**: 1-13.
- Heinrich, E.W. 1976. A comparison of three major lithium pegmatites: Varuträsk, Bikita, and Bernic Lake. United States Geological Survey Professional Paper, **1005**: 50-54.
- Henry, D.J., and Guidotti, C.V. 1985. Tourmaline as a petrogenetic indicator mineral: an example from the staurolite-grade metapelites of NW Maine. *American Mineralogist*, **70**: 1-15.
- Howe, A.C.A., and Rowntree, J.C. 1967. Geology and economic significance of the Bernic Lake pegmatite, Canada. *Minig and Metalurgy Bulletin* 1967, 207-212.
- Hutchinson, R.W. 1959. Geology of the Montgary pegmatite. *Economic Geology*, **54**: 1525-1542.
- Jahns, R.H., and Burnham, C.W. 1969. Experimental studies of pegmatite genesis: I. A model for the derivation and crystallization of granitic pegmatites. *Economic Geology*, **64**: 843-864.
- Kapustin, Y.L., Pudovkina, Z.V., and Bykova, T.E. 1980. Dorfmanite, a new mineral. *Zapiski Vsesoyuznogo Mineralogitsheskogo Obshtchestva*, **109**: 211-216.
- Kissin, S.A., Owens, D.R., and Roberts, W.L. 1978. Černýite, a copper-cadmium-tin sulfide with the stannite structure. *Canadian Mineralogist*, **16**: 139-146.
- Krogh, T.E., Harris, N.B.W., and Davis, G.L. 1976a. Archean rocks from the eastern Lac Seul region of the English River gneiss belt, north-western Ontario, Part 2. Geochronology. *Canadian Journal of Earth Sciences*, **13**: 1212-1215.
- Krogh, T.E., Davis, E.L., Ermanovics, I., and Harris, N.B.W. 1976b. U-Pb isotopic ages of zircons from the Berens block and English River gneiss belt. *Proceedings of the 1976 Geotraverse Conference, University of Toronto, Ont. Abstracts* **12-1**: 46.
- Kuzmenko, M.V. 1976. Rare-element granitic pegmatite fields (geochemical specialization and distribution). Nauka, Moscow, 332 pp.
- Lagache, M. 1995. New experimental data on the stability of the analcime-pollucite series: application to natural assemblages. *European Journal of Mineralogy*, **7**: 319-323.
- London, D. 1982. Stability of spodumene in acidic and saline fluorine-rich environments. *Carnegie Institution Geophysical Laboratory Annual Report*, **81**: 331-334.
- London, D. 1983. The magmatic-hydrothermal transition in rare-metal pegmatites: fluid inclusion evidence from the Tanco mine, Manitoba. *Transactions of the American Geophysical Union*, **65**: 549.
- London, D. 1984. Experimental phase equilibria in the system  $\text{LiAlSiO}_4\text{-SiO}_2\text{-H}_2\text{O}$ : a petrogenetic grid for lithium-rich pegmatites. *American Mineralogist*, **69**: 995-1004.
- London, D. 1986a. Magmatic-hydrothermal transition in the Tanco rare-element pegmatite: evidence from fluid inclusions and phase-equilibrium experiments. *American Mineralogist*, **71**: 376-395.
- London, D. 1986b. Formation of tourmaline-rich gem pockets in miarolitic pegmatites. *American Mineralogist*, **71**: 396-504.
- London, D. 1986c. Holmquistite as a guide to pegmatitic rare metal deposits. *Economic Geology*, **81**: 704-712.
- London, D. 1990. Internal differentiation of rare-element pegmatites; a synthesis of recent research. *In Geological Society of America Special Paper* **246**. Edited by H.J. Stein, and J.L. Hannah: 35-50.
- London, D. 1992. Application of experimental petrology to the genesis and crystallization of granitic pegmatites. *Canadian Mineralogist*, **30**: 499-540.
- London, D., Černý, P., Loomis, J.L., and Pan, J.C. 1990. Phosphorus in alkali feldspars of

- rare-element granitic pegmatite. *Canadian Mineralogist*, **28**: 771-786.
- London, D., Hervig, R.L., and Morgan, G.B. 1988. Melt-vapor solubilities and element partitioning in peraluminous granite-pegmatite systems. *Contributions to Mineralogy and Petrology*, **99**: 360-373.
- London, D., Morgan, G.B., and Hervig, R.L. 1989. Vapor-undersaturated experiments on Macusani glass + H<sub>2</sub>O at 200 MPa, and the internal differentiation of granitic pegmatites. *Contributions to Mineralogy and Petrology*, **102**: 1-17.
- London, D., Zolensky, M.E., and Roedder, E. 1987. Diomignite: natural Li<sub>2</sub>B<sub>4</sub>O<sub>7</sub> from the Tanco pegmatite, Bernic Lake, Manitoba. *Canadian Mineralogist*, **25**: 173-180.
- Marshall, P.A. 1972. Selected partition ratios in feldspars and micas from the Bernic Lake (Chemalloy) pegmatite Manitoba. M.Sc. thesis, University of Western Ontario, London, Ont.
- McRitchie, W.D. 1971. The petrology and environment of the acidic plutonic rocks of the Wannipigow-Winnipeg Rivers Region, S.E. Manitoba. *In Geology and Geophysics of the Rice Lake Region, S.E. Manitoba*, Manitoba Mines Branch Publication, **71-1**: 7-62.
- Morgan, G.B., and London, D. 1987. Alteration of amphibolitic wallrocks around the Tanco rare-element pegmatite, Bernic Lake, Manitoba. *American Mineralogist*, **72**: 1097-1121.
- Morteani, G., and Gaupp, R. 1989. Geochemical evaluation of the tantalum potential of pegmatites. *In Lanthanides, Tantalum and Niobium. Edited by P. Möller, P. Černý, F. Saupé*. Springer-Verlag, 380 pp.
- Morteani, G., Preinfalk, C., Spiegel, W., and Bonalumi, A. 1995. The Achala granitic complex and the pegmatites of the Sierras Pampeanas (northwest Argentina): a study of differentiation. *Economic Geology*, **90**: 636-647.
- Mulja, T., Williams-Jones, A.E., Wood, S.A., and Boily, M. 1995. The rare-element-enriched monzogranite-pegmatite-quartzvein system in the Preissac-Lacorne batholith, Quebec, II. Geochemistry and petrogenesis. *Canadian Mineralogist*, **33**: 817-834.
- Mulligan, R. 1957. Lithium deposits of Manitoba, Ontario and Quebec, 1956. *Geological Survey of Canada*, **57-3**, 26 pp.
- Mulligan, R. 1961. Pollucite (caesium) in Canada. *Geological Survey of Canada*, **61-4**, 4 pp.
- Mulligan, R. 1965. Geology of Canadian lithium deposits. *Geological Survey of Canada, Economic Geology Report*, **21**, 131 pp.
- Mulligan, R. 1968. Geology of Canadian beryllium deposits. *Geological Survey of Canada, Economic Geology Report*, **23**, 109 pp.
- Nickel, E.H. 1961. The mineralogy of the Bernic Lake pegmatite, southeastern Manitoba. *Department of Mines and Technical Services, Mines Branch, Technical Bulletin*, **20**, 38 pp.
- Nickel, E.H., Rowland, J.F., and McAdam, R.C. 1963. Wodginite—a new tin-manganese tantalate from Wodgina, Australia, and Bernic Lake, Manitoba. *Canadian Mineralogist*, **7**: 390-402.
- Norton, J.J. 1983. Sequence of mineral assemblages in differentiated granitic pegmatites. *Economic Geology*, **78**: 854-874.
- Penner, A.P., and Clark, G.S. 1971. Rb-Sr age determinations from the Bird River area, southeastern Manitoba. *In Geoscience Studies in Manitoba. Edited by A.C. Turnock*.

- Geological Association of Canada, Special Paper, **9**: 105-109.
- Quensel, P. 1956. The paragenesis of the Varuträsk pegmatite. *Arkiv för Mineralogi och Geologi*, **2**: 9-125.
- Ramik, R.A., Sturman, B.C., Dunn, P.J., and Povarennykh, D.P. 1980. Tancoite, a new Li-Na-Al phosphate from the Tanco pegmatite, Bernic Lake, Manitoba. *Canadian Mineralogist*, **18**: 185-190.
- Rinaldi, R. 1970. Crystallography and chemistry of Li-Rb-Cs bearing micas from the Tanco (Chemalloy) pegmatite, Bernic Lake, Manitoba. M.Sc. thesis, University of Manitoba, Winnipeg, Man.
- Rinaldi, R., Černý, P., and Ferguson, R.B. 1972. The Tanco pegmatite at Bernic Lake, Manitoba. VI, Lithium-rubidium-caesium micas. *Canadian Mineralogist*, **11**: 690-707.
- Rose, R.B. 1956. Lithium deposits of Manitoba. Geological Survey of Canada, Paper **55-26**, 23 pp.
- Shearer, C.K., Papike, J.J., and Laul, J.C. 1987. Mineralogical and chemical evolution of a rare-element granite-pegmatite system: Harney Peak granite, Black Hills, South Dakota. *Geochimica et Cosmochimica Acta*, **51**: 473-486.
- Simpson, F.M. 1974. The mineralogy of pollucite and beryl from the Tanco pegmatite at Bernic Lake, Manitoba. M.Sc. thesis, University of Manitoba, Winnipeg, Man.
- Solodov, N.A. 1971. Scientific principles of perspective evaluation of rare-element pegmatites. Nauka Moscow, 292 pp, in Russian.
- Stewart, D.B. 1963. Petrogenesis and mineral assemblages of lithium-rich pegmatites. Geological Society of America Special Paper, **76**: 159 (Abstract).
- Stewart, D.B. 1978. Petrogenesis of lithium-rich pegmatites. *American Mineralogist*, **63**: 970-980.
- Stewart, D.B., and Wright, T.L. 1974. Al/Si order and symmetry of natural potassic feldspars, and the relationship of strained cell parameters to bulk composition. *Bulletin de la Société Française de Minéralogie et Cristallographie*, **97**: 356-377.
- Taylor, B.E., and Friedrichsen, H. 1983. Light stable isotope systematics of granite pegmatites from North America and Norway. *Isotope Geoscience*, **1**: 127-167.
- Thomas, A.V., and Spooner, E.T.C. 1984. Petrological evidence for downward and upward non-replacive crystallization in the growth sequence lower wall zone, Ta(-Sn) bearing banded albitite, beryl fringe to quartz core, Tanco pegmatite, Manitoba. Geological Association of Canada–Mineralogical Association of Canada, Program with Abstracts, **9**: 111 p.
- Thomas, A.V., and Spooner, E.T.C. 1987. Textural, mineralogical and geochemical evidence for the geometry of crystallization of the Tanco granitic pegmatite, S.E. Manitoba. Geological Association of Canada–Mineralogical Association of Canada, Program with Abstracts, **12**: 95.
- Thomas, A.V., and Spooner, E.T.C. 1988. Fluid inclusions in the system H<sub>2</sub>O-CH<sub>4</sub>-NaCl-CO<sub>2</sub> from metasomatic tourmaline within the border unit of the Tanco zoned granitic pegmatite, S.E. Manitoba. *Geochimica et Cosmochimica Acta*, **52**: 1065-1073.
- Thomas, A.V., and Spooner, E.T.C. 1988. Occurrence, petrology and fluid inclusion characteristics of tantalum mineralisation in the Tanco granitic pegmatite, S.E. Manitoba. *In* CIM Special Volume, **39**. Granite-related mineral deposits. Edited by R.P. Taylor and D.F. Strong, pp. 208-222.
- Thomas, A.V., and Spooner, E.T.C. 1992. The volatile geochemistry of magmatic H<sub>2</sub>O-CO<sub>2</sub> fluid inclusions from the Tanco zoned granitic pegmatite, southeastern Manitoba,

- Canada. *Geochimica et Cosmochimica Acta*, **56**: 49-65.
- Thomas, A.V., Bray, C.J., and Spooner, E.T.C. 1988. A discussion of the Jahns-Burnham proposal for the formation of zoned granitic pegmatites using solid-liquid-vapour inclusions from the Tanco pegmatite, S.E. Manitoba, Canada. *Transactions of the Royal Society of Edinburgh: Earth Sciences*, **79**: 299-315.
- Thomas, A.V., Pasteris, J.D., Bray, C.J., and Spooner, E.T.C. 1990. H<sub>2</sub>O-CH<sub>4</sub>-NaCl-CO<sub>2</sub> inclusions from the footwall contact of the Tanco granitic pegmatite: estimates of internal pressure and composition from microthermometry, laser Raman spectroscopy, and gas chromatography. *Geochimica et Cosmochimica Acta*, **54**: 559-573.
- Timmins, E.A., Turek, A., and Symons, D.T.A. 1985. U-Pb zircon geochronology and paleomagnetism of the Bird River greenstone belt, Manitoba. Geological Association of Canada–Mineralogical Association of Canada Annual Meeting, Program with Abstracts, **10**, A 62.
- Trueman, D.L. 1978. Exploration methods in the Tanco mine area of southeastern Manitoba, Canada. *Energy*, **3**: 293-298.
- Trueman, D.L. 1980. Stratigraphic, structural and metamorphic petrology of the Archean greenstone belt at Bird River, Manitoba. Ph.D. thesis, University of Manitoba, Winnipeg, Man.
- Trueman, D.L., and Macek, J.J. 1971. Geology of the Bird River Sill, Manitoba Mines Branch Preliminary Map Series 1971-A-1.
- Trumbull, R.B. 1990. The age, petrology and geochemistry of the Archean Sinceni pluton and associated pegmatites in Swaziland: A study of magmatic evolution. Ph.D. thesis, Technische Universität Munich, Germany.
- Trumbull, R.B. 1991. Modelling the geochemical evolution of an Archean fertile granite-pegmatite system. *In* Source, transport and deposition of metals. *Edited by* M. Pagel, and J.L. Leroy. Balkema, Rotterdam, 829-832.
- Turek, A., Keller, R., Van Schmus, W.R., and Weber, W. 1989. U-Pb zircon ages for the Rice Lake area, southeastern Manitoba. *Canadian Journal of Earth Sciences*, **26**: 23-30.
- Williams, C.T., and Trueman, D.L. 1978. An estimation of lithium resources and potentials of northwestern Ontario, Manitoba and Saskatchewan, Canada. *Energy*, **3**: 409-413.
- Wright, G.M. 1963. Geology and origin of the pollucite-bearing Montgary pegmatite, Manitoba. *Geological Society of America Bulletin*, **74**: 919-946.



## WINNIPEG'96 GUIDEBOOK ORDER FORM

- A1. Evolution of the Thompson Nickel Belt, Manitoba: Setting of Ni-Cu Deposits in the Western Part of the Circum Superior Boundary Zone**  
*W. Bleeker and J. Macek*.....\$12.00 x no. of copies: \_\_\_\_\_
- A2. Late Holocene Environmental Changes in Southern Manitoba**  
*E. Nielsen, K. D. McLeod, E. Pip and J.C. Doering*..... \$8.00 x no. of copies: \_\_\_\_\_
- A3. Petrology and Mineralization of the Tanco Rare-Element Pegmatite, Southeastern Manitoba.**  
*P. Cerny, S. Ercit and P. Vanstone*.....\$12.00 x no. of copies: \_\_\_\_\_
- A4. Lithostratigraphic Assembly of the Eastern Rice Lake Greenstone Belt and Structural Setting of Gold Mineralization at Bissett, Manitoba.**  
*K.H. Poulson, W. Weber, R. Brommecker and D. Seneshen*.....\$13.00 x no. of copies: \_\_\_\_\_
- A5/B6. Western Superior Transects: Wabigoon-Quetico-Shebandowen and English River-Winnipeg River-Wabigoon**  
*G. Beakhouse, G. Stott, C. Blackburn, F.W. Breaks, J. Ayer, D. Stone, C. Farrow and F. Corfu*.....\$13.00 x no. of copies: \_\_\_\_\_
- B1. Tectonic Assembly of the Paleoproterozoic Flin Flon Belt and Setting of VMS Deposits**  
*E. Syme, A. Bailes and S. Lucas*.....\$15.00 x no. of copies: \_\_\_\_\_
- B2. Geomorphic and Sedimentological History of the Central Lake Agassiz Basin.**  
*J. Teller, H. Thorleifson and G. Matile*.....\$14.00 x no. of copies: \_\_\_\_\_
- B3. Physical Volcanology, Hydrothermal Alteration and Massive Sulphide Deposits of the Sturgeon Lake Caldera**  
*R. Morton, G. Hudak and E. Koopman*.....\$10.00 x no. of copies: \_\_\_\_\_
- B4. Lower to Middle Paleozoic Stratigraphy of Southwestern Manitoba**  
*R. Bezys and H. R. McCabe*.....\$12.00 x no. of copies: \_\_\_\_\_
- B5. Geology of the Lac du Bonnet Batholith, Inside and Out: AECL's Underground Research Laboratory, S. E. Manitoba**  
*R. Everitt, J. McMurry, C. Davison and A. Brown*..... \$10.00 x no. of copies: \_\_\_\_\_
- B7. Industrial Minerals of S.E.Manitoba**  
*B. Schmidtke and J. Bamburak*.....\$3.00 x no. of copies: \_\_\_\_\_

The entire set may be purchased for \$95.00

Subtotal:	
+GST (7%)	
+Postage and Handling	
<b>TOTAL</b>	

Orders should be sent to:

Geological Association of Canada, Winnipeg Section  
 c/o Geological Services Branch, Manitoba Energy and Mines  
 1395 Ellice Ave., Suite 360  
 Winnipeg, Manitoba R3G 3P2

Make cheques or money orders payable to "GAC-MAC '96". Add \$2.00 per book for postage and handling. For entire set add \$10.00.

